

Green Chemistry

Cutting-edge research for a greener sustainable future

www.rsc.org/greenchem

Volume 7 Number 3 | March 2005 | Pages 113–168



ISSN 1463-9262

RSC | Advancing the
Chemical Sciences

de Bruijn
Fuel cells for mobile and stationary
applications

Baba *et al.*
Methoxycarbonylation with a zinc
acetate catalyst

Stepinski *et al.*
Facilitation of metal ion transfer into
ionic liquids

Grant *et al.*
Introducing undergraduates to green
chemistry



1463-9262 (2005) 7:3;1-D

ChemComm - a vibrant blend of high quality research from across the chemical sciences



ChemComm
...the perfect mix

Celebrating in 2005:

- **40 years** of successful publication
- An increase in frequency to **weekly publication** – improving print publication times even further
- An increase to **three page communications** – providing authors with more flexibility to develop their results and discussion

www.rsc.org/chemcomm

IN THIS ISSUE

ISSN 1463-9262 CODEN GRCHFJ 7(3) 113–168 (2005)

In this issue...

Introducing the concepts, aims and aspirations of green chemistry to undergraduate students—a focus by Grant *et al.* from the University of Glasgow



Chemical biology articles published in this journal also appear in the *Chemical Biology Virtual Journal*:
www.rsc.org/chembiol

**Cover**

Fuel cell bus in daily operation in Amsterdam, as part of the world's largest fuel cell bus trial, sponsored by the EU, in the CUTE project. Thirty fuel cell buses, developed by Daimler Chrysler and Ballard, are operated in Europe under various climate conditions in Amsterdam, Barcelona, Hamburg, London, Luxemburg, Madrid, Porto, Reykjavik, Stuttgart and Stockholm. The buses run on hydrogen, produced by electrolysis of water and by reforming of natural gas.

Image reproduced by permission of René van den Burg from F. de Bruijn, *Green Chem.*, 2005, 7(3), 132.

CHEMICAL TECHNOLOGY

T9

Chemical Technology highlights the latest applications and technological aspects of research across the chemical sciences.

Chemical Technology

March 2005/Volume 2/Issue 3

www.rsc.org/chemicaltechnology

HIGHLIGHT

119

Highlights

FOCUS

121

Introducing undergraduates to green chemistry: an interactive teaching exercise

Steven Grant, Andrew A. Freer, John M. Winfield, Craig Gray and David Lennon*

EDITORIAL STAFF

Managing editor

Harpal Minhas

Deputy editor

Rowena Milan

Assistant editor

Merlin Fox

News writer

Markus Hölscher

Publishing assistant

Jackie Cockrill

Team leader, serials production

Stephen Wilkes

Technical editors

Katherine Davies, Christopher Ingle, Kathryn Lees

Editorial secretaries

Sonya Spring, Julie Thompson, Rebecca Gotobed

Publisher

Adrian Kybett

Green Chemistry (print: ISSN 1463-9262; electronic: ISSN 1463-9270) is published 12 times a year by the Royal Society of Chemistry, Thomas Graham House, Science Park, Milton Road, Cambridge, UK CB4 0WF.

All orders accompanied by payment should be sent directly to Portland Customer Services, Commerce Way, Colchester, Essex, CO2 8HP. Tel +44 (0) 1206 226050; E-mail sales@rscdistribution.org

2005 Annual (print + electronic) subscription price: £795; US\$1310. 2005 Annual (electronic) subscription price: £715; US\$1180. Customers in Canada will be subject to a surcharge to cover GST. Customers in the EU subscribing to the electronic version only will be charged VAT.

If you take an institutional subscription to any RSC journal you are entitled to free, site-wide web access to that journal. You can arrange access via Internet Protocol (IP) address at www.rsc.org/ip. Customers should make payments by cheque in sterling payable on a UK clearing bank or in US dollars payable on a US clearing bank. Periodicals postage paid at Rahway, NJ, USA and at additional mailing offices. Airfreight and mailing in the USA by Mercury Airfreight International Ltd., 365 Blair Road, Avenel, NJ 07001, USA.

US Postmaster: send address changes to Green Chemistry, c/o Mercury Airfreight International Ltd., 365 Blair Road, Avenel, NJ 07001. All despatches outside the UK by Consolidated Airfreight.

Advertisement sales: Tel +44 (0)1223 432243; Fax +44 (0)1223 426017; E-mail advertising@rsc.org

Green Chemistry

Cutting-edge research for a greener sustainable future

www.rsc.org/greenchem

Green Chemistry focuses on cutting-edge research that attempts to reduce the environmental impact of the chemical enterprise by developing a technology base that is inherently non-toxic to living things and the environment.

EDITORIAL BOARD

Chair

Professor Colin Raston,
Department of Chemistry
University of Western Australia
Perth, Australia
E-mail clraston@chem.uwa.edu.au

Professor Joan Brennecke,
University of Notre Dame, USA
Professor Steve Howdle, University
of Nottingham, UK
Dr Janet Scott, Centre for Green
Chemistry, Monash University,
Australia

Professor Roshan Jachuck,
Clarkson University, USA
E-mail rjachuck@clarkson.edu
Dr Paul Anastas, Green Chemistry
Institute, USA
Email p_anastas@acs.org

Scientific editor

Professor Walter Leitner,
RWTH-Aachen, Germany
E-mail leitner@itmc.rwth-aachen.de

Dr A Michael Warhurst,
WWF, Brussels, Belgium
Professor Tom Welton,
Imperial College, UK
E-mail t.welton@ic.ac.uk

Associate editor for the Americas

Professor C. J. Li, McGill
University, Canada
E-mail cj.li@mcgill.ca

International advisory board

James Clark, York, UK
Avelino Corma, Universidad
Politécnica de Valencia, Spain
Mark Harmer, DuPont Central
R&D, USA
Makoto Misono, Kogakuin
University, Japan

Robin D. Rogers, Centre for Green
Manufacturing, USA
Kenneth Seddon, Queen's
University, Belfast, UK
Roger Sheldon, Delft University of
Technology, The Netherlands
Gary Sheldrake, Queen's
University, Belfast, UK

Pietro Tundo, Università ca
Foscari di Venezia, Italy
Tracy Williamson, Environmental
Protection Agency, USA

INFORMATION FOR AUTHORS

Full details of how to submit material for publication in Green Chemistry are given in the Instructions for Authors (available from <http://www.rsc.org/authors>). Correspondence on editorial matters should be addressed to: Harpal Minhas, Managing Editor, The Royal Society of Chemistry, Thomas Graham House, Science Park, Milton Road, Cambridge, UK CB4 0WF. Tel +44 (0) 1223 432137; Fax +44 (0) 1223 420247; E-mail green@rsc.org. Submissions should be sent via Resource: <http://www.rsc.org/resource>.

Authors may reproduce/republish portions of their published contribution without seeking permission from the RSC, provided that any such republication is accompanied by an acknowledgement in the form: (Original citation) – Reproduced by permission of the Royal Society of Chemistry.

© The Royal Society of Chemistry 2005. Apart from fair dealing for the purposes of research or private study for non-commercial purposes, or criticism or review, as permitted under the Copyright, Designs and Patents Act 1988 and the Copyright and Related

Rights Regulations 2003, this publication may only be reproduced, stored or transmitted, in any form or by any means, with the prior permission in writing of the Publishers or in the case of reprographic reproduction in accordance with the terms of licences issued by the Copyright Licensing Agency in the UK. US copyright law is applicable to users in the USA. The Royal Society of Chemistry takes reasonable care in the preparation of this publication but does not accept liability for the consequences of any errors or omissions.

Ⓢ The paper used in this publication meets the requirements of ANSI/NISO Z39.48-1992 (Permanence of Paper).

Royal Society of Chemistry: Registered Charity No. 207890

The Society is not responsible for individual opinions expressed in *Green Chemistry*. Editorials do not necessarily express the views of Council.

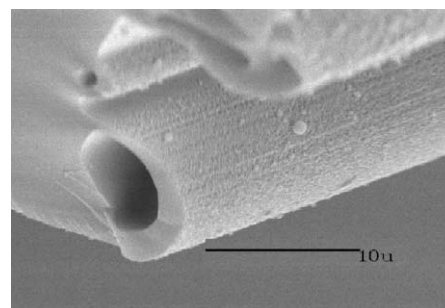
COMMUNICATION

129

Crystallization and processing of carbohydrates using carbon dioxide

Poovathinthodiyil Raveendran,* Marc A. Blatchford, Michael L. Hurrey, Peter S. White and Scott L. Wallen*

Acetylation of sugars renders them highly CO₂-philic. This strategy enables the processing of these materials using CO₂ as a green processing medium in the gaseous, liquid and supercritical states.



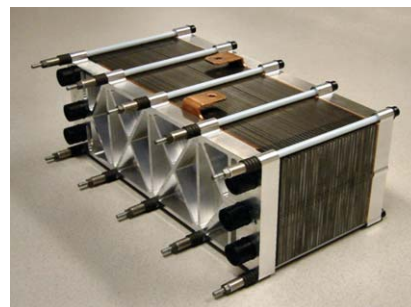
TUTORIAL REVIEW

132

The current status of fuel cell technology for mobile and stationary applications

Frank de Bruijn

The use of fuel cells in transport and for combined heat and power generation can save an appreciable amount of energy, while at the same time reducing emissions of non-greenhouse gases. The status of fuel cell technology is reviewed.



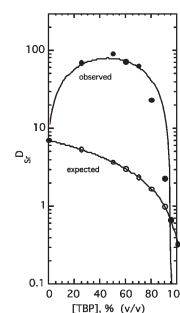
PAPERS

151

Synergistic effects in the facilitated transfer of metal ions into room-temperature ionic liquids

Dominique C. Stepinski, Mark P. Jensen, Julie A. Dzielawa and Mark L. Dietz*

Strontium extraction by dicyclohexano-18-crown-6 from nitric acid into certain 1-alkyl-3-methyl-imidazolium bis[(trifluoromethyl)sulfonyl]imides is enhanced by addition of tri-*n*-butyl phosphate, thus providing the first example of synergistic adduct formation in an ionic liquid.

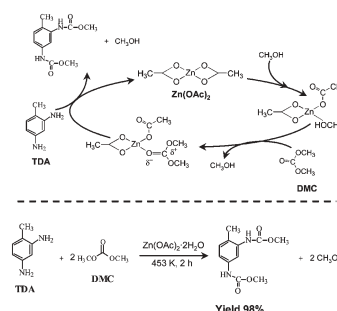


159

Characteristics of methoxycarbonylation of aromatic diamine with dimethyl carbonate to dicarbamate using a zinc acetate catalyst

Toshihide Baba,* Akane Kobayashi, Yukio Kawanami, Koji Inazu, Akio Ishikawa, Tsuneo Echizen, Kazuhito Murai, Shinji Aso and Masamitsu Inomata

The activation mechanism of dimethyl carbonate with zinc cations was investigated by IR measurement and calculations using MOPAC PM3. These findings are important for the development of new catalysts and methoxycarbonylation reactions of diamines with dimethyl carbonate to form dicarbamates.



AUTHOR INDEX

Aso, Shinji, 159
 Baba, Toshihide, 159
 Blatchford, Marc A., 129
 de Bruijn, Frank, 132
 Dietz, Mark L., 151
 Dzielawa, Julie A., 151
 Echizenn, Tsuneo, 159

Freer, Andrew A., 121
 Grant, Steven, 121
 Gray, Craig, 121
 Hurrey, Michael L., 129
 Inazu, Koji, 159
 Inomata, Masamitsu, 159
 Ishikawa, Akio, 159


Jensen, Mark P., 151
 Kawanami, Yukio, 159
 Kobayashi, Akane, 159
 Lennon, David, 121
 Murai, Kazuhito, 159
 Raveendran, Poovathinthodiyil,
 129

Stepinski, Dominique C., 151
 Wallen, Scott L., 129
 White, Peter S., 129
 Winfield, John M., 121

FREE E-MAIL ALERTS


Contents lists in advance of publication are available on the web *via* www.rsc.org/greenchem - or take advantage of our free e-mail alerting service (www.rsc.org/ej_alert) to receive notification each time a new list becomes available.


* Indicates the author for correspondence: see article for details.

 Electronic supplementary information (ESI) is available *via* the online article (see <http://www.rsc.org/esi> for general information about ESI).

ADVANCE ARTICLES AND ELECTRONIC JOURNAL

Free site-wide access to Advance Articles and the electronic form of this journal is provided with a full-rate institutional subscription. See www.rsc.org/ejs for more information.



 **INCA**
 INTERUNIVERSITY CONSORTIUM
 CHEMISTRY FOR THE ENVIRONMENT

Summer School on Green Chemistry


Eighth event
4 - 10 September 2005
Venezia, Italy

Participants are eligible for full scholarships
 Apply online at: www.unive.it/inca , deadline **15 June 2005**

TOPICS

- ALTERNATIVE SOLVENTS
- CLEAN FEEDSTOCKS AND PRODUCTS
- CATALYSIS, PHOTOCATALYSIS AND BIOCATALYSIS
- NEW REACTION CONDITIONS

Contacts: Pietro Tundo, director: tundop@unive.it; Alvise Perosa, organizer: alvise@unive.it



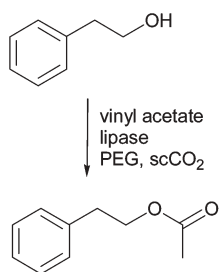
Highlights

DOI: 10.1039/b500904a

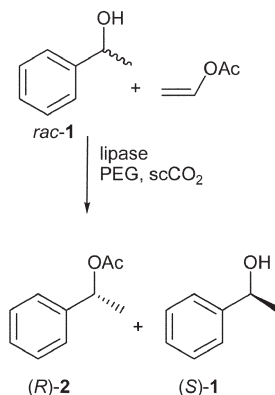
Markus Hölscher reviews some of the recent literature in green chemistry

Lipase-catalyzed esterification in liquid poly(ethylene glycol) and supercritical CO₂

As acylation of chiral and achiral alcohols catalyzed by lipase is a standard tool in organic chemistry, the development of environmentally benign processes would be very helpful to avoid the commonly used organic solvents which are toxic in many cases. In the past, different systems were tried and combinations of supercritical CO₂ (scCO₂) and ionic liquid (IL) proved to be quite successful. However, the combination of scCO₂ and poly(ethylene glycol) (PEG) is also an efficient solvent system in transition metal-catalyzed processes, which makes it an interesting candidate for lipase-catalyzed reactions. Reetz and Wiesenhöfer from the Max Planck Institute for Coal Research, Mülheim, succeeded recently in developing such a system (*Chem. Commun.*, 2004, 2750–2751). The lipase-catalyzed acylation of 2-phenylethanol by vinyl acetate could be accomplished in PEG and the product was extracted with scCO₂ with yields of *ca.* 74%.



The experiment was repeated using a continuous process which gave an excellent conversion of *ca.* 90% for at least 25 h. Kinetic resolution of *rac*-1-phenylethanol, *rac*-1, was also possible yielding (*R*)-2 and (*S*)-1 with *ee*'s of *ca.* 98 and 99%, respectively. Recyclability was shown to be very effective leaving conversions (*ca.* 50%) and enantioselectivities nearly unchanged for 11 consecutive runs.



Mesoporous chromium oxide as efficient removal/oxidation material for volatile organic compounds

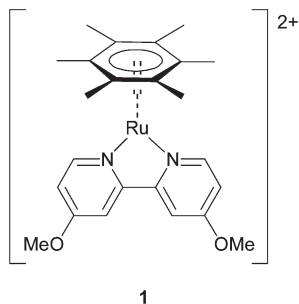
Air pollution by volatile organic compounds (VOCs) has been a matter of growing concern over the past decade which has resulted in strict legislation for controlling nearly any kind of chemical emission into the atmosphere. One favorable approach for dealing with VOCs is catalytic combustion yielding CO₂ and H₂O as final reaction products. Transition metal oxides are the catalysts of choice, however bulk materials suffer from mass transfer limitations, which has made the development of porous alternatives an interesting target. However, this has been accomplished for only a few elements to date. Sinha and Suzuki from the central Toyota R&D laboratories, Japan, have recently shown that mesoporous chromium oxide is readily available when chromium nitrate is mixed with a nonaqueous ethylene glycol-propanol medium in the presence of poly(alkylene oxide) block copolymers as template, aged and heated to form a cubic templated chromium oxide material that can be calcined for template removal (*Angew. Chem.*, 2005, **117**, 275–277). Interestingly the as-synthesized form of the material can be indexed in cubic space group *Im3m* with a largest lattice spacing *d* of 173 Å, whereas the

calcined form is more reminiscent of the rhombohedral phase of crystalline Cr₂O₃, the maximum *d* spacing being 150 Å. The catalytic behaviour of the calcined materials was tested using toluene as a typical VOC. 52% toluene removal was achieved at room temperature with a sample previously calcined at 500 °C. Formation of CO₂ was observed with 2% conversion (11 ppm). The toluene removal ability increased to 65% when the temperature was increased to 85 °C. Complete toluene removal and 100% conversion resulted at a temperature of 350 °C. According to XPS analyses the material contains chromium in different oxidation states. A comparison with mesoporous silica with a much larger surface area showed toluene removal to be much less effective under otherwise identical conditions, and commercially available hexavalent and trivalent chromium oxide samples also showed poor performance. The development of a dual function material for the selective adsorption of toluene at low temperature and efficient combustion at high temperature without the need to recover the catalyst seems possible in the near future.

Water soluble ruthenium catalysts for catalytic reduction of CO₂ to HCOOH

The hydrogenation of CO₂ is an interesting approach to the utilization of carbon dioxide ecologically and economically as a C₁ source. In the past, hydrogenations of HCO₃⁻ under basic conditions were developed, however, the base used had to be removed at the end of the reaction by neutralization. A catalytic alternative, preferably in aqueous media without employing large amounts of base, would be favorable, and Ogo and Fukuzumi *et al.* recently took an important step in this direction (*Chem. Commun.* 2004, 2714–2715). They described the synthesis and catalytic performance of ruthenium complex **1**,

which proved to be an efficient catalyst for the hydrogenation of CO₂ under acidic conditions.

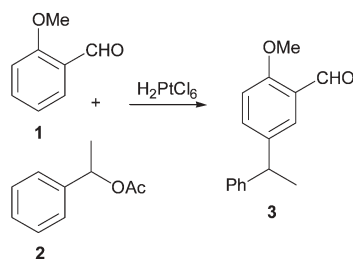


The authors showed the turnover number (TON) to have a maximum at *ca.* 45 °C, whereas it increased linearly with rising CO₂ pressures. Under optimized conditions a TON of 55 was reached. The mechanism relies on the cleavage of a coordinated H₂ molecule yielding the corresponding ruthenium hydride and H₃O⁺. CO₂ subsequently inserts into the Ru–H bond forming the corresponding formate complex, which is then protonated releasing formic acid and regenerating **1**.

Benylation of arenes and heteroarenes with transition metal complexes

A vast amount of pharmaceutically, and agrochemically important compounds contain arene or heteroarene units which during synthesis have to be modified by appropriate functionalizations at the aromatic core to yield the desired product properties. Although a large number of classic organic transformations is available most of these reactions suffer from one or more of the following disadvantages: drastic reaction conditions, low regioselectivities, generation of large amounts of salts. Direct C–C coupling reactions which can be carried out in an environmentally friendly way

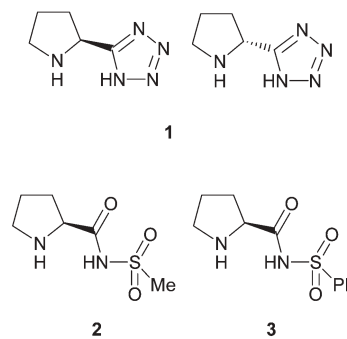
are clearly advantageous. Beller *et al.* from the University of Rostock recently screened a number of transition metal catalysts for direct benzylation of a large number of arenes and heteroarenes and reported quite remarkable results (*Angew. Chem.*, 2005, **117**, 242–246). In a series of test experiments using *o*-xylene as substrate and 1-phenylethylacetate as benzylating agent a catalyst screening showed IrCl₃, H₂[PdCl₄] and H₂[PtCl₆] to result in 100% conversion and 99% yield of the desired benzylated product. Subsequently the authors tested different substrates and found many arenes and heteroarenes to be efficiently benzylated with high yields and regioselectivities. Remarkably 2-methoxybenzaldehyde **1** (free aldehyde group) could be selectively benzylated with 1-phenylethylacetate **2** with a yield of 67% and 99% regioselectivity for the *para*-product **3**.



Novel proline derivatives as organocatalysts in multiple asymmetric C–C bond forming reactions

Organocatalysis has developed into a field with the potential to effectively complement transition metal-catalyzed reactions and the search for new highly active and enantioselective catalysts is an ongoing quest in organic chemistry. If asymmetric organocatalysts can be made available for a substantial number

of transformations, these compounds could, in combination with one of the different environmentally benign and chemically effective innovative solvent systems (supercritical solvents, ionic liquids, polymer based solvent systems), develop into powerful alternatives to commonly used noncatalytic reactions and solvent systems. One of the steps to be taken is the development of novel organocatalysts. Proline has been in use as an organocatalyst since the 1970's, however it has a few disadvantages such as limited solubility and the need for relatively high catalyst loading. Ley *et al.* from the University of Cambridge reasoned that the substitution of the COOH group of proline by a tetrazole ring should increase the solubility in solvents like methanol, dichloromethane and tetrahydrofuran (*Org. Biomol. Chem.*, 2005, **3**, 84–96). Although these solvents are certainly not green, this development is interesting for potential application in supercritical reaction media.



In a first step test reactions were run in conventional solvents. With catalysts like **1**, **2** and **3** different Mannich-, nitro-Michael- and Aldol-reactions, respectively, were investigated and especially in asymmetric Mannich additions of ketones to imines the catalysts proved to be highly enantioselective (*ee*'s > 99% in many cases).

Introducing undergraduates to green chemistry: an interactive teaching exercise

Steven Grant,^a Andrew A. Freer,^a John M. Winfield,^a Craig Gray†^b and David Lennon*^a

DOI: 10.1039/b412664e

An interactive teaching unit (ITU) is described that aims to introduce undergraduate students to some of the concepts and themes of the Green Chemistry movement. It assumes no prior awareness of green chemistry and uses the concept of the atom economy to evaluate the overall efficiencies of a variety of chemical processes. Although the examples presented have all been described elsewhere, the selected reactions and the format of the ITU package represent a stimulating means of getting chemistry students to think about sustainable resources and efficient processes. Catalysis is identified as an enabling technology and examples are presented where the application of catalysts result in substantial improvements in the operational efficiency of well established industrial-scale processes. The ITU format additionally provides participating students with the opportunity to give short oral presentations in a small group environment. Student coursework and the outcome of student evaluation exercises are also described.

1. Introduction

In an effort to enthuse our students for their elected subject and to expose them to the broad range of topics typically encountered by chemists outside a university environment, we have recently constructed three teaching exercises that invoke the concepts of problem based learning.^{1–3} We have named these exercises Interactive Teaching Units (ITUs). The first ITU (ITU1, 'The Age of Refrigeration') examines the issues of replacement refrigerants,⁴ the second (ITU2, 'Mercury, Membrane or Diaphragm') explores issues surrounding the industrial scale manufacture of chlorine and sodium hydroxide,⁴ whilst the third exercise (ITU3) concentrates on the manufacture of titanium dioxide on the industrial scale.⁵ All three ITUs operate within our 2nd year undergraduate teaching programme (≡1st year in England, Wales and Northern Ireland). An underlying theme for this initiative was to inform the students about the importance of operating large-scale chemical operations in a sustainable manner and to, *indirectly*, introduce the concepts of Green Chemistry.⁶ These three units have been

well received by the student body and also by the staff who have to operate them. They offer diversity in the student learning experience, supplement aspects of the lecture programme and provide an opportunity to foster communication skills. However, it was recognised that the diet was skewed towards physical and inorganic chemistry and, crucially, did not specifically address Green Chemistry. Thus, against this background, it was decided to construct a new ITU, which would include a formal introduction to Green Chemistry. The selection of an organic topic was additionally favoured so that our portfolio included the three major sub-disciplines.

The topic chosen for the new unit (ITU4) to illustrate the concepts of Green Chemistry was that of the Atom Economy.⁷ Whilst we recognise that this has been described comprehensively in numerous publications,^{e.g.7–9} it was not prominent in our 1st or 2nd year undergraduate programme and, furthermore, it is a topic that can be readily appreciated by junior undergraduates. The theme of atom efficiency is maintained throughout the whole unit and, whilst there is nothing particularly novel about the chemical systems contained within the ITU, the examples selected have connectivity to material covered within the lecture programme and thus,

collectively, represent an effective package to engage and inform chemistry undergraduates.

The original aim was to use examples from the booklet by Michael Cann and Marc Connelly on 'Real World Cases in Green Chemistry'⁸ and include them within our ITU format.^{4,5} However, in order to reach a wide audience, that publication offers a fairly general perspective and it was deemed that additional examples with increasing technical depth were required to keep our 2nd year undergraduates gainfully employed for the 3 hour duration of the ITU exercise. To this end, material not contained within the Cann and Connelly document⁸ was compiled and worked up into a common template, with which the students were asked to engage, understand and disseminate to their fellow classmates. Overall, ITU4 is presented as a teaching package that aims to demonstrate clearly to junior undergraduate students the importance and value of green chemical issues in an increasingly competitive and environmentally aware world. This communication describes the aims, organisational framework and content of ITU4 and, in conjunction with references 4 and 5 completes the description of the ITU portfolio currently operating at the University of Glasgow.

† Deceased.

*d.lennon@chem.gla.ac.uk

2. Aims

The following aims were identified for ITU4:

1. To make the students aware of the significance of waste in modern industrial chemistry.
2. To introduce the concepts of Green Chemistry and to inform the students of the importance of sustainable products and processes.
3. To introduce the students to the concept of *atom economy* and to involve them in group exercises where the atom economies are determined for a wide range of industrially relevant processes.
4. To illustrate the advantages of homogeneous and heterogeneous catalysis for the efficient manufacture of materials with high selectivity to the desired product(s).
5. To provide a forum which allows every student in the class the opportunity to give a short oral presentation, in

addition to producing a written report for assessment.

3. Exercise structure and organisational framework

Our 2nd year class typically comprises *ca.* 144 students, who are allocated prescribed ITU days so that each ITU class contains about 36 students. The ITU session is then repeated on four consecutive days, with a different set of tutors responsible for each session. This arrangement has the advantage of exposing the student body to a large number of staff who, otherwise, might not have been involved with the 2nd year programme.

ITU4 follows the same structure plan as developed for ITU3.⁵ It is composed of six sections (A–F), each of which is outlined in Fig. 1. During Sections B–E, the class is sub-divided into 4 tutorial groups of 9 students, with each tutorial

group operating independently in separate locations. An academic member of staff is assigned to each tutorial group, which is further required to form small sub-groups of just 3 students (Sub-Groups 1–3) to work together through a series of exercises. The sub-groups are provided with handouts that describe the main issues of the topic they are to investigate at that time. The students are allowed a reading period and then work within their sub-group to decide how best to present their material in an oral presentation to the tutorial group. To assist them in this exercise, and to prevent them going off at a tangent to the intended direction, pre-prepared overhead projector acetates are provided. These acetates provide a crude template, which provides structure to the presentation. The students are responsible for the details to be added to the acetate to convey successfully their 'message' to the tutorial group. This format has proven to

	A	B	C	D	E	F
	INTRODUCTION. (36)	INTRINSIC ATOM ECONOMIES OF THE MAIN REACTION CLASSES. (3 × 3)	ATOM ECONOMY CASE STUDY: THE INDUSTRIAL SYNTHESIS OF IBUPROFEN. (3 × 3)	POOR ATOM ECONOMY IN INDUSTRY: CATALYSTS FOR CHANGE. (3 × 3)	ITU 4 PRINCIPLES OF GREEN CHEMISTRY. (9)	PLENARY SESSION. (36)
Sustainable development.		Sub-Group 1 <i>Addition reaction: Bromination of cyclohexene.</i> OHP	Sub-Group 1 Stereochemical and pharmacological aspects of Ibuprofen. OHP	Sub-Group 1 <i>'Stoichiometric' ethylene oxidation vs Catalytic ethylene oxidation.</i> OHP	Tutorial group discussion	Tutorial group presentations.
Concept of atom economy.		Sub-Group 2 <i>Substitution reaction: Ammonolysis of ethyl propionate with methyl amine.</i> OHP	Sub-Group 2 <i>The Boots Company synthesis of Ibuprofen.</i> OHP	Sub-Group 2 <i>'Stoichiometric' nitrobenzene reduction vs Catalytic nitrobenzene reduction.</i> OHP		Tutor summary of ITU 4.
Outline of ITU 4.		Sub-Group 3 <i>Elimination reaction: Dehydrohalogenation of 2-bromo-2-methylpropane.</i> OHP	Sub-Group 3 The BHC Company synthesis of Ibuprofen. OHP	Sub-Group 3 <i>'Stoichiometric' aromatic nitration vs Catalytic aromatic nitration.</i> OHP		Coursework.
		Tutor summary and questions.	Tutor summary and questions.	Tutor summary and questions.	Tutor to lead discussion. Assign tutor group representative.	Post-evaluation.

Fig. 1 Structure plan for ITU4. The bold letters indicate the six sections described in the text. The numbers in parentheses represent the number of students participating in each section. OHP signifies the requirement by a member of each sub-group (Sub-Groups 1–3) to make an oral presentation, based around pre-prepared overhead projector acetates, to the tutorial group.

work well in previous ITUs,^{4,5} with the ITU team impressed how much moderate level information the students can competently assimilate and disseminate in relatively short periods of time.

Sections B, C and D require each member of the sub-group to make a short oral presentation to the tutorial group and the tutor, who manages the whole exercise. Section E requires the tutorial group of 9 students to come together to propose their own 'Five Principles of Green Chemistry'. In Section F, the 4 tutorial groups recombine for the plenary session and their suggestions for the 'Five Principles of Green Chemistry' are presented to the whole class *via* a short oral presentation, given from a volunteer from each tutorial group. The 3 hour session ends with the lead tutor presenting a summary of the 'Principles of Green Chemistry', as described by several authors,^{6,10} and the class are then informed of the coursework requirement for the exercise.

Thus, as constructed, the unit represents an exercise in parallel learning,⁵ with each sub-group of 3 students educating their tutorial group of 9 students with different aspects of examples of Green Chemistry in action. Having 3 groups of students working concurrently on 3 different, but related, problems means that the class can be exposed to a broad range of issues within the allotted time.

4. Course content

A description of the individual Sections of the ITU now follows:

Section A. Introduction to the ITU

This Section is handed out to the class 3 days before commencement of the ITU programme, with the intention of giving

the students time to prepare and consider what the forthcoming exercise is all about. Prior questioning of the students' awareness of the Green Chemistry movement in 2001 had tended to yield blank faces and no response, so it was deemed that some advance priming of the topics to be encountered would be beneficial.

The Section starts with extracts from a paper by Lancaster. They are used to illustrate some of the concerns over waste emanating from the chemicals industry.¹¹ The students are then informed that the concept of sustainable products and processes has been popularised under the Green Chemistry banner⁶ and probably represents the fastest growing area of chemistry today. The chemical industry's connection to this movement is easy to understand, given the obvious economic benefits.

The roots of the Green Chemistry movement are traced back to the US Green Chemistry Programme established in 1991 and the Pollution Prevention Act of 1992.¹² Green Chemistry is then defined as the design of chemical products and processes that reduce or eliminate the use or generation of hazardous substances.¹² 'Twelve Principles of Green Chemistry' due to Anastas and Warner are mentioned, though not described, at this stage.^{6,8}

The concept of an atom economy is then briefly introduced, without examples. At this juncture the students are simply informed that it is a means by which chemists consider how many reactant atoms end up in the desired product of a chemical synthesis and, moreover, how many atoms contribute to the formation of waste products. Finally, the students are provided with a list of relative atomic masses and asked to bring a calculator to their designated ITU session.

Section B. Intrinsic atom economies of the main reaction classes

The methodology of the atom economy is well described in several texts⁷⁻⁹ and readily engages the students. They are already well versed in the themes of high yields and high selectivities, although our 2nd year class are unaware that certain synthetic pathways are intrinsically predisposed to the production of waste. This point is illustrated with the Wittig reaction,^{13a} Fig. 2.

The yield of 86%^{13a} shows this reaction to be highly efficient in converting a ketone to an alkene. However, what the yield calculation fails to take into account is the stoichiometric quantities of phosphine oxide by-product generated. Furthermore, the molecular weight of the phosphine oxide waste (278 g mol⁻¹) is almost three times that of the desired alkene product (96 g mol⁻¹). Consequently, the waste in this particular reaction is of significantly greater mass and volume than the actual product itself.^{6,8}

Trost's ideas of an atom economy are then highlighted⁷⁻⁹ and his award of a Presidential Green Chemistry Challenge in 1998 is noted. The % atom economy is defined by eqn. (1).

$$\% \text{ atom economy} = \frac{\text{formula weight of all atoms used}}{\text{formula weight of all reactants used}} \times \frac{100}{1} \quad (1)$$

Table 1 is presented which reveals the Wittig reaction to exhibit an atom economy of only 26%.

To illustrate the point that different reaction categories favour different atom economies, the sub-groups of each tutorial group are asked to examine a specific reaction type. Sub-Group 1 look

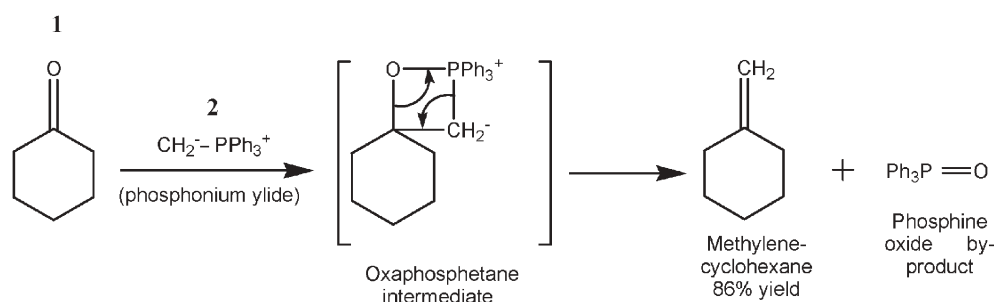


Fig. 2 A reaction scheme outlining the key steps of the Wittig reaction.^{13a}

Table 1 Atom economy for the Wittig reaction. The table is adapted from a format presented in reference,⁸ with permission from the American Chemical Society

Reactants		Utilised		Not utilised	
Formula	Formula mass/g mol ⁻¹	Formula	Formula mass/g mol ⁻¹	Formula	Formula mass/g mol ⁻¹
1 C ₆ H ₁₀ O	98	C ₆ H ₁₀	82	O	16
2 C ₁₉ H ₁₇ P	276	CH ₂	14	C ₁₈ H ₁₅ P	262
Total		Methylene-cyclohexane		Total	
C ₂₅ H ₂₇ PO	374	C ₇ H ₁₂	96	C ₁₈ H ₁₅ PO	278

% Atom economy = $96/374 \times 100 = 26\%$

at the bromination of cyclohexene,^{13b} Sub-Group 2 the ammonolysis of ethyl propionate with methylamine to yield methyl propionate^{14a} and Sub-Group 3 the dehydrohalogenation of 2-bromo-2-methyl-propane with sodium ethoxide to form isobutene.^{14a} A member of each sub-group then presents their results to the tutorial group using an overhead projector and a pre-prepared OHP acetate. They are required to describe the chemistry involved by means of (i) a reaction scheme, (ii) a table similar to Table 1 detailing the utilised and non-utilised components, (iii) the atom economy and (iv) the reaction type. They are encouraged to comment on the significance of their results and the tutor will gently question them on aspects of their presentation. Once all three presentations are complete, the tutor briefly summarises this Section of the ITU by noting the following atom economies: Sub-Group 1 (addition) 100%, Sub-Group 2 (substitution) 65% and Sub-Group 3 (elimination) 27%. The take home message from this section is that increased atom economy correlates with increased environmental friendliness.

Section C. Case study: the industrial synthesis of ibuprofen

Remaining in their sub-groups, the students move on to consider the industrial synthesis of the analgesic Ibuprofen. This is a popular example of successful green chemical practice, that has been comprehensively described in the literature.⁸ However, here the Ibuprofen tale is partitioned so that each sub-group has to understand a specific aspect of the associated chemistry. Then, in turn, each sub-group explains their individual aspect to the whole tutorial group. This structure and interplay between participating

students is a novel aspect of the ITU exercise. Sub-Group 1 concentrate on pharmacological aspects of Ibuprofen, Sub-Group 2 examine the original Boots synthesis of the drug, and Sub-Group 3 present aspects of the contemporary BHC Company synthesis.

All 3 sub-groups are given the size of the pharmaceuticals sector, with sales in 2000 exceeding £207 billion, illustrating the industry's contribution and importance to the global economy.¹⁵ Ibuprofen is the active ingredient in many analgesics and current production is in excess of 13 000 t a⁻¹.⁸ The students can identify popular brand names such as Nurofen, Brufen and Ibuleve, which incorporate Ibuprofen to provide their analgesic action. Additionally, they are informed that Ibuprofen is a member of the non-steroidal anti-inflammatory (NSAI) group of drugs, which combat swelling and inflammation.

Sub-Group 1 use Fig. 3(a) to demonstrate that the compound exerts its action through reversible competitive inhibition of the cyclo-oxygenase (COX) enzyme, which is active in the arachidonic acid cascade.¹⁶ This C₂₀ tetra-unsaturated fatty acid is an important precursor for a range of biologically important molecules. Inhibition of COX by Ibuprofen blocks the synthesis of cyclic endoperoxides and, consequently, prostaglandin derivatives.

Sub-Group 1 are also required to consider how the stereochemistry of Ibuprofen can affect its efficacy.¹⁷ Ibuprofen's success as a COX inhibitor depends on its ability to 'fit' into the enzyme's active site and, subsequently, to form compatible bonding interactions (mainly hydrophobic).¹⁸ The enantiomers of Ibuprofen are presented in Fig. 3(b). Given that there is the scope for enantiomers to display very different

properties *in vivo*,¹⁹ it may be surprising to learn that Ibuprofen is widely marketed as a mixture of the (*R*)- and (*S*)- forms, *i.e.* as the racemate.²⁰ Although only the (*S*)-enantiomer delivers the desired therapeutic action, the physiological enzyme *mandelate racemase* readily converts inactive (*R*)-Ibuprofen to the active enantiomorph.²⁰ Nevertheless, single (*S*)-enantiomer versions of Ibuprofen are currently being developed, with the benefits cited as a reduction in the required dose and a shorter time for therapeutic levels to be reached.²¹ Finally, Sub-Group 1 are expected to disseminate to the class the trend within the pharmaceutical industry towards the production of single enantiomer compounds.

Sub-Group 2 are presented with a reaction scheme for the six-step Boots synthesis of Ibuprofen.⁸ In a similar manner to that encountered in Section B, one member of the Group uses an overhead projector to (i) describe the chemistry involved by means of a reaction scheme, (ii) present a table detailing the utilised and non-utilised components and (iii) define the atom economy. The tutor would normally ask a few questions on aspects of the chemical steps of the overall synthesis, to ensure that the students have some appreciation of the underlying chemistry.

Sub-Group 3 are required to explain the intricacies of the BHC Company's synthesis of Ibuprofen.^{8,22} The 3 stage synthesis offers clear advantages to the traditional route and permits a discussion with the students of the benefits of catalysis (homogeneous and heterogeneous) in designing atom and economically efficient processes.

The second step in the BHC synthesis is the heterogeneously catalysed hydrogenation of 4-*isobutyl*acetophenone to 1-(4-*isobutylphenyl*)-ethanol.⁸ The students are asked to emphasize how the separation of the liquid reagents from the solid catalyst can be readily achieved by simple filtration, highlighting a major advantage of heterogeneous catalysis. The final step is the selective carbonylation to yield Ibuprofen, which is achieved using carbon monoxide in the presence of a soluble palladium catalyst complex, PdCl₂(PPh₃)₂, in an acidic medium.^{22,23} The students are not only asked to consider the advantages in selectivity

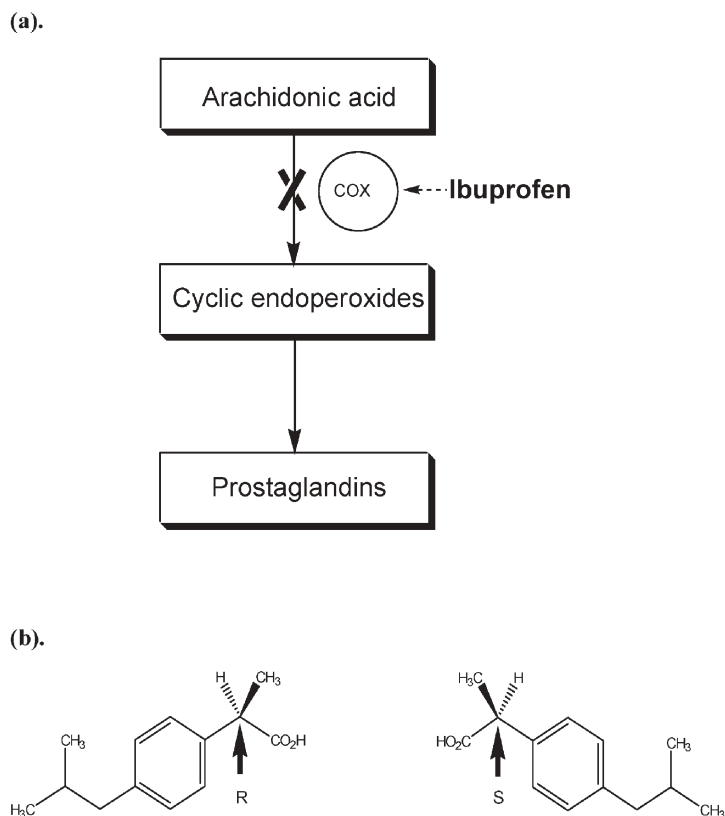


Fig. 3 (a). Schematic representation of how Ibuprofen inhibits the action of the cyclooxygenase enzyme (COX) by blocking the synthesis of cyclic endoperoxides and, in sequence, prostaglandin derivatives. The figure is adapted from reference¹⁶ with permission from John Wiley and Sons, Inc. (b). The *R*- and *S*-enantiomers of Ibuprofen.

that homogeneous catalysis can offer but also to realise that product–catalyst separation problems need to be overcome. In this case, Ibuprofen is removed from the reaction mixture by vacuum distillation.²²

By cutting the number of steps to three, all catalytic, the BHC synthesis has dramatically reduced waste quantities associated with Ibuprofen manufacture. Moreover, larger volumes of the drug can be produced in less time and with less capital expenditure.⁸ Therefore, as well as being environmentally superior to the traditional synthesis, the BHC route also offers more favourable production economics. The tutor summarises the main points from this section and acknowledges that innovative chemistry and process technology has dramatically reduced the environmental burden associated with the production of Ibuprofen. The BHC synthesis is now widely regarded as a benchmark for environmental and production efficiency within the pharmaceutical industry.²⁴

Section D. Poor atom economy in industry: catalysts for change

This is the last session where the sub-groups need to present an oral presentation to the tutorial group. It outlines a specific issue that has been explained in pre-prepared handouts. The theme of catalysis as an enabling technology for Green Chemistry is highlighted by consideration of the improvements catalysis offers to three bulk chemical manufacturing options.

Sub-Group 1 examine the industrial synthesis of ethylene oxide. They first describe the antiquated chlorohydrin process,^{25a,26} and evaluate the associated atom economy (23%). The heterogeneous catalytic process involving a silver based catalyst is described briefly, its atom economy evaluated (100%, as it is effectively an addition reaction) and compared with the older route. The tutor ensures that they appreciate the size of the market for ethylene oxide and have some understanding of its role as a chemical feedstock.^{25a}

The industrial synthesis of aniline is covered by Sub-Group 2. After presentations identifying market size and downstream uses for aniline,²⁵ the traditional Béchamp process is introduced.²⁷ The atom economy for this process is estimated at 35%. Catalytic hydrogenation is presented as the modern alternative, with the reaction occurring in the gas phase, typically over a sulfided nickel catalyst,^{25b} and providing a selectivity for aniline of >99%.^{25b} As with the Béchamp reduction, the catalytic hydrogenation of nitrobenzene proceeds through a series of intermediates. Although not accounting for dimeric intermediates, Fig. 4 outlines the catalytic hydrogenation pathway from nitrobenzene to aniline.²⁸ This process scores favourably, coming in with an atom economy of 72%. The atom economy increases to 100% if water is considered to be an innocuous by-product.

The situation for Sub-Group 3 is not as clear-cut as that encountered by the other two groups. Similarly, the students are asked to consider a traditional route for the manufacture of a commodity chemical, nitrobenzene,^{25b,29,30} but their alternative technology is speculative and not proven on the industrial scale.³¹ This scenario is intended to illustrate to the tutorial group that the replacement of old and dirty processes by new greener alternatives requires a substantial degree of development and financial investment, that will inevitably take time to implement for a large-scale operation.

Although the selected catalytic alternative is not a realistic alternative on the industrial scale at this time, it does represent innovative green chemistry applicable to a real problem. Chris Braddock's team at Imperial College, London have demonstrated that aromatic nitration, on a laboratory scale, can be effected using lanthanide(III) triflate catalysts.³¹ Utilising a ytterbium triflate ($\text{Yb}(\text{OTf})_3$) catalyst, the researchers have shown that nitrobenzene (>95% conversion) can be prepared according to Fig. 5.³¹ An atom economy of 87% is calculated, with water identified as the only by-product. Two main reasons are cited as to why the catalytic nitration (Fig. 5) represents a more efficient and environmentally friendly process than the classical route. Firstly, the only by-product formed is water and,

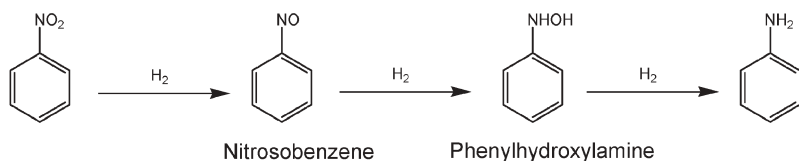


Fig. 4 The pathway for the hydrogenation of nitrobenzene to form aniline.²⁸

secondly, the catalyst is easily recovered and can be reused for further nitrations without any decrease in performance.³¹ Despite this considerable promise, the sub-group are asked to communicate the difficulties in applying this technology outside a laboratory environment.

Section E. Green chemistry principles

At this stage the tutor recombines the three sub-groups and guides the tutorial group in a discussion on the likely five most important guiding principles for Green Chemistry. The students are informed that several authors have examined this topic and their suggestions will be compared with the accepted wisdom in the plenary session. After a short discussion, one member of the tutorial group is elected to present the group's five principles to the whole class by means of an OHP acetate.

Following a timetable, all the tutorial groups reassemble in the main lecture theatre for the plenary session, where the representatives of the four tutorial groups outline their suggestions for the most important green chemistry principles. Somewhat reassuringly, the students invariably highlight topics as outlined by opinion formers such as Anastas and Warner⁶ In fact, given the relative simplicity of the exercise and the clarity of the message, the students regularly note their surprise on the youthfulness of the green chemistry movement, given the well established environmental burden commonly attributed to the chemical industry by the non-scientific media.

5. Coursework

As in all our ITU exercises, the coursework accounts for a generous 5% of the

year's total assessment. This ensures that the class take the exercise seriously and positively engage in the oral presentations and group discussions. A written scientific report is the favoured mode of assessment as this medium is a vital aspect of scientific communication but, regrettably, one that tends to be neglected in our junior classes, where the relatively large numbers can make essay marking arduous. A representative assessment would be one where the students are presented with Sheldon's E factors in the chemical industry³² that show, somewhat against undergraduate expectations, that the pharmaceutical industry produces more waste per kg of product than the oil refining, bulk chemicals and fine chemicals industries.³² The students are asked to write a report (*ca.* 1000 words) on approaches that could lead to a reduction in the pharmaceutical industry's excessive E factor. To broaden their exposure to relevant examples, the students are encouraged to read a recent review article by Anastas and Kirchoff entitled 'Origins, Current Status and Future Challenges of Green Chemistry'.³³

6. Student evaluation

The 3 hour ITU session ends with the students completing a short questionnaire that allows the ITU team to track the success of the general ITU exercise and, specifically, to evaluate the relative acceptance of each ITU package. Representative results from student evaluation of the 2003–2004 class are shown in Table 2.

Question 1 attempts to gauge indirectly the class's response to the ITU exercise. 71% see the chemicals

industry as providing the opportunity for a stimulating career. The magnitude of this positive response is encouraging given that, historically, a substantial proportion of the class tend to opt for life sciences-based courses in their 3rd year of study.

Question 2 asks the students to assess their knowledge of the atom economy, with 61% claiming either a 'good' or 'very good' knowledge of the topic. This is particularly reassuring, as the students had effectively no working knowledge of the concept prior to the ITU session. This number rises to 98% if one accepts an 'average' awareness as a positive outcome.

Question 3 shows a resounding 94% of the class claiming to have enjoyed participating in the ITU exercise. One acknowledges that the students may not describe the experience as 'fun' but, nevertheless, the informal approach and emphasis on small group exercises does seem to be well received by the student body.

Finally, Question 4 enquires whether the students would like to see more ITUs within their degree programme. 72% of the class responded favourably, which is broadly consistent with the responses to the preceding questions and demonstrates that the ITU format can offer a beneficial supplement to traditional teaching packages. The 27% of the class that were unsure, or who wished to see no further roles for ITU exercises in their teaching diet, are thought to represent a substantial body of the class who are uncomfortable with giving oral presentations to their classmates. This reluctance is understandable but should not be over-played, as it is important for career development that students acquire regular practice in written and spoken communication skills. The ITU format is a useful vehicle for achieving this objective, whilst also exposing the students to new chemistry in an unorthodox format.

7. Concluding remarks

Green Chemistry has come a long way since its probable inception in 1991.¹² In order to maintain the vitality of the initiative, it is crucial that undergraduate chemistry students are exposed to the concepts, aims and aspirations of the movement in the early stages of their

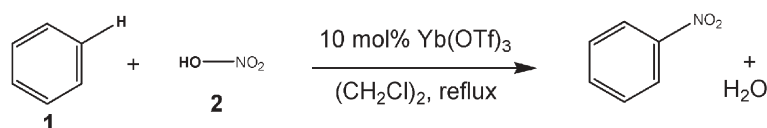


Fig. 5 A reaction scheme outlining the laboratory scale catalytic nitration of benzene.³¹

Table 2 Examples of student evaluation results. The sample relates to the response received from 90 students spread over three sessions in January 2004

Sample Evaluation Questions	Response				
	Strongly Agree	Agree	Not Sure	Disagree	Strongly Disagree
1. The interactive unit was designed to give you an insight into issues current within the chemical industry. Do you think that working within the chemical industry would provide you with a varied and stimulating career?	11 (12%)	53 (59%)	22 (24%)	4 (4%)	0 -
2. How would you rate your current understanding of the concept of atom economy?	Very Poor 0 -	Poor 2 (2%)	Average 33 (37%)	Good 48 (53%)	Very Good 7 (8%)
3. Did you enjoy participating in this exercise?	Yes 85 (94%)		No 5 (6%)		
4. Would you like to see more of these interactive teaching units as part of your degree programme?	Yes 65 (72%)		No 22 (24%)	Not Sure 3 (3%)	

university career. To this end, the materials selected and topics explored must be manageable and accessible to the student audience. The ITU package outlined here has operated in our second year undergraduate class for 3 years and has received strong support and endorsement from staff and students alike. Ideally, more elaborate exercises could be developed for our higher-grade classes, so that the students leave university with a firm grasp of the importance of sustainable products and processes. From February 2005, all four of the University of Glasgow ITU teaching packages will be available via the Education and Professional Development section of the Royal Society of Chemistry website (<http://www.rsc.org/lap/education/rsedhome.htm>).

Acknowledgements

The University of Glasgow Learning and Teaching Development Fund is thanked for the support of a research assistantship (SG). The assistance of the ITU team is gratefully acknowledged. Dr

Susan Armstrong, Dr John Dymond, Dr Richard Hartley, Mr Stephen Jones, Professor Pavel Kocovsky, Dr David MacNicol, Dr Andrei Malkov, Dr David Procter, Professor David Robbins and Dr David Rycroft have provided wonderful support as tutors. Mr Bob Munro, Mr Ted Eason and Mrs Kim Wilson have assisted with document preparation and Mrs Lesley Bell provided administrative support.

Steven Grant,^a Andrew A. Freer,^a John M. Winfield,^a Craig Gray^{†b} and David Lennon^{*a}

^aDepartment of Chemistry, Joseph Black Building, University of Glasgow, Glasgow, UK G13 8QQ. E-mail: d.lennon@chem.gla.ac.uk; Fax: +(44)-(0)-141-330-4888.; Tel: +(44)-(0)-141-330-4372

^bTeaching and Learning Service, Florentine House, 53 Hillhead Street, University of Glasgow, Glasgow, UK G12 8QQ

References

- 1 T. Platt, E. Barber, A. Yoshinaka and V. Roth, *Biochem. Mol. Biol. Educ.*, 2003, **31**, 132.
- 2 E. T. Washington, J. W. Tysinger, L. M. Snell and L. R. Palmer, *Medical Teacher*, 2003, **25**, 136.

- 3 D. Raine and J. Collett, *Eur. J. Phys.*, 2003, **24**, 541.
- 4 D. Lennon, A. A. Freer, J. M. Winfield, P. Landon and N. Reid, *Green Chem.*, 2002, **4**, 181.
- 5 S. Grant, A. A. Freer, J. M. Winfield, C. Gray, T. L. Overton and D. Lennon, *Green Chem.*, 2004, **6**, 25.
- 6 (a) P. T. Anastas and J. C. Warner, *Green Chemistry: Theory and Practice*, OUP, Oxford, 1998, pp. 29; (b) P. T. Anastas and J. C. Warner, *Green Chemistry: Theory and Practice*, OUP, Oxford, 1998, pp. 33.
- 7 B. M. Trost, *Science*, 1991, **254**, 1471.
- 8 M. C. Cann and M. E. Connelly, *Real-World Cases in Green Chemistry*, ACS, Washington, 2000.
- 9 M. A. Rouhi, *Chem. Eng.*, 1995, June 19, 32.
- 10 N. Winterton, *Green Chem.*, 2001, **3**, 73.
- 11 M. Lancaster, *Green Chem.*, 2000, **2**, 3, G65.
- 12 Green Chemistry Program Fact Sheet, <http://www.epa.gov/greenchemistry> (accessed Oct 2002).
- 13 (a) J. Clayden, N. Greeves, S. Warren and P. Wothers, *Organic Chemistry*, OUP, Oxford, 2001, p. 814; (b) J. Clayden, N. Greeves, S. Warren and P. Wothers, *Organic Chemistry*, OUP, Oxford, 2001, p. 515; (c) J. Clayden, N. Greeves, S. Warren and P. Wothers, *Organic Chemistry*, OUP, Oxford, 2001, p. 1220.
- 14 (a) R. J. Fessenden and J. S. Fessenden, *Fundamentals of Organic Chemistry*,

- Harper & Row, New York, 1990, p. 407; (b) R. J. Fessenden and J. S. Fessenden, *Fundamentals of Organic Chemistry*, Harper & Row, New York, 1990, p. 252.
- 15 S. C. Stinson, *Chem. Eng.*, 2000, Oct. 1, 79.
- 16 R. A. Nugent, *Kirk-Othmer Encyclopedia of Chemical Technology*, 4th edn, John Wiley, New York, 1991, **2**, p. 739.
- 17 A. A. Freer, J. M. Bunyan, N. Shankland and D. B. Sheen, *Acta Crystallogr., Sect. C*, 1993, **49**, 1378.
- 18 H. P. Rang and M. M. Dale, *Pharmacology*, Churchill Livingstone, Edinburgh, 1987, p. 204.
- 19 T. W. G. Solomons and G. B. Fryhle, *Organic Chemistry*, John Wiley, New York, 2000, p. 193.
- 20 D. T. Witiak, *Kirk-Othmer Encyclopedia of Chemical Technology*, 4th edn, John Wiley, New York, 1991, **18**, p. 511.
- 21 M. Strong, *Food Drug Law J.*, 1999, **54**, 463.
- 22 I. Kim, *Chem. Eng.*, 1997, **104**, 11, EC-64.
- 23 R. V. Chaudhari, A. Seayad and S. Jayasree, *Catal. Today*, 2001, **66**, 371.
- 24 I. Kim, *Chem. Eng.*, 1993, **100**, 12, 94.
- 25 (a) K. Weissermel and H.-J. Arpe, *Ind. Org. Chem.*, 3rd edn, Wiley-VCH, Weinheim, 1997, p. 143; (b) K. Weissermel and H.-J. Arpe, *Ind. Org. Chem.*, 3rd edn, Wiley-VCH, Weinheim, 1997, p. 373.
- 26 R. J. Fessenden and J. S. Fessenden, *Organic Chemistry*, 4th edn, Brooks/Cole, Pacific Grove, CA, 1990, p. 307, p. 420.
- 27 S. L. Schilling, *Kirk-Othmer Encyclopedia of Chemical Technology*, 4th edn, John Wiley, New York, 1991, **2**, p. 482.
- 28 L. R. Augustine, *Heterogeneous Catalysis for the Synthetic Chemist*, Marcel Dekker Inc., New York, 1996, p. 480.
- 29 R. L. Adkins, *Kirk-Othmer Encyclopedia of Chemical Technology*, 4th edn, John Wiley, New York, 1991, **17**, p. 133.
- 30 P. Y. Bruice, *Organic Chemistry*, Prentice-Hall, London, 2nd edn, 1998.
- 31 C. Braddock, *Green Chem.*, 2001, **3**, 2, G26.
- 32 R. A. Sheldon, *Pure Appl. Chem.*, 2000, **72**, 7, 1233.
- 33 Paul T. Anastas and Mary Kirchoff, *Acc. Chem. Res.*, 2002, **35**, 9, 686.

Crystallization and processing of carbohydrates using carbon dioxide

Poovathinthodiyil Raveendran,^{†*} Marc A. Blatchford, Michael L. Hurrey, Peter S. White and Scott L. Wallen*

Received 22nd November 2004, Accepted 11th January 2005

First published as an Advance Article on the web 26th January 2005

DOI: 10.1039/b417564f

In this work we demonstrate how CO₂ in the gaseous, liquid and supercritical states can be utilized in a wide range of industrially relevant processes, namely, crystallization, glassification, material processing of carbohydrates as well as the dispersion of biologically important macromolecules.

Non-toxicity, non-flammability, recyclability, ease of solvent removal, and readily tunable solvent parameters make gaseous, liquid, and supercritical (sc) CO₂ an excellent “green” alternative medium,^{1–5} for industrial applications involving biomaterials⁶ and pharmaceutical substances. Carbohydrates are an important class of inexpensive, abundant, and renewable biomaterials that have been the focus of recent research activity in a range of chemical, food and pharmaceutical applications as well as material science.^{7,8} The CO₂-phobic nature of these polyhydroxyl systems, however, makes them insoluble in liquid and scCO₂. In the past, we had shown that by replacing the hydroxyl groups with the CO₂-philic acetate groups, it is possible to make these compounds highly miscible with CO₂.^{9,10} Each acetate–CO₂ interaction provides a stabilization energy of $-2.82 \text{ kcal mol}^{-1}$ and this facilitates the solvation of acetylated carbohydrates in liquid and supercritical carbon dioxide.¹⁰ In this communication we present how CO₂ in the gaseous, liquid and supercritical states can be utilized in several processes namely, separation, crystallization, glassification, and processing of carbohydrates as well as in the dispersion of biologically important compounds, including proteins and pharmaceuticals, in these renewable systems.

One of the most direct and pharmaceutically important applications is the selective separation and controlled crystallization of carbohydrate-containing biomolecules from liquid and scCO₂. As a model system, we have performed the crystallization of 1,2,3,4,6-pentaacetyl β-D-galactose (BGAL). A 5 wt% scCO₂ solution ($P = 110 \text{ bar}$ and $T = 40.0 \text{ °C}$) of BGAL was prepared in a high pressure view cell. Slow expansion of the supercritical solution (SESS) through a capillary restrictor resulted in the nucleation and growth of relatively large, single crystals in sizes ranging from 0.1 mm–2 mm, and these were subsequently analyzed by X-ray diffraction. Although the crystal structure of BGAL has been recently reported,¹¹ we carried out further X-ray studies to investigate whether the crystals grown thus are sufficiently good for X-ray structure determination (scCO₂ being a highly diffusive solvent system) and to explore whether the structure from CO₂ is any different from those grown from other

solvents. To the best of our knowledge, this work represents the first controlled crystallization of a biomolecule from scCO₂ solution in which X-ray structure determination is possible. The structure[†] (Fig. 1) is found to be identical compared to those grown from conventional solvents. Extended networks of C–H···O hydrogen bonds (or short C–H···O contacts) are observed in the crystal (the dotted lines in Fig. 1b) and almost all the carbonyl groups and the methyl hydrogen atoms of the acetate groups are involved in C–H···O contacts. These relatively weak contacts collectively can make significant stabilization energy guiding the supramolecular assemblage of molecules in the crystal. We presume that such solute–solute C–H···O interactions are overcome by the solute–CO₂ interactions rather easily enabling their solvation in CO₂.^{9,10}

Sustainable methods in material processing are also quite challenging, especially in the preparation of nanoporous materials. Previous studies on the utilization of scCO₂ as a “green” solvent for material processing and CO₂-assisted impregnation of polymeric systems and biomaterials have been reviewed elsewhere.^{12–14} The preparation of carbohydrate based materials such as glasses and tubular materials with micro- and nanosized interior tubes, is also important due to their potential applications in biomedical engineering and nanotechnology. The preparation of carbohydrate glasses using CO₂ avoids the disadvantages associated with heating such as caramelization and those associated with freeze drying since all the processes can be performed at room temperature. Cyclodextrins,¹⁵ including their acetylated versions^{16,17} are of interest as potential components of many pharmaceutical preparations as sustained release carriers of drugs and biomolecules. We prepared a 2 wt% solution of peracetylated β-D-cyclodextrin

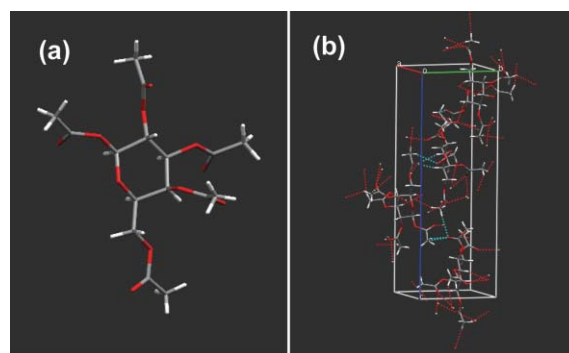


Fig. 1 (a) The crystal structure of BGAL. The crystals were grown by the slow expansion of a supercritical solution prepared by dissolving the solute in scCO₂ at 40.0 °C and 110 bar. (b) Packing of BGAL molecules in the unit cell (the blue dotted lines indicate the C–H···O contacts in the lattice.¹⁰

[†] Present address: Supercritical Fluid Research Center, National Institute for Advanced Industrial Science and Technology, 4-2-1, Nigatake, Miyagino-ku Sendai, 983-8551 Japan.

*ravi@ni.aist.go.jp (Poovathinthodiyil Raveendran)
wallen@email.unc.edu (Scott L. Wallen)

(Cerestar) at $P = 275$ bar and $T = 35.0$ °C. Rapid depressurization to ambient pressure yielded a CO₂-gel from which we could readily pull glassy fibers. An optical microscope photograph of a glass fiber pulled from the CO₂-gel is shown in Fig. 2A. The microscope image suggests that the glass fibers have several capillary pores or are layered. Examination of the microstructure of these glasses was performed using scanning electron microscopy (SEM). An SEM image showing the cross section of this glass fiber is presented in Fig. 2B.

The typical pore radii varied from 500 nm to several microns. Since the depressurized gel contains a significant amount of entrained CO₂, the majority of the fibers pulled from the CO₂ gel have micro- and nanosized tubular pores. It was possible to pull out cyclodextrin fibers having one metre length from the CO₂-melt suggesting a high CO₂-retention capacity of these systems.

These peracetylated cyclodextrins are hydrophobic in nature and are somewhat resistant to moisture suggesting potential biomedical applications. The same method can be applied in other polymeric acetates such as polyvinyl acetate, which melts in gaseous CO₂ around 45 bar at 25.0 °C.

Another important application of the deliquescence and high solubility of these carbohydrate derivatives in CO₂ is their use in the dispersion of enzymes and other biologically important molecules in sugar acetates using CO₂ as the dispersing medium. Carbohydrates generally represent one of the safe solid dispersion media for pharmaceuticals and CO₂ possesses many favorable properties as a dispersing solvent. The low critical temperature of CO₂ (31.1 °C) ensures the non-degradation of biomolecules and allows the processing of these materials in a non-toxic medium. Acetylated carbohydrates^{16,17} may easily be used with CO₂ as a medium for dispersing guest materials at relatively low

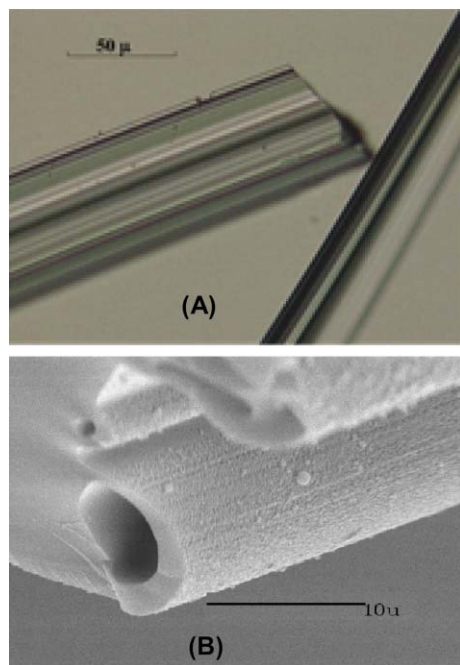


Fig. 2 Fibers of peracetylated β -D-cyclodextrin pulled from a CO₂ melt after rapid depressurization to ambient conditions. (A) Optical microscope image; (B) SEM image of the fiber cross-section revealing the micro- and nanosized pores.



Fig. 3 Photograph showing the dispersion of cytochrome-C in the CO₂-induced melt of BGLU at 55.9 bar pressure and 23.0 °C.

temperatures with respect to the normal melting temperatures of the carbohydrate systems. Both the solution method as well as the CO₂-induced melt method can be utilized for this purpose. As a proof of concept, we have prepared a dispersion of a protein, horse heart cytochrome-c (Sigma), in a glass forming system as well as a dispersion of a pharmaceutical, (*S*)-ibuprofen, in crystalline and glass forming systems using the CO₂-induced melt method. In the former case we added 2.0 grams of β -D-glucose pentaacetate (BGLU) and 0.010 g of cytochrome-c to a high pressure view cell and CO₂ was slowly pumped into the cell. At a pressure of 55.9 bar and a temperature of 23.0 °C, BGLU underwent deliquescence resulting in a thick fluid phase. Continuous stirring with a magnetic stirrer yielded a somewhat clear dispersion of cytochrome-c in the melted BGLU as shown in Fig. 3. On rapid depressurization we obtained a glassy solid of BGLU with cytochrome-c dispersed in the sugar acetate.

In the case of (*S*)-ibuprofen, it is possible to dissolve the drug in either a crystal forming (BGAL) or a glass forming (sucrose octaacetate (SOA)) sugar acetate melt induced by contact with CO₂. The dispersions were prepared by adding 2.0 g of the sugar acetate and 0.050 g of ibuprofen to a high pressure view cell. CO₂ was added until the liquid-vapor equilibrium pressure was reached at 25.0 °C and then the cell was filled to approximately 0.75 of its volume. The system was stirred for 10 minutes, rapidly depressurized, and the solid was collected. Optical spectroscopic studies revealed that these dispersions are very homogeneous. While the guest molecular systems we studied do not have any considerable solubility in scCO₂, they are miscible with the CO₂-gel of the carbohydrate systems upon vigorous stirring.

In summary, we have shown that CO₂ can be used as a medium for processing carbohydrates that are CO₂-philized by acetylation. We have demonstrated the growth of defect-free single crystals of acetylated carbohydrates, preparation of mesoporous materials and the dispersion of biomolecules in acetylated sugars using CO₂. The results indicate that the CO₂ offers a “green” technology platform for processing renewable materials.

Acknowledgements

We acknowledge partial financial support from the STC Program of the National Science Foundation under

Agreement No. CHE-9876674, the Department of Education GAANN Fellowship, Pfizer Analytical Graduate Fellowship and the UNC Chemistry Department Morrison Fellowship (M.A.B.) and a generous gift from Merck & Co., Inc.

Poovathinthodiyil Raveendran,^{†*} Marc A. Blatchford, Michael L. Hurrey, Peter S. White and Scott L. Wallen*
Department of Chemistry and NSF STC for Environmentally Responsible Solvents and Processes, The University of North Carolina, Chapel Hill, North Carolina 27599-3290, USA.
E-mail: ravi@ni.aist.go.jp; wallen@email.unc.edu

Notes and references

[†] A single crystal (*ca.* 0.2 × 0.2 × 0.4 mm) of BGAL grown from scCO₂ solution was selected for X-ray structure determination [Orthorhombic, space group *P*2₁2₁2₁, *a* = 8.3930(3), *b* = 9.0538(3), *c* = 25.4777(9) Å, *V* = 1936.01 Å³, *Z* = 4].

- 1 C. A. Eckert, B. L. Knutson and P. G. Debenedetti, *Nature*, 1996, **373**, 313.
- 2 J. M. DeSimone, Z. Guan and C. S. Elsbernd, *Science*, 1992, **267**, 945.
- 3 K. P. Johnston, K. L. Harrison, M. J. Clarke, S. M. Howdle, M. P. Heitz, F. V. Bright, C. Carlier and T. W. Randolph, *Science*, 1996, **271**, 624.
- 4 T. Sarbu, T. Styranec and E. J. Beckman, *Nature*, 2000, **405**, 165.
- 5 M. Ji, X. Y. Chen, C. M. Wai and J. L. Fulton, *J. Am. Chem. Soc.*, 1999, **121**, 2631.
- 6 B. Subramanian, R. A. Rajewski and K. Snavely, *J. Pharm. Sci.*, 1997, **86**, 885.
- 7 P. Collins and R. Ferrier, *Polysaccharides: Their Chemistry*, Wiley, Chichester, 1995, 478.
- 8 R. A. Cross and B. Kalra, *Science*, 2002, **297**, 803.
- 9 P. Raveendran and S. L. Wallen, *J. Am. Chem. Soc.*, 2002, **124**, 7274.
- 10 P. Raveendran and S. L. Wallen, *J. Am. Chem. Soc.*, 2002, **124**, 12590.
- 11 D. P. Thibodeaux, G. P. Johnson, E. D. Stevens and A. D. French, *Carbohydr. Res.*, 2002, **337**, 2301.
- 12 A. I. Cooper, *Adv. Mater.*, 2001, **13**, 1111.
- 13 D. L. Tomasko, H. Li, D. Liu, X. Han, M. J. Wingert, L. J. Lee and K. W. Koelling, *Ind. Eng. Chem. Res.*, 2003, **42**, 6431.
- 14 H. M. Woods, M. M. C. G. Silva, C. Nouvel, K. M. Shakesheff and S. M. Howdle, *J. Mater. Chem.*, 2004, **14**, 1663.
- 15 A. R. Hedges, *Chem. Rev.*, 1998, **98**, 2035.
- 16 K. Uekama, T. Horikawa, M. Yamanaka and F. Hirayama, *J. Pharm. Pharmacol.*, 1994, **46**, 714.
- 17 F. Hirayama, M. Yamanaka, T. Horikawa and K. Uekama, *Chem. Pharm. Bull.*, 1995, **43**, 130.

The current status of fuel cell technology for mobile and stationary applications

Frank de Bruijn

Received 4th October 2004, Accepted 10th January 2005

First published as an Advance Article on the web 10th February 2005

DOI: 10.1039/b415317k

This review of fuel cell technology gives an overview on the status of low and high temperature fuel cells, both on materials and component level as well as on a system level. Their application in transport and the combined generation of heat and power is discussed in relation to their environmental benefits.

1. Introduction

Fuel cells are generally considered as a clean, efficient and silent technology that can produce electricity and heat from fossil fuels, biofuels as well as hydrogen produced from renewable energy sources such as wind energy and solar energy. The expectations with respect to their commercial introduction in transport as early as 2003^{1–3} and stationary applications by 2001^{1,4,5} held since the mid 1990s have not yet been realised. The main hurdles preventing commercial introduction still are too high cost, lack of durability, too high system complexity and a lack of fuel infrastructure. To better understand the issues to be discussed in this review on fuel cells, the basic principles of fuel cells are explained in this introduction.

1.1. Fuel cell principle and fuel cell types

The basic principle of the fuel cell is illustrated in Fig. 1. The core of each fuel cell consists of an electrolyte and two electrodes. At the negative anode, a fuel such as hydrogen is being oxidized, while at the positive cathode, oxygen is reduced. Ions are transported through the electrolyte from one side to the other. The type of electrolyte determines the temperature window of operation. This window of operation in its turn determines the catalyst that can be used, and the purity of the fuel to be used. At open circuit, the voltage of a

hydrogen–oxygen fuel cell is 1.23 V at 298 K. Under load conditions, the cell voltage is between 0.5 and 1 V.

Six types of fuel cells have evolved in the past decades. A brief summary of these six fuel cell types is given below. This review focuses on the PEMFC and SOFC, as worldwide the most research and development is performed on these two fuel cells.

Alkaline fuel cell, AFC. The electrolyte of the AFC consists of liquid potassium hydroxide. The operating temperature is around 80 °C, but can be as high as 200 °C. The AFC is currently being used for power generation on spacecrafts. The use of AFC's is limited because practically only pure hydrogen can be used as fuel. Air needs to be cleaned from CO₂, which limits the application for terrestrial applications considerably. The power density of the AFC is in the range of 0.1–0.3 W cm⁻². Alkaline fuel cells are especially available in the kW range.

Proton exchange membrane fuel cell, PEMFC. The electrolyte of the PEMFC consists of a cation-exchange membrane. The operating temperature is around 80 °C. Cold start, below 0 °C, is possible. For transport applications, the PEMFC is the fuel cell of choice. For stationary applications, PEM fuel cells are developed as well. The PEMFC is rather sensitive towards impurities in the fuel. The power density of the PEMFC is in the range of 0.35–0.7 W cm⁻². PEM fuel cells are in development in the 1 W to 250 kW range.

Direct methanol fuel cell, DMFC. The direct methanol fuel cell is a variation of the PEMFC; it uses the same type of



Frank de Bruijn, born in 1966, is leading the Fuel Cell Technology unit at the Energy research Centre of the Netherlands. He studied electrochemistry in Utrecht and received his PhD in Chemical Engineering in Eindhoven. In 1996, he joined ECN where he worked on Fuel Cells and Applied Catalysis. At ECN, more than 50 people are working on the research and development of materials and components for fuel cell systems and on system integration.

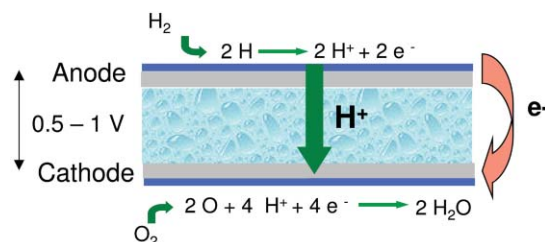


Fig. 1 Basic principle of a fuel cell, for the case where a proton-conducting electrolyte is used as separator.

electrolyte. Instead of using hydrogen as fuel, a solution of methanol in water is directly oxidized to CO_2 . The power density of the DMFC is considerably lower than that of the PEMFC. Maximum power densities, 0.25 W cm^{-2} are obtained at a cell voltage as low as $0.2\text{--}0.3 \text{ V}$.^{6,7} Compared to the PEMFC, high noble metal loadings are used,⁶ 1.2 mg cm^{-2} or higher.⁷ The DMFC is in development mainly for portable applications in the $1\text{--}100 \text{ W}$ range. The high energy density of methanol offers a potential to replace batteries with micro fuel cell systems.

Phosphoric acid fuel cell, PAFC. Liquid phosphoric acid is the electrolyte of the PAFC. The operating temperature is around $200 \text{ }^\circ\text{C}$. The PAFC can use reformat with CO concentrations up to $1\text{--}2\%$. Commercially the most successful fuel cell at this moment, in 2003, 245 of the 200 kW systems have already been installed.⁸ The power density of the PAFC is in the range of 0.14 W cm^{-2} .

Molten carbonate fuel cell, MCFC. A molten mixture of lithium, sodium and potassium carbonate is used as the electrolyte in the MCFC. The operating temperature is between 600 and $700 \text{ }^\circ\text{C}$. Due to the high operating temperature, internal reforming of hydrocarbon fuels is possible. The power density of the MCFC is in the range of $0.1\text{--}0.12 \text{ W cm}^{-2}$. The power of MCFC systems is in the 50 kW to 5 MW range.

Solid oxide fuel cell, SOFC. Yttrium stabilised zirconia is generally used as the solid electrolyte in the SOFC. Depending on the electrolyte and the material composition of the electrodes, the SOFC can be operated between $600 \text{ }^\circ\text{C}$ and $1000 \text{ }^\circ\text{C}$. Fuels ranging from hydrogen to natural gas and higher hydrocarbons can be used. The SOFC is mainly in development for stationary power generation for systems in the 1 kW to 5 MW range. However, it is also considered an important option for auxiliary power units on board of vehicles in the 5 kW range. The power density of the SOFC is in the range of $0.15\text{--}0.7 \text{ W cm}^{-2}$.

1.2. Fuel cell setup: from single cell to systems

Single cell. Besides conducting ions from one electrode to the other, the electrolyte serves as gas separator and electronic insulator. The electrodes are the sites at which the electrochemical reactions take place. Besides containing the suitable catalysts, the electrode architecture should be such that transport of reactants to and products from the catalyst–electrolyte interface is taking place at the maximum possible rate.

A single fuel cell, as displayed in Fig. 2, produces the power, which results from the area \times the current density of the cell \times the cell voltage. The typical cell voltage under load conditions amounts to 0.7 V , which is too low for practical applications.

Stacks. It is therefore common practice to put a number of cells in series, resulting in a so-called fuel cell stack. Flow plates connect two adjacent cells. These flow plates, also called separator plates or bipolar plates when a single plate is used

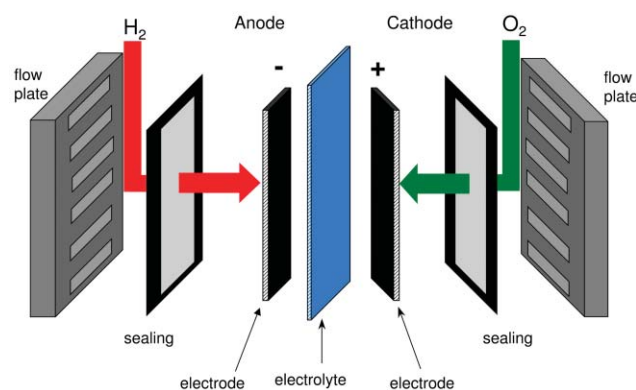


Fig. 2 Fuel cell components of a single cell.

for the anode side of one cell and for the cathode side of the other cell, should have a high electronic conductance, and should act as a gas separator between the two adjacent cells. The flow plates contain flow patterns on the cell side to generate an even distribution of reactants across the cell area. On the backside, cooling liquid flow patterns transport the heat to a heat exchanger in the system. The stack power and voltage is obtained by the number of cells \times the individual cell power and voltage. A three-cell stack is schematically drawn in Fig. 3. Besides the repeating units displayed in Fig. 2, a stack contains two endplates and two current collector plates from which the current is collected.

Systems. The fuel cell is the core of each fuel cell system, but it does need a number of additional components to make it operate and to let it carry out its function in its application. Fig. 4 gives a schematic, simplified display of a typical fuel cell system. The components other than the fuel cell stack and the fuel processor are often called balance of plant components. Both with respect to system cost, as well as to system efficiency and durability, these balance of plant components play an important role.

In low temperature fuel cells, except the DMFC, hydrogen is oxidized at the anode to protons. The hydrogen can either be fed from a hydrogen storage container, or produced from another fuel in a so-called fuel processor. Generally, hydrocarbons or alcohols are used as fuels to feed fuel processors. The complexity of the fuel processing depends strongly on the fuel cell type and the primary fuel. In high temperature fuel

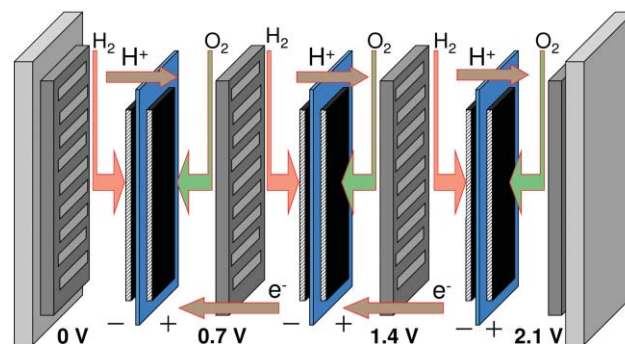


Fig. 3 Schematic, simplified overview of a fuel cell stack.

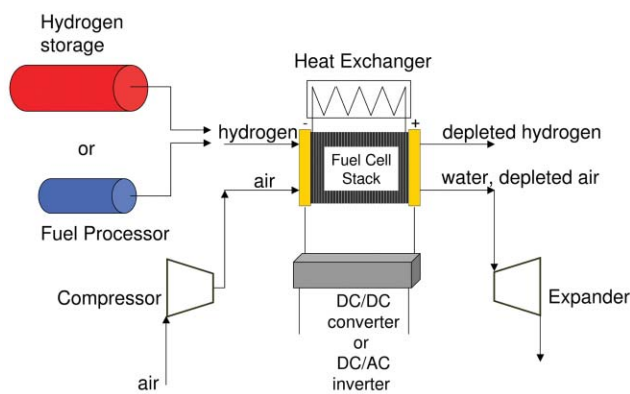


Fig. 4 Schematic, simplified overview of a PEM fuel cell system.

cells, such as the MCFC and SOFC, fuel processing can be done in the fuel cell itself. This process is referred to as internal reforming. In section 4 fuel processing will be further discussed.

The air pressure needs to be elevated from ambient pressure up to a level, which depends on the operation pressure and the pressure drop in the complete system. This can range from a gauge pressure of 100 mbar to several bars. The power of the fuel cell stack generally increases with increasing pressure; the parasitic loss of the compression however increases as well.

The voltage of the fuel cell stack is the product of the number of cells \times the individual cell voltage, which is typically 0.6–0.7 V DC. For mobile applications, the voltage should be increased to several hundred Volts and conditioned to the needs of the electric motor. For stationary applications, generally AC voltage is needed, which requires a DC/AC inverter.

1.3. System efficiency

The efficiency of the fuel cell stack (Eff_{FC}), the hydrogen production (Eff_{H_2}), the utilization of the hydrogen ($Util_{H_2}$) and power consumed by the balance of plant components ($Power_{BOC}$) determine the total system efficiency:

$$Eff_{el, sys} = Eff_{H_2} \times Eff_{FC} \times Util_{H_2} \times (1 - (Power_{BOC}/Power_{Fuel\ cell\ system}))$$

In all cases, the full fuel to electricity chain efficiency should be considered, and not only the efficiency of the fuel cell system itself. Especially the production and transportation of hydrogen can cause considerable loss of energy before the hydrogen is converted in the fuel cell system.

The fuel cell efficiency for hydrogen–oxygen fuel cells, based on the higher heating value of hydrogen, which is 142 MJ kg^{-1} , can be obtained by dividing the cell voltage at operation by 1.48 V. The maximum theoretical efficiency of a hydrogen–oxygen fuel cell at 298 K and atmospheric pressure is $1.23/1.48 = 0.83$.⁹ Hydrogen–oxygen fuel cells operated at 0.7 V thus have an electrical efficiency of 0.47. Often, efficiencies in literature are referred to as Lower Heating Value (LHV) efficiencies. As the Lower Heating Value of hydrogen amounts to 120 MJ kg^{-1} , these LHV efficiencies are 1.18 times higher than the HHV efficiency.¹⁰

2. Current status of PEM fuel cells

The Proton Exchange Membrane Fuel Cell (PEMFC) is the most widely used fuel cell in transport applications. Since 2000, more than 90% of all fuel cell vehicles on the road have been equipped with a PEMFC.¹¹ The low temperature of operation and its high power density both at its operating temperature as well as during start-up, make it the most suitable fuel cell for transport applications.

The large research and development efforts put into the PEMFC, combined with the potentially large production volumes and low cost targets associated with the automotive markets, have made the PEMFC an attractive candidate for application in stationary applications as well.

2.1 Electrolytic membranes

The vast majority of PEMFCs use a perfluorosulfonic acid–tetrafluoroethylene copolymer as membrane material. Membranes in PEM fuel cells nowadays have a thickness between 30 μm and 100 μm , depending on whether they are reinforced or not. The main supplier of the non-reinforced membranes is Dupont, selling the perfluorosulfonic acid membrane under the trade name Nafion.¹² It can be operated at temperatures between 0 and 80–90 $^{\circ}\text{C}$, depending on the cell pressure. Dehydration of this type of membrane has to be prevented, as its conductivity, typically 0.1 S cm^{-1} at normal operating conditions, dramatically decreases when its water content drops below full saturation.¹³ The requirement for full hydration of the membrane leads to a fuel cell system operation with very complicated water and heat management, especially at low operating pressures.¹⁴

All PEM fuel cells in commercial development use this membrane or one of its analogues. One of these analogues is the Aciplex membrane, commercialized by Asahi Chemical. Reinforced membranes are commercialized by Gore, and consist of a porous polytetrafluoroethylene (PTFE) matrix, the pores of which are filled with a Nafion-type electrolyte.^{15,16} The benefit of this composite membrane concept is that the thickness of the membrane can be very small, typically 30 μm or even less, due to the strength of the PTFE matrix. Thin membranes have a very low resistance¹⁵ and it is much easier to keep them hydrated than a thick membrane.

Alternative membranes for the PEMFC have been developed initially mainly for reasons of lower cost. All membranes used for PEM fuel cells to be operated at temperatures below 100 $^{\circ}\text{C}$, contain sulfonic acid groups for proton conduction. A few examples are sulfonated polyether-sulfone,^{17,18} sulfonated polyetheretherketone¹⁹ and sulfonated α,β,β -trifluorostyrene.^{18,20} It has proven to be difficult to develop cheaper alternatives that can meet the requirements on durability.^{21,22} Peroxy radicals formed in the oxygen reduction reaction make most polymers with C–H bonds susceptible to degradation. The fully fluorinated Nafion membrane or its analogues can stand this harsh environment for a long time, although some fluoride is lost.¹² Modifications of Nafion can lead to lower fluoride losses.¹²

Two important factors have led to an increase in research and development effort towards high temperature (120–180 $^{\circ}\text{C}$) proton conducting membranes: too low CO tolerance and

poor heat transfer on a system level associated with the PEMFC being operated at temperatures between 70 and 80 °C.

CO tolerance means that low concentrations of CO in the fuel cell feed does not lead to an extreme loss in fuel cell performance. In the state-of-the-art PEMFC, a CO level of 10 ppm leads to a loss in fuel cell power of 20–50%, depending on the type of catalyst being used at the anode, and the conditions with respect to fuel humidity and pressure. Complete removal of CO in the fuel processor is only effective in the complete absence of CO₂, as the reverse water gas shift reaction between CO₂ and H₂ leads to formation of CO and water.²³

Much work has been devoted to the use of phosphoric acid doped polybenzimidazole (PBI) membranes, which can be operated at a temperature between 125 °C and 200 °C.²⁴ This is immediately the drawback of this type of membrane: the proton conductivity at temperatures below 100 °C is too low, such that the cold-start properties of the classic PEMFC are lost.

The benefit of fuel cell operation at temperatures above 100 °C with respect to CO tolerance is demonstrated by Li *et al.*²⁵ The use of phosphoric acid doped PBI enabled them to investigate the influence of temperature on the CO tolerance of the PEMFC in the temperature range between 125 °C and 200 °C. Even when using unalloyed platinum catalysts, the effect of CO is very limited. At 125 °C, the effect of 1000 ppm CO is already minor. At 200 °C, 3% CO can be tolerated with a very small drop in performance. The power output at 200 °C is around 0.5 W cm⁻², at 125 °C it is less than 0.25 W cm⁻². Compared to a Nafion based PEMFC, this means that while at 200 °C power density is satisfactory, at temperatures below 125 °C it is too low for practical application.

Extensive reviews of alternative membranes under development for high temperature operation have been published by Savogado²⁶ and Li *et al.*²⁷ It should be noted that it will take a long time before alternative membranes will be used in practical fuel cell systems which have comparable performance and proven endurance compared to Nafion based fuel cell systems.

The high cost of the perfluorosulfonic acid–tetrafluoroethylene copolymer membranes has been the driving force for the development of cheap alternatives. The cost level of these Nafion membranes used to be in the order of \$800 m⁻².²⁸ Developers of alternative membranes were aiming at a cost level of \$30–50 m⁻².^{28,29} Probably, the development of cheap alternatives for Nafion has been frustrated by the forecast that the cost level of Nafion would drop when the markets would demand it to \$50 m⁻².^{22,30} At a cell power density of 0.5 W cm⁻², and an active area/total area ratio of 80%, a cost level of \$50 m⁻² corresponds to \$12.5 kW⁻¹.

2.2. Catalysts and electrodes

Only platinum based catalysts have sufficient activity in the 80–100 °C temperature range to meet power density targets set for mobile and stationary applications. 20–40 wt% Noble metal catalysts are commonly used. Electrode layer thickness amounts to 10 μm, in order to minimize the transport resistance for reactants and protons.³¹

For the anode, the composition depends on the fuel being used. When hydrogen is used with CO levels below the ppm range and with CO₂ levels not exceeding the percentage level, platinum on carbon suffices. Noble metal content at the anode is typically 0.2 mg per cm² active cell area. Even lower noble metal contents have been reported.^{32,33} Lowering the platinum loading at the anode to 0.05 mg cm⁻² does lead to a negligible reduction in cell power density.³³ Using such a low anode loading would result in platinum usage for the anode of 0.08 g Pt kW⁻¹.

When reformed hydrocarbons, alcohols or ethers are being used as hydrogen fuel, CO levels of 10 ppm and higher are commonly present, as well as CO₂. Platinum catalysts are severely poisoned by CO. PtRu and PtMo show superior tolerance towards CO compared to unalloyed Pt.³⁴ In addition, CO₂ present in the reformat in concentrations of 10–25%, leads to CO by the so-called reversed water gas shift reaction.³⁵ Thermodynamically, a 3 : 1 H₂ : CO₂ mixture at the PEM fuel cell operating conditions is in equilibrium with 25 ppm CO or higher, depending on the water content, pressure and temperature.²³

The formation of CO from CO₂ and its effect can be mitigated by alloying platinum with ruthenium.²³ However, the power density on pure or nitrogen-diluted hydrogen cannot be matched as long as CO is part of the fuel. This leads generally to lower fuel cell efficiency and to higher noble metal contents. The negative impact of carbon monoxide can in many systems be mitigated by dosing a small amount of air, typically 2%,³⁶ to the reformat stream. By this, the CO is oxidized to CO₂, which at the same concentration level has a much smaller impact on the fuel cell performance than CO.³⁷ With respect to the noble metal loading under reformat conditions, a minimum of 0.2 mg cm⁻² gives acceptable performance when 2% air bleeding is applied in the presence of 100 ppm CO. Lower noble metal loadings lead to an extra voltage loss of 0.2 V.³²

PEM fuel cells using electrodes containing 0.18 mg cm⁻² Ru and 0.02 mg cm⁻² Pt have been reported to give an acceptable power density of 0.3 W cm⁻² both on hydrogen as well on hydrogen with 50 ppm CO with an air bleed. The durability of the fuel cell using these low noble metal loadings is promising, but needs further improvement.³³ State-of-the-art PtRu anodes would result in 0.3 g PtRu kW⁻¹, at 1 A cm⁻² at 0.65 V. Note that the air-bleed will result in a lower fuel cell efficiency, as the air not used for CO oxidation will lead to the non-electrochemical oxidation of hydrogen.

At the cathode, platinum on carbon is used. Platinum alloys are under investigation, as especially PtCr shows improved performance.³⁸ The gains are however minor, and up till now fuel cell stacks generally do not make use of cathode catalysts other than unalloyed platinum. The noble metal content amounts to 0.2–0.4 mg cm⁻². To prevent voltage losses at the cathode, electrode optimization is important, to prevent mass transport limitation of oxygen. Inefficient removal of product water has an extremely strong influence on the fuel cell performance as it can completely block the transport of oxygen to the reaction interface.³⁹ When an optimized electrode structure is used, 0.2 mg cm⁻² Pt gives acceptable PEMFC performance, resulting in 0.32 g Pt kW⁻¹.³²

For hydrogen–air systems, noble metal loading could be as low as 0.4 g Pt kWe⁻¹. For reformat–air systems the noble metal loading would increase to 0.3 g PtRu and 0.3 g Pt kWe⁻¹. These required noble metal loadings are based on short-term performance measurements and not on full life endurance tests. Especially contaminants in reformat systems can lead to catalyst poisoning. Higher noble metal loadings can in the case of poisoning extend fuel cell life considerably.

Noble metal usage in the fuel cell stack at low noble metal loading amounts to \$10 kWe⁻¹ for hydrogen systems and \$15 kWe⁻¹ for reformat systems, using \$25 per gram of noble metal. Catalyst and electrode manufacturing cost will lead to additional costs. Due to the relatively high noble metal loadings of 20–40 wt%, these additional costs are expected to be relatively insignificant.

2.3 Flow plates

The component which has the highest impact on the weight and volume of the fuel cell stack, is the flow plate. Whereas the flow plates used to be made from high-density graphite, nowadays the material of choice is a mouldable graphite–polymer composite material. Although the latter has a somewhat lower conductivity, it enables due to its higher mechanical strength and its higher flexibility the use of plates with lower thickness than when using pure graphite plates. This directly leads to reduction of stack weight and volume. A major advantage of polymer–graphite plates is the fact that they can be manufactured by means of injection moulding.⁴⁰

An alternative to graphite and polymer–graphite material plates are metal plates.^{41–43} The main advantage of metal plates is the fact that very thin metal sheets can be used, and mass manufacturing techniques are available for forming flow patterns in these sheets. The power density of stacks based on metal bipolar plates has been demonstrated to be as high as 1.6 kW l⁻¹.⁴⁴ To resist the corrosive environment of the PEMFC, either a special stainless steel alloy,^{41,44} or coated plates^{44,45} have to be used.

For very large quantities, the manufacturing procedure for steel plates, being stamping, could be cheaper than the moulding procedure. It could very well be that the power density requested by automotive applications, combined with its relatively short operating lifetime of typically 3000–5000 hours for passenger cars, leads to the use of metal plates in automotive fuel cells. In stationary applications, where operating lifetime should exceed 40 000 hours, and where a high power density is not as stringent as in automotive applications, it is more likely that mouldable flow plates will be preferred.

Moulded graphite–polymer composite plates can in large quantities be manufactured at a cost of €1.4 per plate of 625 cm²,⁴⁶ or €0.7 per plate of 200 cm²,⁴⁰ corresponding to approximately €8–12 kW⁻¹, at a cell power density of 0.5 W cm⁻².

Graphite–polymer bipolar plate costs calculated in the DoE Hydrogen and Fuel Cell Program add up to \$46 m⁻², corresponding to \$18 kWe⁻¹ at 0.5 W cm⁻².⁴⁷

For metal plates, costs are calculated in the DoE program to amount to \$117–\$171 m⁻², corresponding to \$45–\$67 kWe⁻¹

depending on whether SS316 or SS904L is used as base material.⁴⁷ Probably these figures for metal plates are over-estimated, as in the first place the plate thickness assumed is 1 mm, where it can be as thin as 0.1–0.25 mm. Second, the coating costs are assumed to cause more than 50% of the total plate costs, \$63 m⁻², leaving much room for further cost reduction.

2.4 PEMFC—state of the art performance

Table 1 summarizes the state-of-the-art performance of PEM fuel cells under different conditions. Cell power densities of 0.5 W cm⁻² at a cell voltage of 0.7 V can be regarded as state-of-the-art for PEM fuel cells operated at temperatures of 80 °C and lower, at a pressure of 1.5 bar g. Lower pressures render lower power densities.

PEMFC stacks have been developed for both transport as well as stationary applications. In the case of transport, the design is focused on integrating the fuel cell stack into passenger vehicles, such that a stack producing typically 70 kW or more fits in the floor or under the hood of the car. The power density of these stacks is typically above 1 kW l⁻¹, when operated on hydrogen at a pressure of 1 to 2 bar g and 80 °C.^{44,51,52} Table 2 gives an overview of state-of-the-art stack performance levels.

Stack technology has been improved considerably during the past decade. Whereas in the early 1990s stack power density was 0.2 kW l⁻¹,^{54,55} nowadays stack power densities over 1.5 kW l⁻¹ are realized by several companies.

The power density of fuel cell stacks developed for automotive applications and operated on hydrogen is significantly

Table 1 PEMFC state-of-the-art performance under various conditions. For materials used, see cited reference. All cases refer to humidified conditions, and an operating temperature of maximally 80 °C

	Cell power density/W cm ⁻² at 0.7 V _{cell}	Company	Ref
H ₂ –O ₂ , 0.5 bar g	0.84	Johnson Matthey	48
H ₂ –air ambient pressure	0.56	UTC Fuel Cells	49
	0.35	Umicore	15
H ₂ –air, 0.5 bar g	0.42	Johnson Matthey	48
H ₂ –air, 1.5 bar g	0.5	General Motors	32
	0.7	Gore	50
Reformat + air bleed–air 1.5 bar g	0.5	General Motors	32

Table 2 PEMFC stacks for automotive (a) and stationary (s) applications

	Ref	Power/kW	Power density		Conditions
			kW l ⁻¹	kW kg ⁻¹	
Ballard Mark 902 (a)	51	85	1.13	0.88	H ₂ –air; 1–2 bar g; 80 °C
GM HydroGen 3 (a)	52	94	1.60	0.94	H ₂ –air; 1.5 bar g; 80 °C
Regenesys (s)	44	15	1.54	0.33	H ₂ –air; 2 bar g; 65 °C
Teledyne NG1000 (s)	53	1.7	0.20	—	Ref–air; 0.4 bar g

larger than those developed for stationary applications. First, stationary systems are generally operated and designed for lower pressures, below 0.5 bar g. Second, stationary systems are operated on natural gas reformat with hydrogen concentration between 40–75%, depending on the reformer technology used. Third, efficiency requirements are more important and volume requirements less stringent than for automotive applications, so cells are operated at higher cell voltage and lower power density. Especially for micro combined heat and power systems of 1–5 kWe, the end plates, current collector plates and tie rods make a relatively large contribution to the total stack volume and weight.

2.5. PEMFC durability

When accepting a maximum efficiency loss of 10%, *i.e.* a voltage drop of 70 mV from 0.7 V to 0.63 V over the total lifetime of the stack, the degradation rate for stationary systems should be less than $1.7 \mu\text{V h}^{-1}$, assuming 40 000 hours for the lifetime. For transport systems, where 5000 hours lifetime is taken for passenger cars, the maximum degradation rate should be less than $14 \mu\text{V h}^{-1}$. Due to the voltage loss, electrical efficiency will degrade and more heat will be released. In the case of combined heat and power (CHP) generation, the heat can be used. In transport applications, cooling problems have to be anticipated when degradation becomes too significant.

Both the electrodes as well as the proton conducting membrane are susceptible to ageing effects that will lead to performance loss of the PEMFC during its operating life. Performance loss can occur both in operation as well as when residing at rest.⁵⁶ The proton-conducting polymer, present in the membrane as well as in the electrodes, can lose its conductivity by dehydration⁵⁷ and by contamination with metal ions.⁴¹

The presence of ammonia in the fuel, which can be the case when operating on reformed fuels, has been shown to lead to irreversible performance loss.⁵⁸ Ammonia reacts as a base with the acidic membrane, leading to a lowering of the proton conductance in the electrode.⁵⁸ Pollutants in the air, notably NH_3 ,⁵⁹ SO_2 ⁵⁹ and NO_2 ⁶⁰ can lead to performance loss, both temporary and permanent.

Using pure hydrogen (99.9%) and oxygen (99.8%), PEMFC stack performance was monitored during an 11 000 hour life test,⁶¹ in order to test the feasibility of the PEMFC stack for use in space shuttle applications. The degradation observed was very low, and amounted to a mere 16 mV at a current density of 0.86 A cm^{-2} over the total test time. The only component that showed some degradation was the sealant material. As relatively high noble metal loadings were used in the tested PEMFC stack, 4 mg cm^{-2} Pt at the cathode and 4 mg cm^{-2} Pt and 1.2 mg cm^{-2} Rh at the anode, the degradation associated with electrode poisoning might be much higher in PEMFC stacks with lower noble metal loadings. Also less pure hydrogen and ambient air will probably lead to higher degradation rates.

Use of fuel cells in transport applications means they should resist freezing conditions. Without precautions, freezing of the

water contained in the membrane–electrode assembly leads to physical damage of the membrane–electrode interface.⁶² Effective removal of the water is possible by either gas purging^{36,62} or washing away with antifreeze liquids,⁶² preventing performance loss of the fuel cell. Membrane–electrode assemblies using reinforced membranes are much less affected by freeze–thaw cycles.⁶³

Fuel starvation is another well-known cause of degradation of fuel cells.³⁶ In a series of fuel cells, all cells are obliged to generate the same current. As long as all cells perform equally well and are supplied with enough fuel, all cells are operated at the same cell voltage and no degradation should occur. When however a single cell is not supplied with enough fuel, the cell materials are sacrificed to sustain the cell current. Cell materials to be oxidized are the carbon support of the catalyst³⁶ and the bipolar plate material. Degradation can occur by fouling of the catalyst by their oxidation products, by increasing contact resistance or by complete loss of the electrode catalysts.³⁶ Strategies to protect the fuel cell components from oxidation in case of fuel starvation focus on the promoting of water oxidation.³⁶

Oxidant starvation leads to the recombination of protons to molecular hydrogen at the cathode.³⁶ Although also in the case of oxidant starvation the cell voltage can drop below zero, physical damage is less severe than in the case of fuel starvation.

Pinholes in the electrolytic membrane are another well-known failure. They can be caused either by mechanical damage, or by local heat generation. Pinholes lead to direct mixing of hydrogen and air, which will react with formation of reaction heat leading to more cell damage.

PEMFC systems running on reformed fuels face, in addition to all durability issues addressed in the previous section, difficulties which stem from impurities present in the fuel reformat. Depending on the primary fuel, contaminants present in the reformat with negative effects on fuel cell lifetime are carbon monoxide,³⁶ ammonia⁵⁸ and sulfur containing components.^{60,64} The noble metals in the electrodes are easily poisoned by low concentrations of impurities. While the effect of CO and CO_2 is reversible, sulfur components in the ppm range lead to irreversible loss of fuel cell performance, whether as part of the inlet air or fuel.^{59,63}

As mentioned before, the negative impact of carbon monoxide is in many systems mitigated by using an air bleed. The catalytic reaction between CO and O_2 can however lead to hot spots when the flow design of the fuel cell is not optimal.³⁶

Most tests aiming at studying the PEMFC performance on reformed fuels are done using simulated reformat. While this covers the effect of operation on diluted hydrogen, CO_2 , and CO, effects of partly unknown impurities remain unaddressed.

For operation on simulated methane reformat, a degradation rate of $0.5 \mu\text{V h}^{-1}$ over 13 000 hours of operating time has been demonstrated.³⁶ Osaka Gas has measured a degradation rate of $2 \mu\text{V h}^{-1}$ over more than 12 000 hours using simulated reformat gas.⁶⁵ Operation of a 7400 hour field trial on real methane reformat has been completed successfully, without disclosing the degradation rate.³⁶

3. Current status of solid oxide fuel cells

The Solid Oxide Fuel Cell is a strong candidate for stationary power generation, especially in the power range of 1–200 kWe. Its high operating temperature allows operation on a wide range of fuels without the need for extensive reforming and gas clean-up steps as required in PEMFC systems. The cell reactions in the SOFC are depicted in Fig. 5.

Both the electrolyte as well as the electrodes consist predominantly of ceramic materials. Only the anode contains metallic nickel for electron transport and catalysis of hydrogen oxidation. The basic cell concept does not require noble metals. The electrolyte is a ceramic oxygen ion conductor.

Whereas the system of an SOFC is much less complex compared to the system of low temperature fuel cells, the major challenges are on cell and stack level.

Generally, SOFC developers consider three cell configurations: electrolyte-supported cells, anode-supported cells and metal-supported cells, depending on which component is the thickest and serves as the mechanical basis. In this order, these fuel cell configurations are also referred to as first generation, second generation and third generation. The temperature of operation decreases through these generations from 900–1050 °C for the electrolyte supported cell, to 700–800 °C for the anode supported and 500–700 °C for metal supported cells. Operation at lower temperatures is aimed at because of sealing issues and the need for using cheap, iron based heat resistant steels for separator plates (called interconnects in SOFC) and system components.

Due to the high operating temperature, an important factor in the design of a solid oxide fuel cell stack is the matching of thermal expansion of the cell components and interconnects, to prevent cracking of the intrinsically brittle ceramic cells, gas leakage and loss of electrical contact.

3.1. Electrolytes

The electrolyte that is generally used in the SOFC is yttria stabilised zirconia, abbreviated as YSZ, either ZrO₂ doped with 3 mol% Y₂O₃ (3YSZ) or with 8% Y₂O₃ (8YSZ). The dopant concentration has a strong influence on ion conductivity and mechanical properties.⁶⁶ In electrolyte-supported cells, the electrolyte is typically 120–150 μm thick. Because the conductivity is proportional to the temperature, operating at lower temperatures requires thinner electrolytes. At around 850 °C the electrolyte thickness must be so thin, that it cannot mechanically support the cell anymore. For

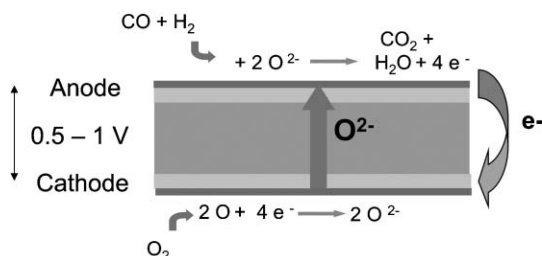


Fig. 5 Basic principle of the SOFC, for the case where both hydrogen and CO are in the anode feed.

operation between 600–800 °C, electrolyte layers are typically less than 20 μm.⁶⁷

An alternative for operation at lower temperature is the application of other electrolyte materials, for example CeO₂ doped with 10 mol% GdO, abbreviated as GCO. Electron conduction that occurs at reducing conditions in the anode environment, leading to short-circuiting is an issue for this alternative electrolyte.⁶⁷ For operation at 600 °C or even lower, La_{0.9}Sr_{0.1}Ga_{0.8}Mg_{0.2}O_{2.85} electrolytes offer superior conductivity, but exhibit stability problems caused by evaporation of Ga, and low mechanical stability and high gallium costs.⁶⁷ Scandium doped ZrO₂ offers improved oxygen ion conductivity and relatively high mechanical strength, at the expense of using high cost scandium.⁶⁷

3.2. Electrodes

SOFC anodes are generally composed of Ni–YSZ. Besides catalysing H₂ oxidation and facilitating electron conduction, nickel is active in reforming of carbon containing fuels, which is an attractive feature of the SOFC. As steam reforming of methane is an endothermic reaction, the heat produced at the anode can directly be used for the steam reforming reaction. Water formation at the anode side helps as well. A critical issue however is coke formation, which occurs at lower water contents. Direct injection of fuels such as ethanol and iso-octane has been shown to lead to immediate loss of SOFC performance caused by coke formation.⁶⁸ Oxidation–reduction cycles can form another threat to anode stability. Anodes composed of nickel and gadolinium doped ceria appeared to have a much better resistance towards these oxidation–reduction cycles than Ni–YSZ anodes.⁶⁹ Completely ceramic anodes, not containing nickel, show good oxidation–reduction cyclability.⁷⁰ Another positive effect of replacing nickel is a better tolerance towards sulfur.⁷⁰ However, the main challenge is to increase the electrochemical performance of the full-ceramic anode to the same level of the Ni based anode.

SOFC cathodes consist of single-phase La_{0.75}Sr_{0.2}MnO₃ (LSM) or of mixtures of this compound with YSZ. As in the other fuel cell types, the oxygen reduction largely determines the efficiency of the SOFC.⁶⁷ Substitution of manganese with cobalt gives improved cathode performance.⁶⁷ The mechanical properties of cobalt containing cells are however poorer, as the thermal expansion coefficient of the cobalt containing cathode is twice that of YSZ, and formation of low conductivity products at the electrolyte–cathode interface leads to decreasing power output.⁷¹ Cathodes using La_{0.6}Sr_{0.4}Co_{0.2}Fe_{0.8}O₃ (LSCF) have the advantages of lower losses at lower temperatures (600–700 °C) and are additionally reported to be less sensitive to Cr-poisoning. As in other fuel cells, electrode optimisation is focused on improvement of the conductivity throughout the electrode for ions and electrons and the accessibility for oxidant.

Loss of cathode performance is associated with changes of microstructure and phase composition at load conditions. In combination with Cr containing steels for the interconnects, important degradation occurs due to poisoning of the cathode by Cr which evaporates from the steel and preferably condensates at catalytic sites. In general the rates of these

degradation mechanisms decrease with decreasing operating temperature.⁷²

In contrast to the PEMFC where electrolyte and electrodes can be manufactured separately and joined together at a later stage, solid oxide fuel cell manufacturing comprises electrolyte and electrode manufacturing in close conjunction.

Future SOFC cell cost needs to be less than US\$500 m⁻², leading to a cost of less than US\$250 kWe⁻¹ when operating at cell power densities of 0.2 W cm⁻².⁷³

Current price level estimates are US\$2000–5000 kWe⁻¹ for electrolyte-supported cells⁷³ and US\$12000 kWe⁻¹ for anode-supported cells.⁷³ Cheaper raw materials, simpler manufacturing procedures and above all mass manufacturing of cells are the keys to lower cell costs.⁷³

3.3. Separator plates—interconnects

Separator plates are in SOFC mostly called interconnects. At high temperatures, one option is to use ceramic interconnects. The ceramic plates are based on LaCrO₃. Doping with Ca, Sr or Mg leads to higher electrical conductivity.⁷⁴ Pure ceramic plates have the tendency to be partially reduced at the anode side, leading to warping and breakage of the sealing.⁷⁵ Besides, more cost effective materials and fabrication methods are needed for bringing this technology to the commercial stage.⁷⁵ Metallic interconnects would lead to lower fabrication costs, are less brittle and have a higher electrical and thermal conductivity.⁷⁴

An extensive review on high temperature alloys and their suitability for application in the SOFC has been published recently.⁷⁵ At temperatures below 800 °C, metallic interconnects, such as ferritic steels can be used. The advantages are lower costs and simpler manufacturing.⁷² Chromium containing alloys are used to ensure high temperature oxidation resistance and sufficient electron conductivity of the corrosion scale. Evaporation of this chromium, and its subsequent deposition at the cathode–electrolyte interface is one of the causes of SOFC degradation when using chromium-containing metallic interconnects.⁷² The application of contact coatings on the alloy can prevent the degradation caused by chromium evaporation and increase the electronic conductivity of the cell interconnect assembly.⁷⁶ The typical requirements imposed by the SOFC conditions have led to a few new alloys, specially designed for application in the SOFC.⁷⁷

3.4. SOFC—state-of-the-art performance

Table 3 summarizes the state-of-the-art performance of Solid Oxide Fuel Cells under different conditions. Planar cell power

densities of 0.6–0.9 W cm⁻² at a cell voltage of 0.7 V can be regarded as state-of-the-art for anode supported Solid Oxide Fuel Cells operated at temperatures of 750 °C and lower, at atmospheric pressure. Much higher power densities are reported at low fuel utilisation, typically 25%. Such low fuel utilisations are, from an efficiency point of view, not realistic for practical systems and therefore only data at fuel utilisation of 60% and higher are reported here.

Electrolyte-supported cells give much lower power densities. Many stack and system developers still use electrolyte-supported cells as their robustness is better established.

Two SOFC stack configurations are in development: planar and tubular. The tubular SOFC is being developed by Siemens Westinghouse and Rolls-Royce. One of the main advantages of the tubular concept is the relative ease whereby the sealing between anode and cathode compartments can and has been solved. Thermal stress is a concern in the tubular design. As the tubular configuration is targeting large stationary applications with more or less continuous operation,⁸⁴ this should not be a major barrier.

The power densities demonstrated with planar cells however are much higher, especially because current collection is much more effective than in the tubular cells.

It is generally believed that although the tubular SOFC is at present the most developed, in the long term planar SOFCs offer a better cost perspective and higher power densities.⁸⁴

Power densities for SOFC stacks are not reported frequently. SOFC stacks are, besides their application in Auxiliary Power Units (APUs), primarily designed for stationary power generation and the focus in SOFC development is predominantly on increasing lifetime and robustness, more than on increasing the power density. Power densities as reported in Table 4, are on first sight considerably lower than for PEMFC stacks. When comparing the power density with the atmospheric PEMFC stack of 1.5 kWe, it must be concluded that both power densities are in the same range.

3.5 SOFC durability data

The durability of the SOFC is primarily determined by processes occurring during thermal cycles, oxidation–reduction cycles, more than accumulation of contaminants, as is the case for the PEMFC. Sulfur is an exception. Even at the high temperatures at which the SOFC is operated, sulfur is adsorbed by the anode and causes performance loss.⁸⁸

An important cause of degradation is loss of activity of the anode. Nickel sintering and coke formation when operated on carbon containing fuels lead to a loss of active surface area.⁷²

Table 3 SOFC state-of-the-art performance under various conditions. For materials used, see cited reference

	Cell power density/W cm ⁻² at 0.7 V _{cell}	Cell type	Company/laboratory	Ref
H ₂ –air ambient pressure, 750 °C	0.6 ^a	ASC	Global T.	78
	0.9	ASC	PNNL	79
Methane + air ambient pressure, 720 °C	0.55	ASC	FZ Jülich	80
Simulated reformat + air ambient pressure, 750 °C	0.44	ASC	Delphi/Batelle	81
Natural gas + air ambient pressure, 850 °C	0.1	ESC planar	CFCL	82
Natural gas + air ambient pressure, 1000 °C	0.14	ESC tube	Siemens W.	83

Global T. = Global Thermoelectric; PNNL = Pacific NorthWest National Laboratory; Siemens W. = Siemens Westinghouse. ^a Power density higher than 0.6 W cm⁻² at fuel utilisation lower than 0.6.

Table 4 SOFC stacks for stationary applications

	Ref	Power/kW	Power density/kW l ⁻¹	Conditions
Siemens Westinghouse tubular	85, 86	125	0.1 ^a	Natural gas–air; 0 bar g; 900–1000 °C
General Electric ASC planar	87	1.1	0.53	Hydrogen–air; 0 bar g; 800 °C
CFCL ESC planar	82	1–10	0.3	Reformate–air; 0 bar g; 850 °C

^a Roughly calculated from available data.

Another factor which has been mentioned before is the deposition of chromium from the interconnect on the cathode–electrolyte interface.

An averaged degradation rate of 1% per 1000 hours over a total test period of 12 000 hours has been reported by Global Thermoelectric for a single cell under realistic load, using hydrogen as fuel and at an operating temperature of 750 °C.⁸⁹ A short stack operated on 50% hydrogen at 850 °C by Haldor Topsoe hardly suffered from any degradation⁹⁰ during a 3000-hour operation period.

Pressurised tubular stacks have been operated by Mitsubishi Heavy Industries for 7000 hours, the degradation rate is not reported.⁹¹

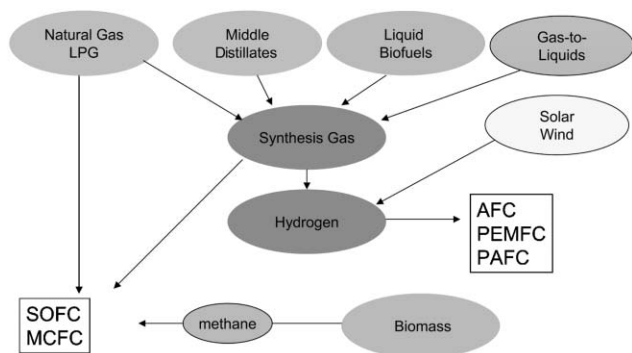
If the degradation rate is limited to 0.25% per 1000 hours, the power output can probably be maintained by increasing the stack temperature by 15 °C or lowering the fuel utilisation.⁹⁰ For larger degradation rates, these solutions become less feasible.

For application in vehicles as Auxiliary Power Units, breaking of ceramic cells caused by vibrational forces is a real concern. Global Thermoelectric has shown that a 500 W stack can survive vibration of 10 G at 185 Hz.⁷⁸

4. Hydrogen storage, transport and production

The Direct Methanol Fuel Cell is the only fuel cell in which a fuel other than hydrogen is electrochemically oxidized. In all other fuel cells, hydrogen or a hydrogen–carbon monoxide mixture (synthesis gas) is electrochemically oxidized. Hydrogen can be either generated internally, as is done in the MCFC and in large fraction of the SOFC stacks, or be supplied externally. As displayed in Fig. 4, the hydrogen can be supplied as pure hydrogen, or generated within the system in a so-called fuel processor or reformer.

Fig. 6 gives an overview of a variety of the most common fuel supply chains in combination with the fuel cell types.

**Fig. 6** Fuel routes for fuel cells.

For obtaining hydrogen from solar and wind power, electrolyzers are commonly used. Electrolyser technology is not covered in this review. Electrolyser efficiencies of commercial alkaline electrolyzers are in the 65–75% range.⁹²

For the generation of hydrogen from fossil fuels as well as biofeedstocks, thermal conversion processes are used, either as the central production unit, as a decentral unit or as part of the fuel cell system. For stationary applications, natural gas will be the preferred fuel in the coming decades, as supplies are sufficient and existing distribution networks can be used. For vehicles, pure hydrogen is considered as one of the options. In that case, distribution networks as well as storage need to be available.

4.1. Hydrogen storage and transport

4.1.1. Hydrogen storage. For transport applications, the on-board storage of hydrogen has to be developed aggressively in order to realize a driving range comparable to gasoline or diesel cars at an acceptable use of volume, weight and cost. The DoE targets for on-board hydrogen storage devices⁹³ are displayed in Table 5. The targets are based on the amount of hydrogen needed for a passenger car to have a driving range of 600 km. The 2015 targets lead to a storage tank with 56 kg weight, 62 l volume at a cost of \$333, containing 5 kg hydrogen. A refueling time of 2.5 minutes is regarded as acceptable.⁹⁴

Several options are in development: liquid hydrogen, pressurized hydrogen, metal hydrides, borohydrides and storage in carbon structures.

State-of-the-art compressed hydrogen storage consists of lightweight tanks using polymers and carbon fibers containing hydrogen compressed to 700 bar. Liquid hydrogen, stored at –253 °C, is stored in tanks that are engineered in such a way that boil-off losses are minimised.⁹⁶ It strongly depends on the driving behaviour whether boil-off losses are acceptable or not.⁹⁵ The workday driver with a minimum driving range of 25 km per day would not suffer from loss of fuel, while the

Table 5 State-of-the-art hydrogen storage options *versus* DoE targets for on-board hydrogen storage for transport applications. All numbers are based on the Lower Heating Value of hydrogen

	Volumetric density/kWh l ⁻¹	Gravimetric density/kWh kg ⁻¹	Cost/\$ kWh ⁻¹	Ref
DoE target	3	2.7	2	94
Compressed H ₂ 350 bar	0.8	2.1	12	94
Compressed H ₂ 700 bar	1.25	1.0		95
	1.3	1.9	16	94
Liquid H ₂	1.6	2.0	6	94
Metal hydride	0.6	0.8	16	94

weekend driver driving 50 km per day would suffer from 15% loss of fuel.⁹⁵

To avoid the energetic losses associated with compression and liquefaction of hydrogen (see next section), metal hydrides have been under investigation for quite some time. Lightweight elements are under special consideration, to meet the weight target of the storage vessel. Mg, LiN and NaAlH₄ are lightweight candidates, but suffer from the high temperatures, 200–300 °C, at which desorption takes place.⁹⁷

Hydrogen storage in carbon nanotubes has up to this moment not fulfilled initial expectations.⁹⁸ Zeolites are under consideration as hydrogen storage materials as well.^{97,98}

4.1.2. Transport and distribution. Small numbers of vehicles in demonstration programs can easily be supplied by local hydrogen stations, of which several have been placed in 2003 in the 10 cities participating in the EU-funded CUTE project.⁹⁹ For large-scale introduction a fuel supply network is needed which is of comparable density to the present petrol supply network. In a densely populated western country such as the Netherlands, 3750 petrol stations are present in a total area amounting to 42 000 km², approaching a refueling density of 1 per 10 km². The USA has 187 000 petrol stations, Western Europe 80 000.

An infrastructure consisting of hydrogen fuel stations will cost approximately 10 times that for new liquid fuels as methanol or ethanol.¹⁰⁰ Using existing gasoline and diesel infrastructure would impose no extra infrastructural cost. For safety reasons, a hydrogen filling station will be quite different from the gasoline stations, as we know today.

Also from an energetic point of view, large-scale transportation of hydrogen, and the necessary compression or liquefaction of hydrogen can be highly unattractive.¹⁰¹ Both compression (10–20%)^{97,101} and liquefaction (25%–40%)^{97,101} consume an unacceptable part of the energy content of the hydrogen. New methods of liquefaction, such as magnetic and acoustic refrigeration, could diminish the energy use for liquefaction.⁹⁷ In addition, transport by trucks or through pipelines over large distances should be avoided: hydrogen trucks consume 20% of the energy content of the hydrogen transported per 100 km delivery distance, pipeline transport consumes 10% of the hydrogen energy content per 1000 km.¹⁰¹

Production of hydrogen at the “petrol” station would avoid the efficiency losses associated with transport of hydrogen.

4.2. Fuel processor technology

On site generation of hydrogen can speed up the introduction of fuel cell systems without the presence of a widespread hydrogen infrastructure. The generation of hydrogen from hydrocarbons is a multi-step process, which is schematically displayed in Fig. 7.

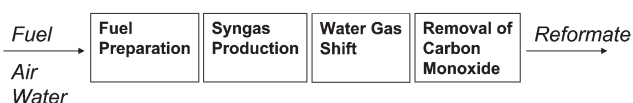


Fig. 7 Schematic overview of hydrogen generation by means of fuel processing.

The purpose of the fuel processing is to generate a reformat which is most suitable for the fuel cell in question. The tolerance towards carbon monoxide strongly depends on the temperature level of the fuel cell. The MCFC and SOFC can be fed with carbon monoxide, while the concentration of CO that can be tolerated by the PEMFC is in the range between 10–50 ppm. Other impurities with a negative impact on fuel cell performance and durability have to be removed as well.

4.2.1. Fuel processors for mobile applications. Methanol fuel processors have been demonstrated in the Daimler Chrysler Necar 3 and Necar 5.¹⁰⁰ Emission characteristics are displayed in Table 11, which shows the absence of NO_x formation in the fuel processor, due to its low operating temperature.¹⁰² Whereas the CO emission is very low, the hydrocarbon content is still comparable to that of a modern gasoline internal combustion engine (ICE) car. As the Necar 5 is still at a relatively early development stage, one should expect that it is possible to lower this hydrocarbon emission.

Gasoline fuel processors are quite scarce. A partially integrated gasoline fuel processor for a 10 kWe PEMFC stack, consisting of an autothermal reformer, a desulfuriser and a single stage shift reactor, was demonstrated by Argonne National Laboratory. The volume of this system, which needs an additional PrOX reactor, amounts to 7 l.¹⁰³

Both Nuvera as well as Hydrogen Source (A Shell/UTC Fuel Cells joint venture, liquidated mid 2004) have developed a gasoline fuel processor, which is suitable for use in passenger vehicles. The Hydrogen Source gasoline fuel processor has a cold start-up time of 4 minutes, which is relatively short, but still too long to meet the DoE target of 30 seconds.

The Nuvera Star gasoline fuel processor,¹⁰⁴ which can be operated on ethanol and natural gas as well, has an efficiency of 80% and can generate the hydrogen for a 62 kWe fuel cell system. The CO concentration in the reformat amounts to 50 ppm, while the volume of the system amounts to 75 l.

Daimler Chrysler concluded on the basis of simulations that while methanol fuel processors can be highly integrated, leading to a compact fuel processor, gasoline fuel processors couldn't be integrated far enough, due to too large temperature differences between the several stages.¹⁰⁰ Both dynamics and efficiency would be poor to compete successfully with *e.g.* diesel internal combustion engines.¹⁰⁰

Based on the current status of fuel processors for transport, as displayed in Table 6, the DoE has decided mid 2004 to terminate the funding of the development of gasoline on-board fuel processors for vehicle propulsion.

Important factors in the decision of the DoE are:

- the progress made with hybrid ICE vehicles with respect to fuel economy
- the expectation that the extra effort put into supporting a hydrogen based transport system by the Hydrogen Fuel Initiative of the Bush administration, will shorten the time a transition technology such as gasoline–fuel cell vehicles will be used.¹⁰⁵
- automotive manufacturers do not show much interest in the option of on-board fuel processing anymore.

Table 6 Selected DoE targets and current status for on-board fuel processors for transport¹⁰⁵

	Power density/kWe l ⁻¹	Efficiency (%)	Start-up energy/MJ (50 kWe) ⁻¹	Durability/h	Start-up time/s	Cost/\$ kWe ⁻¹
DoE 2004 target	0.7	78	<2	2000	<60	—
DoE 2010 target	2	80	<2	5000	<30	<10
Status 2004	0.7	78	7	1000	600	<65

4.2.2. Fuel processors for stationary applications. Steam reforming can be used for small-scale generation of hydrogen from natural gas for residential fuel cell applications. For 0.5–1 kWe systems, Osaka Gas has developed a small fuel processor, based on its technology developed for the phosphoric acid fuel cell systems.¹⁰⁶ The fuel processor, combining a desulfuriser, a steam reformer, water gas shift section and a single stage preferential oxidation reactor is able to generate reformat with a CO content of less than 1 ppm and a hydrogen concentration of 75% (dry basis). Endurance has been proven for more than 10 000 hours, and lifetime is expected to be more than 90 000 hours. The high hydrogen concentration is a major advantage of steam reforming. The start-up time is 1 hour, which is relatively long for residential applications. The volume of the complete fuel processor amounts to 48 l, including thermal insulation.

Similar fuel processors have been developed by Tokyo Gas,¹⁰⁷ Nuvera,¹⁰⁸ Plug Power, Johnson Matthey and many others for natural gas or, amongst others, by Sanyo for propane.¹⁰⁹

Shell/Hydrogen Source developed a 2 and 5 kWe integrated fuel processor for natural gas and propane based on catalytic partial oxidation.

5. Fuel cell systems and field trials

Fuel cell field trials play an extremely important role in the improvement of fuel cells and their introduction into the market. Both in transport as well as in stationary markets, fuel cells replace technologies which have been on the market for more than a century, meet customer requirements satisfactorily and have evolved into a low cost commodity through many years of strong, global competition.

Fuel cells will not be allowed to develop through the development curve in the market as *e.g.* cars were allowed during their first decades. The price : quality ratio that cars have displayed in their first decades, will be totally unacceptable in the present market for the vast majority of consumers, bar a small number of early adapters. A new technology needs to be better than the technology it replaces. Environmental benefits are not enough to convince consumers to switch to a new technology.

The goals of field trials are to evaluate the technology through a wide range of conditions, to show the public the capabilities of the new technology, and not unimportantly, to increase production numbers and thereby reduce cost through economies of scale.¹¹⁰

Early market introduction and demonstration is seen mostly in stationary off-grid applications or as back-up power in critical environments, where operating hours are low and existing technologies, such as diesel generators, have serious

disadvantages. The efficiency, which is at present still too low for many current systems, is not a key factor in these markets. Other niche applications for fuel cells are auxiliary power units in cars and leisure applications, backup power systems in offices and houses, replacing diesel generators. Applications for the military range from power packs for soldiers to MW systems in submarines.

5.1 Stationary applications of PEMFC and SOFC

For decentralised power generation, fuel cell systems are being developed which run mostly on natural gas, sometimes on propane or even kerosene in the case of Japan.¹¹¹ Inside the systems, hydrogen is generated by steam reformer or autothermal reformer based fuel processors.

One of the frontrunners in the demonstration of PEMFC systems for stationary applications is Plug Power. Systems of 5 kWe, operated on either natural gas or propane commercialised under the trade name GenSys, are being demonstrated at the United States Military Academy and other sites by the Department of Defense.^{112,113} The Plug Power CHP systems are operated on natural gas and produce at maximum power 5 kW electric and 9 kW thermal. The electrical efficiency of these GenSys systems amounts to 24.8%, which is an average of different operating set points. NOx and SOx emission concentrations are below 1 ppm. The average availability has been improved from 88% in year 2002/2003 to 92% in year 2003/2004.

In Europe, 31 Plug Power systems are being evaluated within an EU funded project called the Virtual Power Plant. All systems will be grid connected and centrally controlled, in such a way that together these systems form a virtual power plant.⁹⁹

Japanese industries and gas utility companies are very actively developing small micro CHP systems: Hitachi,¹¹⁴ Tokyo Gas,¹¹⁵ Fuji Electric,¹¹⁶ Osaka Gas⁶⁴ and many more. In a Japanese program, called the Millennium Project, micro combined heat and power systems are being evaluated.¹¹⁷ The system size is typically between 1 and 5 kWe (Fig. 8). Participating companies are Toshiba IFC, Sanyo Electric, Toyota, Plug Power, Mitsubishi Electric, Ebara Ballard, Matsushita Electric and UTC Fuel Cells. The electrical efficiency of the Japanese 1 kWe systems is typically 30%.

The systems that are available now should be seen as the first generation, suitable for field trials but not for large-scale market penetration. The necessary reliability and lifetime have not been demonstrated. Besides that, electric efficiency needs to be improved to at least 35%. With respect to the cost level, it is expected that at large volumes the cost target of \$1000–1500 kWe⁻¹ can be met when using the materials available at this moment.



Fig. 8 1–5 kWe Residential fuel cell systems under evaluation in the Japanese Millennium Project.¹¹⁷

PEMFC stationary systems of 250 kWe have been developed by an Alstom–Ballard joint venture.¹¹⁸ Five plants with an electrical efficiency of 34% and a total efficiency of 73% have been tested in field trials since 2000.¹¹⁸ Further commercialisation plans for the 250 kW systems are unclear.

SOFC. Frontrunners in SOFC system development and demonstrations for stationary applications are Sulzer Hexis, aiming at systems of 1 kWe,¹¹⁹ and Siemens Westinghouse, aiming at 250 kWe systems.¹²⁰ A 110 kWe system has been operated on natural gas by Siemens Westinghouse during more than 20 000 hours at an AC efficiency of 46%, without any voltage degradation.¹²⁰ Bigger units, of 170 kWe and 190 kWe have been put in operation since, but not for as long as the 110 kWe system.

Derived from this concept and in collaboration with Siemens Westinghouse, 5 kWe tubular systems have been put in operation by Fuel Cell Technologies. The AC efficiency of these smaller systems is reported to amount to 38%¹²⁰ and they have been in operation for more than 1700 hours.

Sulzer Hexis has concluded a field test with its Hexis 1000 Premiere systems, a 1 kWe system that with an additional burner covers the full heat demand and the base load electrical demand of a single family house. The AC efficiency of this system amounts to 25–32% at full load.^{121,122} For commercial introduction, this generation has shown a too high degradation rate. In addition further reduction in size, weight and cost are needed. A redesign consists, amongst other things, of changing from natural gas steam reforming to catalytic partial oxidation of natural gas and a new design of the metallic interconnect.¹²¹

A 2 kWe system from Global Thermoelectric running on natural gas has been operated for 20 000 hours at a maximum AC efficiency of 29%.¹²³ Better thermal integration and higher fuel utilisation, 60–70%, in the next generation should lead to an increase in efficiency to 35%.¹²³

A pressurised (4 bar g) 10 kWe SOFC module of Mitsubishi Heavy Industries, consisting of 288 SOFC tubes with internal natural gas reformer has been operated with a DC efficiency of 41.5% HHV for 755 hours.¹²⁴ A former generation has been operated for 7000 hours.

A consortium of Wärtsilä and Haldor Topsoe is developing a 250 kWe SOFC system, based on planar SOFC technology. Based on laboratory experiments and detailed engineering calculations the consortium expects that 250 kWe plants can become competitive to 300 kWe gas engine plants between 2010 and 2020.¹²⁵ Total unit price has been calculated to be in the range of 1600–2600 € kWe⁻¹ in 2010 and 676–1100 € kWe⁻¹ in 2020.¹²⁵ Whereas SOFC stacks contribute 310 € kWe⁻¹, balance of plant costs would contribute as much as 490 € kWe⁻¹ to this 2020 cost estimate.¹²⁵

For auxiliary power units, BMW/Delphi is the leading consortium. The ongoing electrification of vehicles is hitting the boundaries of conventional batteries and generators. This has led to the insight that an auxiliary power unit (APU), which consists of a fuel cell system decoupled from the drive train, can generate the power needed on board both when driving as well as during standstill. As the APU might be introduced before fuel cell systems are ready for introduction in the drive train of the vehicle, regularly used fuels such as gasoline and diesel are the fuels of choice. As the available space in existing vehicles for an additional device is limited, SOFC systems are seriously considered by the automotive sector for APU's. For the SOFC, fuel processing of gasoline and diesel will be much less complex than in the case of a PEMFC. Compared to stationary applications, the APU puts more challenging demands on the SOFC with respect to the power density, the start-up time and thermal cycling capability. A gasoline SOFC APU system has been demonstrated by Delphi/BMW integrated in a BMW vehicle.⁷⁹ Their latest generation APU has a start-up time of 60 minutes.¹²⁶

5.2 Application of PEMFC systems for transport

A considerable number of fuel cell vehicles are presently being tested and demonstrated on the road. These tests show the advancement of the fuel cell technology with respect to robustness, compactness and driving performance. It does not give the progress with respect to cost reduction. Table 7 gives an overview of part of the fuel cell vehicle demonstrations.

Daimler Chrysler has been the pioneering car manufacturer since the mid 1990s. Through various generations, system size has diminished tremendously in close cooperation with Ballard. Initially, the fuel cell system was so large that only a minivan could accommodate it (Necar 1 and Necar 2).^{101,102} In the newest model, the fuel cell system is situated in the floor space of a Mercedes A-class passenger vehicle, hardly sacrificing the customer need for space.¹⁰² At present, all major car manufacturers have a development program for fuel cell vehicles. The most active manufacturers are, besides Daimler Chrysler: Toyota, Ford, General Motors and Honda. A complete, actualised overview is available at the website of FuelCells2000.¹²⁷

The majority of the vehicles run on hydrogen. Daimler Chrysler, Toyota and General Motors have demonstrated vehicles, which produced hydrogen on board using fuel processors, mostly running on methanol or specially formulated gasoline type of fuels. At present, most manufacturers are focusing on further development of vehicles with on-board hydrogen storage.

Table 7 Recent field trials in transport

Company	Vehicle type	Type	Fuel	Year	Accomplishment
Daimler Chrysler	Small passenger car	Necar 5	Methanol	2002	USA coast to coast trip, 4500 km ¹³⁰
Volkswagen	Mid size passenger car	Bora HY Power	Hydrogen	2002	Mid winter mountain trip across Simplon Pass (CH) at -9°C
General Motors	Mid size passenger car	HydroGen3	Hydrogen	2004	10 000 km Journey in 38 days
Daimler Chrysler	Small passenger car	Mercedes A F-cell	Hydrogen	2004	60 Cars in operation in Germany, Japan, USA and Singapore ¹⁰²
Daimler Chrysler	Bus	Citaro	Hydrogen	2003	30 Buses in 10 European cities in daily operation ¹⁰²

Field trial programs, in which fuel cell vehicles are tested in realistic environments, are running in California in the California Fuel Cell Partnership¹²⁸ and in Japan within the Fuel Cell Commercialisation Conference of Japan.

Vehicle systems often combine fuel cells with an electricity storage package, which can be either batteries or super capacitors.¹²⁹ Three important reasons for using electricity storage devices in fuel cell vehicles are: improvement of dynamics, decreasing fuel cell stack size and cost, and enabling regenerative braking, which has a positive impact on the total efficiency.

Fuel cell buses have been in development since the 1990s. The advantages of fuel cells in buses are multiple. From a technical point of view, the ample availability of space has made it easy to integrate the system and hydrogen storage in the bus without sacrificing the available space for passengers. Availability of technicians at bus terminals makes a field trial easier to handle, and fuelling of buses is generally done at a central depot. Finally, the dynamics of a bus drive cycle is especially advantageous for a fuel cell system in comparison to a diesel engine. The engine is often operated at partial load, leading to poor diesel engine efficiency. A Scania passenger bus, consisting of a 50 kWe hydrogen fed PEMFC system combined with a 135 kW battery system was tested on Braunschweig and FTP-75 duty cycles. Fuel consumption in the vehicle is 42–48% lower than in its standard diesel ICE version.⁵³ The regenerative braking, which can also be applied in combination with an ICE hybrid vehicle, accounts for roughly half of the fuel saving.

The largest field trial of fuel cell buses is at this moment running in Europe in the EU funded CUTE project, where in 10 cities 30 Daimler Chrysler buses are in daily operation (Fig. 9).

The Department of Energy of the USA government has set technical as well as cost targets for mobile fuel cell systems which have to be met in order to become competitive with conventional cars.⁹³ The direct hydrogen fuel cell power system has to have a 60% electric efficiency at a cost of $\$45\text{ kW}^{-1}$ by 2010 and $\$30\text{ kW}^{-1}$ by 2015, both including hydrogen storage. Alternatively, a reformer based fuel cell power system, operating on clean hydrocarbon or alcohol that meets emission standards, has to have a 45% electric efficiency at a cost of $\$45\text{ kW}^{-1}$ by 2010 and $\$30\text{ kW}^{-1}$ by 2015. The start-up time of a reformer based system should be less than 30 seconds.

The price of today's demonstration vehicles, \$1 million for GM's HydroGen3 vehicle,¹³¹ stands in no relation with the vehicle price when manufactured in series. The cost of fuel cell

systems for mobile applications is estimated to be at present at a level of $\$325\text{ kWe}^{-1}$,¹³⁰ at a production level of 500 000 units per year. According to the DoE 2003 Progress Report, the current cost level, 2003, is $\$250\text{ kW}^{-1}$ at a volume of 500 000 units per year.

5.3 Applications of other fuel cell types

5.3.1. Alkaline fuel cells. The alkaline fuel cell (AFC) is, like the PEMFC, a fuel cell for low temperature operation. The AFC uses liquid potassium hydroxide or a matrix soaked with potassium hydroxide as the electrolyte. A rather extensive review covering alkaline fuel cells has been written by McLean *et al.*¹³²

The major advantage of the alkaline electrolyte is the possibility to use non-noble metal catalysts for both the anode as well as the cathode. For the anode, nickel¹³³ can be used, while silver can be used for the cathode.¹³⁴ Both alternatives do however suffer from degradation.^{133,134}

Due to its intolerance to CO_2 , both as a component in the fuel as well as in the air, its practical use for mobile applications as well as stationary power generation is rather limited. The reaction between CO_2 and KOH leads to precipitation of K_2CO_3 , due to its limited solubility at low temperatures. This precipitated K_2CO_3 blocks the porous electrode structures, especially when using Raney nickel mesh electrodes. Filtering the CO_2 out of the cathode stream (as well as the anode stream) is possible using a limestone filter. This would imply a usage of limestone of 0.1–0.01 kg per kWh of generated electricity.¹³² Another way to deal with CO_2 is by circulating the electrolyte such that the CO_2 and carbonate do not exclusively build up in the electrodes.¹³⁴ The role of CO_2 in



Fig. 9 Fuel cell bus in Amsterdam in daily operation, as part of the EU-CUTE project. Photo by René van den Burg.

the degradation of the AFC was recently shown to be minor, in comparison with the loss of the hydrophobic nature of the PTFE in the electrodes.¹³⁵

The corrosive nature of hot KOH limits the choice of materials. Current collectors, seals and non-noble electrode catalysts are attacked by the KOH, even PTFE which is part of the electrode, suffers from degradation by KOH in combination with radicals formed by partial reduction of oxygen.^{134,135} Alkaline fuel cells with immobilised KOH suffer more from degradation than AFC's with circulating electrolyte, and more in open circuit conditions than under load conditions.¹³⁶ Carbon corrosion at high voltage in open circuit and carbonate build-up are responsible for this degradation.¹³⁶

Cell power density of the AFC on hydrogen–air, at atmospheric pressure and 75 °C is in the range of 0.1–0.3 W cm⁻².¹³² Pressurised systems are generally applied in space applications. In this application, oxygen is used as the oxidant, and power densities can be as high as 0.74 W cm⁻².¹³²

The alkaline fuel cell has been used in the majority of the space missions as power generator and potable water source. The AFC is also in development for small stationary power generation in the kW range. The limited lifetime of the AFC, being not more than 5000 hours, is a major hurdle for large-scale commercialization.¹³⁴

Early transport applications used alkaline fuel cells as well. At present, none of the car manufacturers take AFC's into consideration. The cost of an atmospheric alkaline fuel cell system has been calculated to amount to \$200–1750 kW⁻¹, dominated by the stack costs.¹³²

5.3.2. Molten carbonate fuel cells. The MCFC is a fuel cell, which is operated at 650 °C. The electrolyte consists of a matrix of porous LiAlO₂ filled with LiKCO₃ or a LiNaCO₃ electrolyte, with a thickness of 0.5–1 mm. At the anode Ni–Cr or Ni–Al is used, at the cathode NiO.¹³⁷ Separator plates are based on Ni or modified stainless steels.

The effort put into the development of the molten carbonate fuel cell has been declining since the end of the 1990s. MCFC have been developed for stationary applications of 200 kWe and more. It can be operated on natural gas, sewage gas, and biogas.

The main industrial developers of MCFC units are Fuel Cell Energy and MTU, a subsidiary of Daimler Chrysler. MTU is putting 200 kW so-called HotModules on the market, primarily as demonstration units. The HotModule is operated at ambient pressure and uses internal reforming. Fuel Cell Energy has built a 2 MW plant in California.¹³⁷

Chubu Electric Power Company and Toyota in Japan have both established 300 kWe MCFC units. The Chubu Electric unit is operated on digester gas, the Toyota unit is combined with a gas turbine.

Estimated price level given by MTU amounts to €1300–1500 kWe⁻¹.¹³⁸ HotModule plants have been tested in at least three field trials since 1999 in Germany.¹³⁹ Fuel cell stack efficiency of 52% is reported.¹³⁹

5.3.3. Phosphoric acid fuel cells. Phosphoric acid fuel cells are operated at temperatures of around 200 °C. The phosphoric acid is immobilized in a matrix layer, consisting

of PTFE–SiC.¹⁴⁰ The electrodes are similar to those in the PEMFC, carbon supported platinum or platinum alloy catalysts. Noble metal loadings used are 0.25 mg Pt cm⁻² at the anode and 0.5 mg Pt at the cathode.¹⁴¹

In fact, in the early stages of the PEMFC many components of the PAFC were adopted by the PEMFC. Only later, PEMFC specific optimisations were made which led to rapid improvement of the PEMFC. Due to the operating temperature which is more than 100 °C higher than the PEMFC, the tolerance towards carbon monoxide is much higher, typically 1–2%. Also the heat management is simpler in the case of the PAFC, and the quality of the heat is higher.

The phosphoric acid fuel cell is the fuel cell which has dominated the stationary market in the 1990s, with a (demonstration) market share of more than 80%.¹¹ The PAFC systems are generally in the power range of 50–200 kW.

In recent years, its share has declined, as competing technologies are believed to be more cost effective in the long run. The PAFC can be regarded as being at the end of its cost lowering asymptote. The installation cost of 200–1000 kWe systems are in the range of \$2000–\$4000 kWe⁻¹,^{142,143} which is considerably higher than the \$1000 kWe⁻¹ which is generally believed to be required to be competitive for stationary applications.¹⁴⁴

The cell power density of the PAFC is 0.14 W cm⁻² when operated on hydrogen and air at atmospheric pressure.^{141,145}

Main industrial PAFC developers are UTC Fuel Cells, Fuji, Mitsubishi and Toshiba.

A fleet of 30 PAFC systems of 200 kW electric power, manufactured by ONSI/UTC Fuel Cells under the trade name PC25, has been operated by the Department of Defense from 1997 till 2003 throughout the US at different climate conditions ranging from Alaska to Texas. Most units have been in operation for 30 000–40 000 hours, at an average availability of 66%.¹⁴⁶ The averaged electric efficiency of the units amounted to 31.6%. Desert operation leading to water management troubles and operation in cold sites leading to freezing damage led to retrofits and redesigns, after which the performance and availability improved.¹¹⁰

Degradation rates of the PAFC stacks amounts to 5% per 10 000 hours for the improved versions. Electrolyte depletion is the major cause of stack degradation.¹¹⁰ Emission levels of NO_x, CO and VOC's and SO_x were below 1 ppm, 5 ppm, 1 ppm and the detection limit of SO_x respectively.¹¹⁰

Also in Japan, PAFC systems have been operated for more than 40 000 hours, using UTCFC PC25 systems as well as Fuji FP100 systems.¹⁴⁷ A number of PAFC systems are operated on digester gas instead of natural gas.

6. Environmental benefit of fuel cells

6.1. Fuel cells for transport

The main drivers for fuel cell vehicles are to diminish the polluting emissions and surpass the poor efficiency of conventional transport, to become less dependent on foreign oil and to prepare the society for the after-oil era.

Table 8 EU and USA^a emission standards for gasoline and diesel engine passenger vehicles (EU: ECE 15 + EUDC; USA: FTP test) in g km⁻¹

	CO	NMHC	NOx	PM
Euro IV gasoline (2005)	1	0.10	0.08	—
Euro IV diesel (2005)	0.50	—	0.25	0.025
USA Tier 2 (2007)	2.6	0.056	0.056	0.0062

NMHC = non-methane hydrocarbons; PM = particulate matter.

^a Emission standards for first 100 000 miles of vehicle life cycle.

6.1.1. Current and near-future emission standards. Tightening emission control legislation in the European Union and the USA is forcing the automobile industry to develop cleaner vehicles. For the European Union, and the USA, the existing as well as future emission standards are given in Table 8 for passenger cars.^{148,149} The emission standards for California are even tighter, but phase-in schedules are unsure, and have been postponed several times already.

The USA Tier 2 standard is an average standard which has to be met by a car manufacturer for his whole passenger car fleet. The Tier 2 standard is subdivided into eight so-called Bins, of which the Bin in Table 8 is the average Bin. In contrast to the Euro emission standard, under the USA Tier 2 legislation gasoline and diesel passenger cars have to meet the same emission standards.

6.1.2. Fuel economy and CO₂ emissions. Common practice is to calculate so-called well-to-wheel efficiencies or emissions, taking into account the emissions and efficiencies in the fuel supply chain (well-to-tank) as well as the emissions and efficiency in the vehicle itself (tank-to-wheel).

Table 9 Emission of CO₂ and equivalents (CH₄ and N₂O)^a for the production and transport of various fuels from ref. 150 and supply costs from ref. 146

Fuel	Emission of CO ₂ eq/g MJ _{LHV} ⁻¹	Supply cost/\$ GJ ⁻¹ (cost of fuel, production, transport and refueling)
Gasoline	13	8–10
Natural gas	14	7–9
Liquid hydrogen from NG	124	
Compressed hydrogen from NG	103	12–18 ^b
Compressed hydrogen from EU-mix electricity	208	
Compressed hydrogen from biomass (poplar plantation)	22	14–25
Compressed hydrogen from wind <i>via</i> electrolysis; highest cost for off-shore	0	22–37

^a CO₂ eq includes emissions of CH₄ (=21 × CO₂) and N₂O (=310 × CO₂). ^b Price includes CO₂ storage.

Table 10 Fuel consumption and well-to-wheel emissions for various fuel/traction combinations, based on best estimates in GM report¹⁵⁰

	Fuel consumption/l gasoline eq. (100 km) ⁻¹	CO ₂ eq ^a emission, well-to-wheel/g km ⁻¹
2002 Gasoline ICE car	8.15	224
2010 Gasoline ICE car	7.66	211
2010 Gasoline ICE hybrid vehicle	5.61	154
2010 Diesel hybrid ICE vehicle	5.18	137
2010 Fuel cell hybrid vehicle with on-board fuel processor on gasoline	4.84	133
2010 Fuel cell hybrid vehicle on compressed hydrogen from NG	3.31	108
2010 Fuel cell hybrid vehicle on compressed hydrogen from biomass	3.31	23
2010 Hydrogen ICE car, compressed hydrogen from NG	6.37	209
2010 Hydrogen hybrid ICE car	4.68	153

^a CO₂ eq includes emissions of CH₄ (=21 × CO₂) and N₂O (=310 × CO₂).

A recent study by General Motors and LBST¹⁵⁰ compares a wide variety of fuel pathways and powertrain systems, with respect to their energy use and CO₂ emissions. Table 9 compares greenhouse gas emissions for a variety of fuel pathways.¹⁵⁰ From Table 9 it follows that hydrogen production by electrolysis using electricity from the grid should be avoided, as it leads to the highest CO₂ emission. Production of compressed hydrogen is to be preferred in comparison to liquid hydrogen.

When the choice of the fuel pathway is left to the market, the supply cost will be more important than the CO₂ emissions for the various supply chains. Hydrogen produced by solar PV *via* electrolysis leads to a cost of \$52–82 GJ⁻¹.¹⁴⁶

Fuel consumption as modeled in the GM study for various configurations is given in Table 10.

A clear conclusion from Table 10 is that only hydrogen fuel cell vehicles offer a clear benefit with respect to a reduction of greenhouse gas emissions. Fuel cell vehicles with gasoline fuel processors do not provide such a benefit, in comparison to a diesel hybrid vehicle, neither do vehicles using hydrogen in internal combustion engines.

The data from Table 10 are in line with a recent study from MIT.¹⁵¹ Fuel cell vehicles (hybrid and non-hybrid) using gasoline will not have a significantly lower energy consumption and greenhouse gas emission than a hybrid internal combustion engine running on diesel. As the authors state themselves, fuel cell vehicles will be superior with respect to the emissions of non-greenhouse gases, such as NO_x, SO₂, hydrocarbons, CO and particles. In addition, it should be recognised that if hydrogen replaces gasoline and diesel for other reasons, then fuel cells will convert hydrogen much more efficiently than internal combustion engines.

Table 11 Emissions in g km^{-1} for various existing passenger vehicles

	Toyota Avensis gasoline ¹⁵²	Toyota Prius HSD gasoline ¹⁵²	Mercedes A gasoline ¹⁵²	Mercedes A diesel ¹⁵²	Daimler Chrysler Nectar 5 methanol ^{102,150}	Toyota FCHV-4 hydrogen ^{a153}
Weight/kg	1275	1400	1040	1085	1430	1860
Power/kW	95	57	75	70	75	80
CO ₂ (ttw/wtw ^b)	171/202	104/123	172/212	139/158	—	0/80
CO ttw	0.480	0.180	0.202	0.407	0.008	0
NOx ttw	0.050	0.010	0.024	0.381	0.000	0
HC ttw	0.030	0.020	0.054	0.000	0.036	0
PM ttw	0.000	—	0.000	0.039	—	0

ttw = Tank-to-wheel; wtw = well-to-wheel; — = no data available. ^a Produced by steam reforming of natural gas. ^b Including CO₂ emissions for fuel production, transport and distribution as given in GM study. Fuel Cell vehicle emissions as measured in Japan Drive Cycle.

Whereas well-to-wheel studies compare the same vehicle types with respect to weight, power to weight ratio and other vehicle specific characteristics by model calculations using the same driving cycles, comparison of existing vehicles under these equal circumstances proved unavailable from open sources. Table 11 gives an overview of CO₂, NOx, CO and hydrocarbon (HC) emissions from sets of comparable existing vehicles. The Toyota Prius HSD is based on the same chassis as the Toyota Avensis. The Mercedes A vehicles are based on the same model as the Nectar 5. The shortcoming of such a comparison is the difference in driving cycle (Japan 15 cycle for both fuel cell vehicles, EU drive cycle used in Cleaner Drive, for the other vehicles) and the difference in vehicle weight. It gives nevertheless an insight into the present state of the technology, as well as an idea of the results of well-to-wheel modeling.

The low contribution of ICE hybrid vehicles on reduction of non-greenhouse gases, as shown in Table 11, is confirmed in Toyota's Prius Green report, which evaluates emissions of CO₂, NOx, HC, SO₂ and particles over the entire life cycle of Toyota's newest gasoline ICE hybrid vehicle, the new Prius HSD, in comparison with a gasoline car of comparable size.¹⁵⁴ It appears that besides the 35% reduction in CO₂, the reductions of NOx, HC, SO₂ and particles are respectively 8%, 16%, 4% and -50% (*i.e.* particulate matter emissions are higher for the hybrid vehicle than for the gasoline vehicle). The exhaust emissions of NOx and HC in the driving cycle, as measured in g km^{-1} , are equal for both vehicle types.¹⁵⁴

The emissions of fuel cell vehicles depend on the fuel being used. Tailpipe emissions from hydrogen-fueled vehicles are zero. The Daimler Chrysler Nectar 5 is the fuel cell equivalent of the Mercedes A passenger car and runs on methanol. All tailpipe emissions of the Nectar 5 vehicle are lower than its ICE equivalent.^{102,152} Comparison of Table 11 with Table 8 shows that while modern conventional gasoline vehicles will be able to meet Euro IV and Tier 2 emission standards, even small passenger diesel vehicles will have difficulties in meeting both Euro IV as well as USA Tier 2 standards. An impressive effort is being made to meet today's and future emission standards for diesel cars, by the development of *e.g.* NOx absorbers, hydrocarbon adsorbers, and combinations of regenerable particle filters and NOx traps. Through the introduction of advanced particle filters and NOx absorbers a large reduction potential is present, although the regeneration of soot filters and the NOx absorbers will lead to a considerable fuel penalty.¹⁵⁵ Fuel cell technology offers the potential to reduce

the non-greenhouse gas emissions while at the same time reducing the fuel consumption of the vehicle.

6.2. Decentralised power generation

The generation of electricity and heat at the site of demand can save a significant amount of primary energy compared to the central generation of electricity and the generation of heat on site. Besides dumping the waste heat generated at central production, electricity is lost during transmission and distribution, ranging from more than 6% in the EU15 countries and North America, to more than 10% in developing countries.¹⁴⁶

Both PEMFC and SOFC systems are in development for this combined heat and power generation on the household scale (1–5 kWe). As presented in the previous sections, large scale CHP, PAFC and MCFC systems are available, while SOFC and PEMFC systems are in development. Depending on the consumer price of natural gas and the consumer price of electricity, the ratio of which can vary significantly from country to country, such systems can be operated economically. It was calculated that in Germany, taking into account the heat and electricity demand of the houses and the price of electricity and natural gas and the fee received for electricity sold back to the distribution companies, the penetration of fuel cell systems could be in the order of 30% of natural gas supplied houses and 50% of heating oil supplied houses.¹⁵⁶ An investment cost of less than €1000 kWe⁻¹ was assumed in this calculation for natural gas systems and around €900–1200 kWe⁻¹ for heating oil systems.

For stationary applications, the Department of Energy of the USA government has set the target for fuel cell systems operating on natural gas or propane being 40% electrical efficiency, 40 000 hours durability at a cost of \$400–\$750 kW⁻¹.

In a way similar to well-to-wheel studies, emissions have been calculated for the full fuel chain for stationary applications. For the UK, the environmental impact of combined heat and power systems on a 200 kWe scale has been calculated using diesel engines, gas engines and fuel cell systems in comparison with central electricity production using Combined Cycle Gas Turbines (CCGT) and decentralised heat production using heating boilers.¹⁵⁷ Table 12 gives the energy input and emissions per kWh energy demand for various technologies compared in this study.

Whereas the largest saving of energy originates from the combination of heat and power generation, irrespective of the technology used, the non-greenhouse gas emissions of

Table 12 Energy input and emissions for 200 kWe decentralised systems in comparison with central electricity production and decentralised heat production. Heat/power demand ratio = 1.8 (ref. 157)

	Energy input/ MJ kWh ⁻¹	CO ₂ / g kWh ⁻¹	CH ₄ / g kWh ⁻¹	NO _x / g kWh ⁻¹	SO _x / g kWh ⁻¹	CO/ g kWh ⁻¹
Grid electricity from NG (CCGT) + NG heating boiler	5.65	270	0.194	0.310	0.007	0.141
Diesel CHP engine	4.75	315	0.08	4.432	0.685	0.222
NG CHP engine	4.40	219	0.311	1.246	0.006	0.996
NG-SOFC	4.40	219	0.150	0.021	0.005	0.001

the fuel cell system are much lower than both engine based technologies.

The figures of Table 12 are similar for CHP systems in residential applications, where primary energy savings and CO₂ emission reductions are above 20% when using 1 kWe fuel cell CHP systems instead of using electricity from the grid and generating heat with boilers.¹²²

7. Conclusions

Fuel cells are in development for a variety of applications. Their use in transport and for combined heat and power generation offers a great opportunity to save an appreciable amount of energy, while at the same time reducing emissions of non-greenhouse gases. As the technology of fuel cells becomes more mature, fuel cell vehicles as well as stationary power systems are available for field tests. Commercial introduction can only take place when reliability is proven and cost is reduced. A considerable improvement on materials, component and system level is to be expected before and during the widespread application of fuel cells.

Frank de Bruijn

ECN Fuel Cell Technology, PO Box 1 1755 ZG Petten, The Netherlands.
E-mail: debruijn@ecn.nl

References

- At last, the fuel cell, *The Economist*, October 23rd, 1997.
- T. Klaiber, *J. Power Sources*, 1996, **61**, 61.
- Estimated Economic Impacts and Market Potential Associated with the Development and Production of Fuel Cells in British Columbia*, KPMG report for Ministry of Environment, Lands and Parks, Victoria, BC, Canada, 1996.
- A. Casanova, *J. Power Sources*, 1998, **71**, 65.
- Y. Watanabe, M. Matsumoto and K. Takasu, *J. Power Sources*, 1996, **61**, 53.
- X. Ren, P. Zelenay, S. Thomas, J. Davey and S. Gottesfeld, *J. Power Sources*, 2000, **86**, 111.
- H. Dohle, H. Schmitz, T. Bewer, J. Mergel and D. Stolten, *J. Power Sources*, 2002, **106**, 313.
- R. D. Breault, in *Handbook of Fuel Cells*, ed. W. Vielstich, A. Lamm and H. A. Gasteiger, Wiley, Chichester, UK, 2003, vol. 4, ch. 59.
- F. Barbir and T. Gomez, *Int. J. Hydrogen Energy*, 1996, **21**, 891.
- U. Bossel, *Well-to-Wheel Studies, Heating Values, and the Energy Conservation Principle*, European Fuel Cell Forum, 29th October 2003, available at <http://www.efcf.com>.
- M. A. J. Cropper, S. Geiger and D. M. Jollie, *J. Power Sources*, 2004, **131**, 57.
- D. E. Curton, R. D. Lousenberg, T. J. Henry, P. C. Tangeman and M. E. Tisack, *J. Power Sources*, 2004, **131**, 41.
- A. V. Anantaraman and C. L. Gardner, *J. Electroanal. Chem.*, 1996, **414**, 115.
- R. K. A. M. Mallant, *J. Power Sources*, 2003, **118**, 424.
- J. A. Kolde, B. Bahar and M. S. Wilson, in *Proceedings of the 1st International Symposium on Proton Conducting Membrane Fuel Cells (1995)*, The Electrochemical Society, Pennington, NJ, USA, 1995, vol. **95-23**, p. 193.
- W. Liu, K. Ruth and G. Rusch, *J. New Mater. Electrochem. Syst.*, 2001, **4**, 227.
- D. J. Jones, M. El Haddad, B. Mula and J. Rozière, *Environ. Res. Forum*, 1996, **1-2**, 115-126.
- A. E. Steck and C. Stone, *Development of the BAM Membrane for Fuel Cell Applications*, in *New Materials for Fuel Cell and Modern Battery Systems II*, ed. O. Savogado and P. R. Roberge, Ecole Polytechnique de Montreal, Montreal, Quebec, 1997, p. 792.
- F. Helmer-Metzmann, F. Osan, A. Schneller, H. Ritter, K. Ledjeff, R. Nolte and R. Thorwirth, *Polymer Electrolyte Membrane, and Process for the Production Thereof*, US Pat., 5 438 082, 1995 (Hoechst).
- J. Wei, C. Stone and A. E. Steck, *Trifluorostyrene and Substituted Trifluorostyrene Copolymeric Compositions and Ion-Exchange Membranes Formed Therefrom*, US Pat., 5 422 411.
- F. N. Büchi, B. Gupta, O. Haas and G. G. Scherer, *Electrochim. Acta*, 1995, **40**, 345-353.
- S. Faure, N. Cornet, G. Gebel, R. Mercier, M. Pineri and B. Sillion, in *New Materials for Fuel Cell and Modern Battery Systems II*, ed. O. Savogado and P. R. Roberge, Ecole Polytechnique de Montreal, Montreal, Quebec, 1997, p. 828.
- F. A. de Bruijn, D. C. Papageorgopoulos, E. F. Sitters and G. J. M. Janssen, *J. Power Sources*, 2002, **110**, 117.
- R. Savinell, E. Yeager, D. Tryk, U. Landau, J. Wainright, D. Weng, K. Lux, M. Litt and C. Rogers, *J. Electrochem. Soc.*, 1994, **141**, L46.
- Q. Li, R. He, J. O. Jensen and N. J. Bjerrum, *J. Electrochem. Soc.*, 2003, **150**, A1599.
- O. Savogado, *J. Power Sources*, 2004, **127**, 135.
- Q. Li, J. O. Jensen, R. He and N. J. Bjerrum, in *Proceedings of the 1st European Hydrogen Energy Conference, Grenoble September 2-5, 2003*, Association Française de l'Hydrogene, Paris, 2003.
- K. V. Lovell and N. S. Page, *Membrane Electrolyte Technology for Solid Polymer Fuel Cells*, report ETSU F/02/00110/REP, Cranfield University, Bedford, UK, 1997.
- T. R. Ralph, *Platinum Met. Rev.*, 1997, **41**, 102.
- C. G. M. Quah, *Hydrogen Fuel Cell Lett.*, 1998, **8**, 4, 1-3.
- D. M. Bernardi and M. W. Verbrugge, *J. Electrochem. Soc.*, 1992, **139**, 2477.
- H. A. Gasteiger, J. E. Panels and S. G. Yan, *J. Power Sources*, 2004, **127**, 162.
- K. Sasaki, J. X. Wang, M. Balasubramanian, J. McBreen, F. Uribe and R. R. Adzic, *Electrochim. Acta*, 2004, **49**, 3873.
- T. R. Ralph and M. P. Hogarth, *Platinum Met. Rev.*, 2002, **46**, 117.
- R. J. Bellows, E. P. Marucchi-Soos and D. T. Buckley, *Ind. Eng. Chem. Res.*, 1996, **35**, 1235.
- S. D. Knights, K. M. Colbow, J. St-Pierre and D. P. Wilkinson, *J. Power Sources*, 2004, **127**, 127.
- D. P. Wilkinson and D. Thompsett, in *New Materials for Fuel Cell and Modern Battery Systems II*, ed. O. Savogado and P. R. Roberge, Ecole Polytechnique de Montreal, Montreal, Quebec, 1997, p. 266.
- T. R. Ralph and M. P. Hogarth, *Platinum Met. Rev.*, 2002, **46**, 3.
- M. S. Wilson, J. A. Valerio and S. Gottesfeld, *Electrochim. Acta*, 1995, **40**, 355.
- A. Heinzl, F. Mahlendorf, O. Niemzig and C. Kreuz, *J. Power Sources*, 2004, **131**, 35.

- 41 R. C. Makkus, A. H. H. Janssen, F. A. de Bruijn and R. K. A. M. Mallant, *J. Power Sources*, 2000, **86**, 274.
- 42 J. Scholta, B. Rohland and J. Garche, in *New Materials for Fuel Cell and Modern Battery Systems II*, ed. O. Savogado and P. R. Roberge, Ecole Polytechnique de Montreal, Montreal, Quebec, 1997, p. 330.
- 43 C. Zawodzinski, M. S. Wilson and S. Gottesfeld, in *1996 Fuel Cell Seminar Orlando, FL*, Courtesy Associates, Washington, DC, 1996, p. 659.
- 44 J. Newton, S. E. Foster, D. Hodgson and A. Marrett, *Routes to Commercially Viable PEM Fuel Cell Stack*, ETSU F/02/00155/REP, available at <http://www.dti.gov.uk/energy/renewables/publications>.
- 45 N. Cunningham, D. Guay, J. P. Dodelet, Y. Meng, A. R. Hill and A. S. Hay, *J. Electrochem. Soc.*, 2002, **149**, A905.
- 46 E. Middelman, W. Kout, B. Vogelaar, J. Lenssen and E. de Waal, *J. Power Sources*, 2003, **118**, 44.
- 47 E. J. Carlsson, in *Hydrogen, Fuel Cells and Infrastructure Technologies*, 2003 Annual Progress report, US Department of Energy, Energy Efficiency and Renewable Energy, p IV-13.
- 48 G. Hards, J. Buchanan, T. Ralph, C. de Rouffignac, J. Rowe and D. Thompsett, in *2002 Fuel Cell Seminar Abstracts*, Courtesy Associates, Washington, DC, 2002, p. 854.
- 49 D. Wheeler, T. Clark and S. Motupally, in *2003 Fuel Cell Seminar, Miami*, Courtesy Associates, Washington, DC, 2003, p. 774.
- 50 S. Cleghorn, J. Kolde, R. Reid and O. Teller, in *2003 Fuel Cell Seminar, Miami*, Courtesy Associates, Washington, DC, 2003, p. 832.
- 51 Product sheet Ballard Mark 902, available at <http://www.ballard.com>, July 2004.
- 52 Product sheet General Motors, *GM Fuel Cell Technology for Sustainable Mobility*, Adam Opel AG, Rüsselsheim, 2004.
- 53 Product sheet Teledyne Energy Systems, available at <http://www.teledyne.com>, July 2004.
- 54 A. Folkesson, C. Andersson, P. Alvfors, M. Alakula and L. Overgaard, *J. Power Sources*, 2003, **118**, 349.
- 55 D. P. Wilkinson, in *The Electrochemical Society Interface, Spring 2001*, The Electrochemical Society, Pennington, NJ, 2001, p. 22.
- 56 M. Fowler, J. C. Amphlett, R. F. Mann, B. A. Peppley and P. R. Roberge, *J. New Mater. Electrochem. Syst.*, 2002, **5**, 255.
- 57 C. Handley, N. P. Brandon and R. van der Vorst, *J. Power Sources*, 2002, **106**, 344.
- 58 F. Uribe, T. Zawodzinski and S. Gottesfeld, *ECS Proc.*, 1998, **98-27**, 229.
- 59 J. B. J. Veldhuis, F. A. de Bruijn and R. K. A. M. Mallant, in *1998 Fuel Cell Seminar Abstracts, Palm Springs*, Courtesy Associates, Washington, DC, 1998, p. 598.
- 60 L. Pino, V. Recupero, M. Lagana and M. Minutoli, in *1998 Fuel Cell Seminar Abstracts*, Courtesy Associates, Washington, DC, 1998, p. 671.
- 61 J. St.-Pierre and N. Jia, *J. New Mater. Electrochem. Syst.*, 2002, **5**, 263.
- 62 E. Cho, J.-J. Ko, H. Y. Ha, S.-A. Hong, K.-Y. Lee, T.-W. Lim and I.-H. Oh, *J. Electrochem. Soc.*, 2004, **151**, A661.
- 63 M. Wakizoe, H. Murata and H. Takei, in *1998 Fuel Cell Seminar Abstracts, Palm Springs, CA*, Courtesy Associates, Washington, DC, 1998, abstract 1140.
- 64 P. J. de Wild, R. G. Nyqvist and F. A. de Bruijn, in *2002 Fuel Cell Seminar Abstracts*, Courtesy Associates, Washington, DC, 2002, p. 227.
- 65 S. Ibe, K. Hirai, N. Shinke, O. Yamazaki, S. Higashiguchi, K. Yasuhara, M. Hamabashiri and T. Tabata, in *2003 Fuel Cell Seminar, Miami*, Courtesy Associates, Washington, DC, 2003, p. 941.
- 66 T. Kawada and J. Mizusaki, in *Handbook of Fuel Cells*, ed. W. Vielstich, A. Lamm and H. A. Gasteiger, Wiley, Chichester, UK, 2003, vol. **4**, ch. 70.
- 67 A. Weber and E. Ivers-Tiffée, *J. Power Sources*, 2004, **127**, 273.
- 68 G. J. Saunders, J. Preece and K. Kendall, *J. Power Sources*, 2004, **131**, 23.
- 69 G. Rietveld, P. Nammensma, J. P. Ouweltjes, G. van Druten and R. Huijberts, in *2002 Fuel Cell Seminar, Portland*, Courtesy Associates, Washington, DC, 2002, p. 886.
- 70 O. A. Marina, J. S. Hardy, G. W. Coffrey, S. P. Simner and K. D. Meinhardt, in *2002 Fuel Cell Seminar, Portland*, Courtesy Associates, Washington, DC, 2002, p. 295.
- 71 O. Yamamoto, in *Handbook of Fuel Cells*, ed. W. Vielstich, A. Lamm and H. A. Gasteiger, Wiley, Chichester, UK, 2003, vol. **4**, ch. 71.
- 72 H. Tu and U. Stimming, *J. Power Sources*, 2004, **127**, 284.
- 73 D. Stöver, H. P. Buchkremer and J. P. P. Huijsmans, in *Handbook of Fuel Cells*, ed. W. Vielstich, A. Lamm and H. A. Gasteiger, Wiley, Chichester, UK, 2003, vol. **4**, ch. 72.
- 74 K. Hilpert, W. J. Quadackers and L. Singheiser, in *Handbook of Fuel Cells*, ed. W. Vielstich, A. Lamm and H. A. Gasteiger, Wiley, Chichester, UK, 2003, vol. **4**, ch. 74.
- 75 Z. Yang, S. Weil, D. M. Paxton and J. W. Stevenson, *J. Electrochem. Soc.*, 2003, **150**, A1188.
- 76 K. Fujita, K. Ogasawara, Y. Matsuzaki and T. Sakurai, *J. Power Sources*, 2004, **131**, 261.
- 77 N. Dekker, G. Rietveld, J. Laatsch and F. Tietz, in 6th European Solid Oxide Fuel Cell Forum, Lucerne, 28 June–2 July 2004, European Fuel Cell Forum, Oberrohrdorf, Switzerland, 2004, p. 319.
- 78 D. Ghosh, in *Proceedings of The Fuel Cell World*, 1–5 July 2002, ed. M. Nurdin, European Fuel Cell Forum, Oberrohrdorf, Switzerland, 2002, p. 135.
- 79 J. Zizelman, C. DeMinco, S. Mukerjee, J. Tachtler, J. Kammerer and P. Lamp, in *Proceedings of The Fuel Cell World*, 1–5 July 2002, ed. M. Nurdin, European Fuel Cell Forum, Oberrohrdorf, Switzerland, 2002, p. 306.
- 80 R. Steinberger-Wilckens, I. C. Vinke, L. Blum, J. Rimmel, F. Tietz and W. J. Quadackers, in 6th European Solid Oxide Fuel Cell Forum, Lucerne, 28 June–2 July 2004, European Fuel Cell Forum, Oberrohrdorf, Switzerland, 2004, p. 11.
- 81 S. Shaffer, *Development Update on Delphi's Solid Oxide Fuel Cell System*, 2004 SECA Review Meeting, Boston, available at: <http://www.netl.doe.gov>.
- 82 J. Dinsdale, K. Foger, J. Love, R. Ratnaraj and A. Washusen, in *2003 Fuel Cell Seminar, Miami*, Courtesy Associates, Washington, DC, 2003, p. 884.
- 83 R. A. George, *SECA Project at Siemens Westinghouse*, 3rd Annual Solid State Energy Conversion Alliance Workshop, March 21–22, 2002.
- 84 N. P. Brandon, S. Skinner and B. C. H. Steele, *Annu. Rev. Mater. Res.*, 2003, **33**, 183.
- 85 S. C. Singhal, *Solid State Ionics*, 2002, **152–153**, 405.
- 86 M. C. Williams, J. P. Strakey and S. C. Singhal, *J. Power Sources*, 2004, **131**, 79.
- 87 N. Minh, *Solid Oxide Fuel Cell Technology for Hybrid Power Generation*, 2nd DoE/UN International Conference and Workshop on Hybrid Power Systems, April 2002, available at: <http://www.netl.doe.gov>.
- 88 G. Israelson, *J. Mater. Eng. Perform.*, 2004, **13**, 282.
- 89 B. Borglum and E. Neary, in *2003 Fuel Cell Seminar, Miami*, Courtesy Associates, Washington, DC, 2003, p. 786.
- 90 J. Hansen, J. Pålsson, J. Nielsen, E. Fontell, T. Kivisaari, P. Jumppanen and P. Hendriksen, in *2003 Fuel Cell Seminar, Miami*, Courtesy Associates, Washington, DC, 2003, p. 790, and presentation available at <http://www.fuelcellseminar.com>.
- 91 K. Konishi, J. Iritani, N. Komiyama, T. Kabata, N. Hisatome, K. Nagata and K. Ikeda, in *Proceedings of The Fuel Cell World*, 1–5 July 2002, ed. M. Nurdin, European Fuel Cell Forum, Oberrohrdorf, Switzerland, 2002, p. 95.
- 92 R. Wustler and J. Schindler, in *Handbook of Fuel Cells*, ed. W. Vielstich, A. Lamm and H. A. Gasteiger, Wiley, Chichester, UK, 2003, vol. **3**, ch. 5.
- 93 *Hydrogen, Fuel Cells and Infrastructure Technologies*, 2003 Annual Program Report, US Department of Energy, Energy Efficiency and Renewable Energy, Washington, DC.
- 94 A. Bouza, C. J. Read, S. Satyapal and J. Milliken, 2004 Annual DoE Hydrogen Program Review–Hydrogen Storage, available at: <http://www.eere.energy.gov>.
- 95 M. M. Herrmann and J. Meusinger, 1st European Hydrogen Energy Conference, Grenoble 2–5 September 2003, paper CO2-175.
- 96 J. Wolf, in *Handbook of Fuel Cells*, ed. W. Vielstich, A. Lamm and H. A. Gasteiger, Wiley, Chichester, UK, 2003, vol. **3**, ch. 7.

- 97 R. Harris, D. Book, P. Anderson and P. Edwards, *Fuel Cell Rev.*, 2004, **1**, 17.
- 98 A. Züttel, in Proceedings of the International German Hydrogen Congress, 11–12 February 2004, Essen, ee energy engineers, Essen, Germany, 2004.
- 99 *European Fuel Cell and Hydrogen Projects 1999–2002*, Directorate-General for Research, EUR 20718, Brussels 2003.
- 100 D. zur Megede, *J. Power Sources*, 2002, **106**, 35.
- 101 B. Eliasson and U. Bossel, in *Proceedings of The Fuel Cell World, Lucerne*, 1–5 July 2002, ed. M. Nurdin, European Fuel Cell Forum, Oberrohrdorf, Switzerland, 2002, p. 367.
- 102 F. Panik and O. Vollrath, in *Proceedings of The Fuel Cell World, Lucerne*, 1–5 July 2002, ed. M. Nurdin, European Fuel Cell Forum, Oberrohrdorf, Switzerland, 2002, p. 196.
- 103 M. Krumpelt, J. D. Carter, R. Wilkenhoener, S. H. D. Lee, J.-M. Bae and S. Ahmed, in *2000 Fuel Cell Seminar, Portland*, Courtesy Associates, Washington, DC, 2000, p. 542.
- 104 P. S. Chintawar, B. Bowers, C. O'Brien, Z.-Y. Xue, J. Cross and W. Mitchell, in *Hydrogen, Fuel Cells and Infrastructure Technologies*, 2003 Annual Progress Report, US Department of Energy, Energy Efficiency and Renewable Energy, p IV-157.
- 105 DoE Decision Team Committee Report, On-Board Fuel Processing Go/No Decision, August 2004, available at: <http://www.eere.energy.gov/hydrogenandfuelcells/>.
- 106 M. Echigo, N. Shinke, S. Takami and T. Tabata, *J. Power Sources*, 2004, **132**, 29.
- 107 J. Komiya, N. Fujiwara, H. Fujiki, T. Miura and I. Yasuda, in *2002 Fuel Cell Seminar, Palm Springs*, Courtesy Associates, Washington, DC, 2002, p. 942.
- 108 W. L. Mitchell, in *2002 Fuel Cell Seminar, Palm Springs*, Courtesy Associates, Washington, DC, 2002, p. 952.
- 109 A. Fujii, K. Shindo, O. Tajima and H. Izaki, in *2002 Fuel Cell Seminar, Palm Springs*, Courtesy Associates, Washington, DC, 2002, p. 616.
- 110 M. J. Binder, W. R. Taylor and F. H. Holcomb, 2001 International Gas Research Conference Amsterdam, the Netherlands.
- 111 T. Fukunaga, H. Katsuno, H. Matsumoto, O. Takahashi and Y. Akai, *Catal. Today*, 2003, **84**, 197.
- 112 B. Davenport, *Plug Power Demonstration Project*, United States Military Academy West Point, NY, DACA 42-03-C-0005.
- 113 Site performance of residential fleet on <http://www.dodfuelcell.com/res>.
- 114 T. Mizukami, T. Okusawa, K. Takahashi, N. Imada and Y. Enokizu, in *2003 Fuel Cell Seminar, Miami*, Courtesy Associates, Washington, DC, 2003, p. 1.
- 115 H. Horinouchi, N. Osaka, J. Miyake, M. Kawamura, T. Miura and K. Nishizaki, in *2003 Fuel Cell Seminar, Miami*, Courtesy Associates, Washington, DC, 2003, p. 17.
- 116 I. Nakagawa, T. Kiyota, Y. Chida and T. Koike, in *2003 Fuel Cell Seminar, Miami*, Courtesy Associates, Washington, DC, 2003, p. 81.
- 117 Information on Millenium project available at <http://www.pefc.net>.
- 118 Z. Barisic, in *Proceedings of The Fuel Cell World, Lucerne*, 1–5 July 2002, ed. M. Nurdin, European Fuel Cell Forum, Oberrohrdorf, Switzerland, 2002, p. 105.
- 119 H. Raak, R. Diethelm and S. Riggenschach, in *Proceedings of The Fuel Cell World*, 1–5 July 2002, ed. M. Nurdin, European Fuel Cell Forum, Oberrohrdorf, Switzerland, 2002, p. 81.
- 120 R. George and A. Casanova, in *2003 Fuel Cell Seminar, Miami*, Courtesy Associates, Washington, DC, 2003, p. 895.
- 121 A. Schuler, J. Schild, E. Batawi, A. Rügge, M. Tamas, T. Doerk, H. Raak and B. Doggwiler, in *Proceedings of The Fuel Cell World*, 1–5 July 2002, ed. M. Nurdin, European Fuel Cell Forum, Oberrohrdorf, Switzerland, 2002, p. 128.
- 122 P. F. van den Oosterkamp and P. C. van der Laag, Proceedings AIChE Spring meeting, New Orleans 2003, paper 98G.
- 123 B. Borglum and E. Neary, in *2003 Fuel Cell Seminar, Miami*, Courtesy Associates, Washington, DC, 2003, p. 786.
- 124 K. Konishi, J. Iritani, N. Komiyama, T. Kabata, N. Hisatome, K. Nagata and K. Ikeda, in *Proceedings of The Fuel Cell World*, 1–5 July 2002, ed. M. Nurdin, European Fuel Cell Forum, Oberrohrdorf, Switzerland, 2002, p. 95.
- 125 E. Fontell, T. Kivisaari, N. Christansen, J.-B. Hansen and J. Pålson, *J. Power Sources*, 2004, **131**, 49.
- 126 J. Zizelman, S. Shaffer and S. Mukerjee, in *2003 Fuel Cell Seminar, Miami*, Courtesy Associates, Washington, DC, 2003, p. 888.
- 127 <http://www.fuelcells.org>.
- 128 <http://www.fuelcellpartnership.org/>.
- 129 F. Büchi, A. Tsukada, P. Rodatz, O. Garcia, M. Ruge, R. Kötz, M. Bärtschi and P. Dietrich, in *Proceedings of The Fuel Cell World, Lucerne*, 1–5 July 2002, ed. M. Nurdin, European Fuel Cell Forum, Oberrohrdorf, Switzerland, 2002, p. 218.
- 130 A. Martin, in *Proceedings of The Fuel Cell World, Lucerne*, 1–5 July 2002, ed. M. Nurdin, European Fuel Cell Forum, Oberrohrdorf, Switzerland, 2002, p. 232.
- 131 R. F. Service, The Hydrogen Backlash, *Science*, 2004, **305**, 958.
- 132 G. F. McLean, T. Niet, S. Prince-Richard and N. Djilali, *Int. J. Hydrogen Energy*, 2002, **27**, 507.
- 133 M. Cifrain and K. V. Kordesch, *J. Power Sources*, 2004, **127**, 234.
- 134 M. Schulze and E. Gülzow, *J. Power Sources*, 2004, **127**, 252.
- 135 E. Gülzow and M. Schulze, *J. Power Sources*, 2004, **127**, 243.
- 136 K. Kordesch, V. Hacker, J. Gsellmann, M. Cifrain, G. Faleschini, P. Enzinger, R. Fankhauser, M. Ortner, M. Muhr and R. R. Aronson, *J. Power Sources*, 2000, **86**, 162.
- 137 Y. Mugikura, in *Handbook of Fuel Cells*, ed. W. Vielstich, A. Lamm and H. A. Gasteiger, Wiley, Chichester, UK, 2003, vol. **4**, ch. 66.
- 138 G. Huppmann, in *Proceedings of The Fuel Cell World*, 1–5 July 2002, ed. M. Nurdin, European Fuel Cell Forum, Oberrohrdorf, Switzerland, 2002, p. 171.
- 139 T. Bardewyck, in *Proceedings of The Fuel Cell World, Lucerne*, 1–5 July 2002, ed. M. Nurdin, European Fuel Cell Forum, Oberrohrdorf, Switzerland, 2002, p. 102.
- 140 R.-H. Song, S. Dheenadayalan and D.-R. Shin, *J. Power Sources*, 2002, **106**, 167.
- 141 D. A. Landsman and F. J. Luczak, in *Handbook of Fuel Cells*, ed. W. Vielstich, A. Lamm and H. A. Gasteiger, Wiley, Chichester, UK, 2003, vol. **4**, ch. 60.
- 142 D. Rastler, in *Proceedings of The Fuel Cell World*, 1–5 July 2002, ed. M. Nurdin, European Fuel Cell Forum, Oberrohrdorf, Switzerland, 2002, p. 383.
- 143 R. D. Breault, in *Handbook of Fuel Cells*, ed. W. Vielstich, A. Lamm and H. A. Gasteiger, Wiley, Chichester, 2003, vol. **4**, ch. 59.
- 144 Site performance of PAFC fleet on <http://www.dodfuelcell.com/pafc>.
- 145 J. C. Yang, Y. S. Park, S. H. Seo, H. J. Lee and J. S. Noh, *J. Power Sources*, 2002, **106**, 68.
- 146 World Energy Investment Outlook 2003, International Energy Agency, IEA Publications, Paris.
- 147 K. Kasahara, M. Morioka, H. Yoshida and H. Shingai, *J. Power Sources*, 2000, **86**, 298.
- 148 European Directive 1999/96/EC, from <http://www.dieselnet.com>.
- 149 <http://www.epa.gov>.
- 150 *GM Well to Wheel Analysis of Energy Use and Greenhouse Gas Emissions of Advanced Fuel/Vehicle Systems—a European Study*, L-B Systemtechnik GmbH, Otobrun, 27 September 2002, available at <http://www.lbst.de/gm-wtw>.
- 151 M. A. Weiss, J. B. Heywood, A. Schafer and V. K. Natarajan, MIT report LFEE 2003-001 RP, available at: http://lfec.mit.edu/publications/PDF/LFEE_2003-001_RP.pdf.
- 152 Emission data available at <http://www.emis.vito.be>.
- 153 <http://www.dti.gov.uk>.
- 154 Prius Green Report, Toyota Motor Corporation, June 2003, available at: http://www.toyota.co.jp/en/k_forum/tenji/pdf/pgr_e.pdf.
- 155 D. Basteels and R. A. Searles, *Platinum Met. Rev.*, 2002, **46**, 27.
- 156 G. Erdmann, *Int. J. Hydrogen Energy*, 2003, **28**, 685.
- 157 D. Hart and A. Bauen, *Further Assessment of the Environmental Characteristics of Fuel Cells and Competing Technologies*, ETSU F/02/00153/REP, Imperial College, London, 1998.

Synergistic effects in the facilitated transfer of metal ions into room-temperature ionic liquids†‡

Dominique C. Stepinski, Mark P. Jensen, Julie A. Dzielawa and Mark L. Dietz*

Received 23rd September 2004, Accepted 16th December 2004

First published as an Advance Article on the web 10th January 2005

DOI: 10.1039/b414756a

Addition of tri-*n*-butyl phosphate (TBP) is shown to markedly increase the extraction of strontium from acidic nitrate media into certain 1-alkyl-3-methylimidazolium bis[(trifluoromethyl)sulfonyl]imides by dicyclohexano-18-crown-6 (DCH18C6), the apparent result of the formation of a synergistic adduct between the strontium-DCH18C6 complex and TBP. The magnitude of the synergistic enhancement is shown to depend on the alkyl chain length of the ionic liquid (IL) cation, with the effect diminishing as the cation hydrophobicity increases. The effect also diminishes at high (>50% v/v) TBP concentrations, the likely result of changes in solvent polarity unfavorable to the extraction of metal-crown ether complexes.

Introduction

Efficient transfer of a metal cation from an aqueous medium into an organic phase is most readily achieved by the use of an extractant capable of satisfying both its solvation and coordination requirements. Although in many instances, a single extractant can both saturate the coordination sphere of the cation and produce an electrically neutral, hydrophobic (and thus, extractable) species, in other cases, two different extractants are required. One extractant may, for example, serve to complex the cation and neutralize its charge, while a second serves to replace remaining waters of hydration, thereby yielding a more organophilic metal complex. When the cation partitioning is greater for the combined extractants than the sum for the extractants employed individually, the result is a synergistic extraction system. Such systems offer unique benefits, and have been employed to advantage in numerous metal ion separations.^{1–4}

Recent work in this laboratory in the area of metal ion separations has examined the possibilities afforded by ionic liquids (ILs),^{5–11} low-melting organic salts whose unique physicochemical properties (*e.g.*, low volatility, high ionicity) have garnered them intense interest as potential “green” alternatives to conventional organic solvents in a wide range of applications.^{12–18} Of particular note in our studies is the observation that in contrast to the extraction of strontium-crown ether (CE) complexes into molecular organic solvents, strontium extraction by dicyclohexano-18-crown-6 (DCH18C6) from acidic nitrate media into various 1-alkyl-3-methylimidazolium-based ILs takes place predominantly *via* a mechanism in which the cationic 1 : 1 metal-CE complex is exchanged for the cationic constituent of the ionic liquid. This

is clearly an undesirable pathway if the objective is the development of environmentally benign extraction systems.⁵ Although this problem can be addressed by employing a sufficiently hydrophobic IL cation (*e.g.*, 1-decyl-3-methylimidazolium) to induce a change in the extraction mechanism,¹¹ increased cation hydrophobicity is accompanied by substantially decreased metal ion extraction efficiency, thus diminishing an important advantage of ILs as extraction solvents over ordinary molecular diluents. The exploitation of synergistic effects offers one potential route to overcoming this difficulty. That is, by judicious combination of extractants, it may be possible to boost metal ion extraction efficiencies into ionic liquids incorporating even relatively hydrophobic cations. To date, the possibility of synergistic interactions between extractants in ionic liquids has not been explored, however. In this report, we examine the use of neutral organophosphorus reagents as synergists in the extraction of alkali and alkaline earth cations by crown ethers into 1-alkyl-3-methylimidazolium-based ionic liquids and consider the implications of the results for the design of improved IL-based systems for metal ion separations.

Experimental

Materials

The 1-alkyl-3-methylimidazolium bis[(trifluoromethyl)sulfonyl]imides (abbreviated hereafter as [C_{*n*}mim][Tf₂N]) were prepared and purified according to published methods.¹⁹ Tri-*n*-butyl phosphate (TBP) was obtained from Aldrich Chemical Company (Milwaukee, WI) and distilled prior to use. Diamyl amylophosphonate (DAAP) was obtained from Albright and Wilson (Richmond, VA) and purified by distillation (*T* = 105 °C) at reduced pressure (0.1 mm). For extended X-ray absorption fine structure (EXAFS) measurements and partitioning studies, the *cis-syn-cis* (A) isomer of DCH18C6 (Aldrich, Milwaukee, WI) was employed, while for extraction selectivity studies, a mixture of the *cis-syn-cis* (A) and *cis-anti-cis* (B) isomers was used. Aqueous

† Work performed under the auspices of the Office of Basic Energy Sciences, Division of Chemical Sciences, US Department of Energy under contract number W-31-109-ENG-38.

‡ Electronic supplementary information (ESI) available: *k*³-weighted Sr K-edge EXAFS of Sr-crown ether complexes in RTIL-TBP mixtures, scattering path lengths, energy threshold shifts and Debye-Waller factors. See <http://www.rsc.org/suppdata/gc/b4/b414756a/>

*mdietz@anl.gov

acid solutions were prepared using Milli-Q2 water and Ultrex[®] nitric acid (J. T. Baker Chemical Co.).

Methods

All distribution ratios were determined radiometrically using commercial Sr-85, Na-22 and Ca-45 radiotracers (Isotope Product Laboratories, Burbank, CA) assayed *via* gamma spectroscopy on a Packard Cobra II Auto-Gamma spectrometer (Sr-85 and Na-22) or liquid scintillation counting on a Packard model 2200CA liquid scintillation counter (Ca-45) using standard procedures.

The strontium coordination environment of representative organic phases was probed with X-ray absorption spectroscopy. Liquid samples containing approximately 0.03 M Sr and varying IL/TBP ratios were placed in 6 mm I.D. polyethylene tubes and mounted at 45° to the incident X-ray beam at beamline 12-BM of the Advanced Photon Source.²⁰ The monochromator energy was calibrated against the first inflection point of the K absorption edge of a Zr foil (17.998 keV) before and after the data collection. No drift in the monochromator energy was detected. Data at the Sr K-edge were collected in the fluorescence mode with a 13-element Ge detector, averaging four to seven scans. The EXAFS signal was extracted and analyzed by standard procedures²¹ using IFEFFIT²² with the threshold energy (E_0) set to the measured first inflection point of the Sr K-edge of the samples, 16.114 keV.

The resulting k^3 -weighted EXAFS ($k = 2.5$ – 11.0 \AA^{-1}) were fit in R -space ($R = 1.22$ – 4.22 \AA) to the theoretical phase and amplitude functions generated with FEFF8.00²³ from the atomic positions of $\text{Sr}(\text{NO}_3)_2(18\text{-crown-6})$,²⁴ $\text{Sr}(\text{H}_2\text{O})_2(18\text{-crown-6})^{2+}$, or $\text{Sr}(\text{TBP})_2(18\text{-crown-6})^{2+}$. In the fitting procedure, the values of the amplitude reduction factor ($S_0^2 = 1.0$) and the Debye–Waller factors of the Sr coordinated oxygen atoms ($\sigma_{\text{O}}^2 = 0.0136$) and the carbon atoms of the crown ether ring ($\sigma_{\text{C}}^2 = 0.0108$) were fixed at the values previously determined from the EXAFS of Sr-crown ether complexes.⁶ The number of coordinated crown ether molecules and the number of coordinated nitrate, water, or TBP molecules; the Debye–Waller factors of all other scattering paths; the average scattering pathlengths; and a single threshold energy shift (ΔE_0) were allowed to vary during each fit. The number of parameters varied in each fit was between 7 and 10, depending on the model used (maximum number of floating parameters allowed by the Nyquist criterion = 16).

Results and discussion

Synergistic interactions between extractants have been widely exploited as a means of enhancing metal ion partitioning into a variety of conventional molecular diluents.^{1–3} Extraction systems incorporating crown ethers have been of particular interest, a result of the cation size-selective nature of the synergistic effects in these systems.⁴ Although such effects have been observed for combinations of crown ethers with either acidic or neutral extractants, the latter represents a combination of particular potential utility, as for these systems, metal ion partitioning increases as the aqueous acidity is increased (thereby permitting efficient extraction from aqueous phases

containing high concentrations of acid and facile recovery of extracted metal ions at low acidities). Among the possible combinations of extractants (*i.e.*, acidic–neutral, neutral–neutral, and acidic–acidic), however, the pairing of two neutral extractants typically yields among the weakest synergistic effects.⁴

Previous work concerning the mechanism of strontium ion transfer between acidic nitrate media and $[\text{C}_n\text{mim}][\text{Tf}_2\text{N}]$ ($n = 2$ – 8) ionic liquids in the presence of the crown ether DCH18C6 has shown that strontium partitioning proceeds predominantly *via* exchange of the cationic 1 : 1 $\text{Sr}[\text{DCH18C6}]^{2+}$ complex for the cationic constituent of the IL.⁵ Subsequent EXAFS investigations have shown that the extracted species has a structure in which water molecules occupy the two axial positions in the complex.⁶ As is well known, synergistic effects frequently have their origins in the replacement of coordinated water with molecules of the second extractant.^{25–28} It thus seems reasonable to anticipate that the extraction of strontium by DCH18C6 from acidic nitrate media into these ILs might be more susceptible to synergistic enhancement than is its extraction into a conventional organic solvent (*e.g.*, 1-octanol), in which the extracted complex bears no inner-sphere water molecules.⁶ In fact, significantly improved strontium extraction efficiency might well be obtained simply by pairing the crown ether with a second neutral extractant.

Among neutral extractants, few have received more attention, particularly in the context of the development of processes for metal ion separation, than tri-*n*-butyl phosphate (TBP), which has been extensively investigated both as a metal ion extractant and as a solvent or co-solvent.^{29,30} Earlier work by Visser *et al.*⁹ has shown that various hydrophobic ionic liquids (*e.g.*, $[\text{C}_8\text{mim}][\text{Tf}_2\text{N}]$) can dissolve high (*ca.* 1 M) concentrations of TBP. As might be anticipated from this result, $[\text{C}_5\text{mim}][\text{Tf}_2\text{N}]$ and TBP are miscible in all proportions. Fig. 1A depicts the effect of varying the proportions of these two reagents on the extraction of strontium by DCH18C6-A from aqueous nitric acid. As can be seen, the distribution ratios for strontium obtained with the TBP–IL mixtures exceed the sum of the values obtained for the individual reagents over a wide range, sometimes by a substantial margin. A 1 : 1 (v/v) mixture of $[\text{C}_5\text{mim}][\text{Tf}_2\text{N}]$ and TBP, for example, yields a D_{Sr} of 91.5, more than an order of magnitude greater than the value expected. That the effect is not a peculiarity of this particular combination of ionic liquid and organophosphorus reagent is demonstrated by the results presented in Figs. 1B and C, which depict the results of analogous measurements for $[\text{C}_5\text{mim}][\text{PF}_6]$ –TBP and for $[\text{C}_2\text{mim}][\text{Tf}_2\text{N}]$ –diamyl amyolphosphonate (DAAP), a neutral phosphonate ester that has been employed as a substitute for TBP in various metal ion separations.^{31,32} In each of these two systems, the extraction of strontium into the mixtures also exceeds that expected from its extraction by the individual reagents.

If the influence of TBP addition upon molecular solvents is taken as a guide, this improvement in strontium extraction may have its origins in any of several effects. When used as a co-solvent in a conventional system (*e.g.*, for the modification of paraffinic hydrocarbons to yield the TRUEX process solvent³³), TBP serves primarily to raise the solvent polarity,³⁴ thereby improving the compatibility of the extractant and the

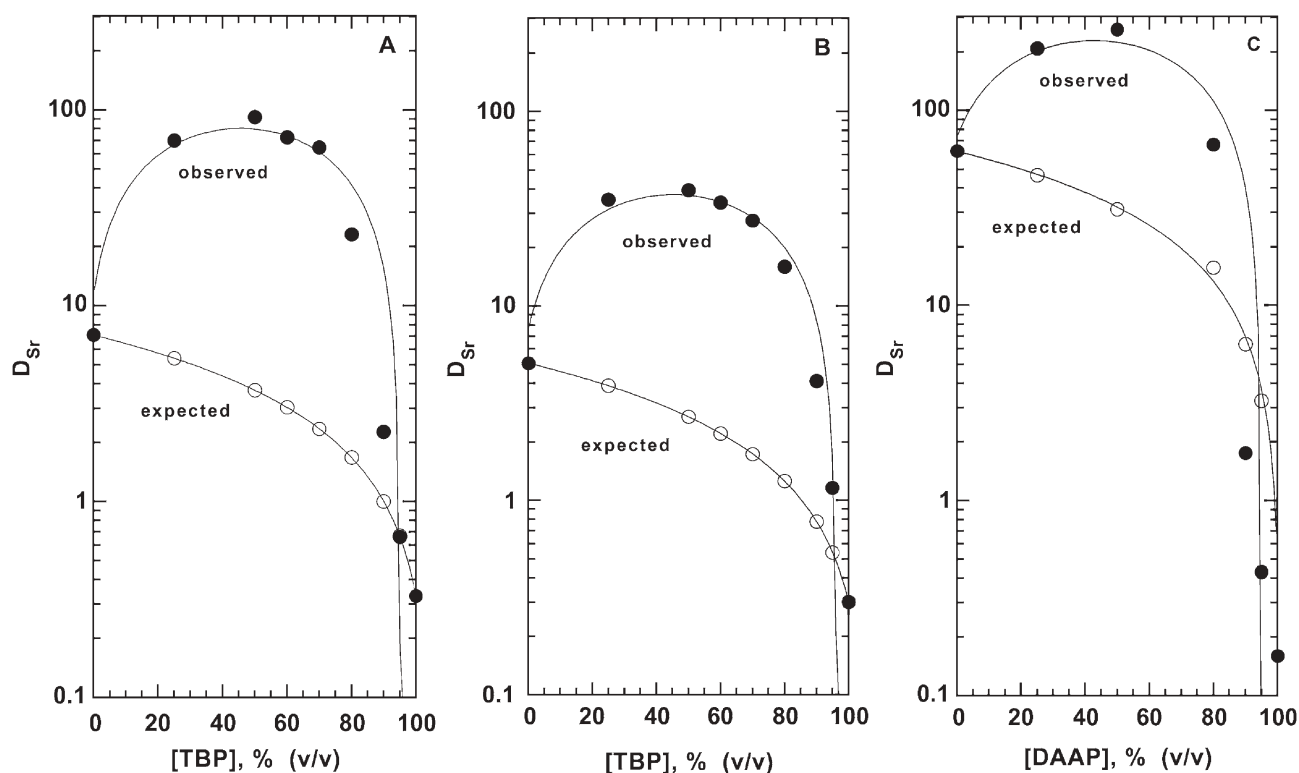


Fig. 1 Effect of co-extractant concentration (expressed as % v/v) on the partitioning of Sr-85 between 1 M HNO₃ and [C₅mim][Tf₂N] (panel A), [C₅mim][PF₆] (panel B), or [C₂mim][Tf₂N] (panel C) containing 0.1 M DCH18C6-A.

metal-extractant complex(es) with the organic phase and thus, increasing the extraction of the metal ion of interest. In the present system, however, addition of TBP, with its dielectric constant of 8.14,²⁹ to [C₅mim][Tf₂N], whose polarity approximates that of methanol ($\epsilon = 32.66$) or acetonitrile ($\epsilon = 35.94$),³⁵ would be expected to have the opposite effect, rendering the mixture less polar and presumably, less suitable as a medium for extraction of hydrated complexes. This is, in fact, a possible explanation for the decline in D_{Sr} values observed at high (>50% v/v) concentrations of TBP (Fig. 1, panels A and B).

A change in extraction mechanism (to strontium-nitrato-crown ether complex extraction) induced by the addition of high concentrations of TBP obviously represents another possible explanation for this decline. As shown in Fig. 2, however, even for an organic phase that is 80% (v/v) TBP, an increase in aqueous acidity leads to a decrease in D_{Sr} , behavior which, as has been noted previously,⁵ is inconsistent with the extraction of a strontium-nitrato-crown ether complex, such as is observed for TBP alone. This observation, while perhaps unexpected, is consistent with the results of ion chromatographic measurements of nitrate ion extraction into various TBP-[C₅mim][Tf₂N] mixtures containing DCH18C6. That is, over the range 10–90% (v/v) TBP, no measurable co-extraction of nitrate ion occurs upon extraction of strontium. That nitrate complex extraction remains an insignificant route for strontium partitioning into [C₅mim][Tf₂N] regardless of TBP concentration is further demonstrated by the results of extended X-ray absorption fine structure (EXAFS) measurements on the organic phases obtained upon extraction of

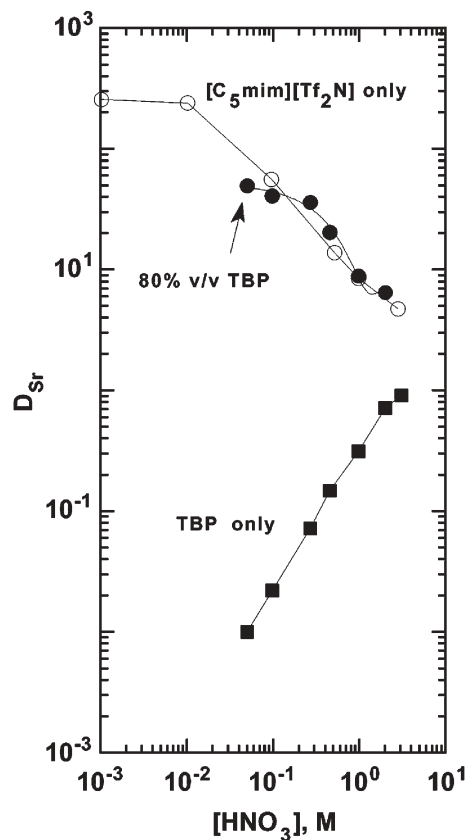


Fig. 2 D_{Sr} nitric acid dependencies for strontium extraction by DCH18C6-A into TBP, [C₅mim][Tf₂N], and an 80 : 20 (v/v) mixture of TBP and [C₅mim][Tf₂N].

Table 1 EXAFS results for the extraction of strontium from aqueous Sr(NO₃)₂ solution into neat tri-*n*-butyl phosphate (TBP) and its mixtures with [C₅mim][Tf₂N]

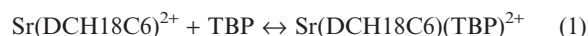
Organic phase	No. DCH18C6	No. coordinated O	No. axial O	No. distal O
[C ₅ mim][Tf ₂ N] (IL)	1.1 ± 0.2	8.7 ± 0.8	2.0	0
40% IL + 60% TBP	0.9 ± 0.2	7.3 ± 0.8	1.9	0
10% IL + 90% TBP	1.0 ± 0.2	7.9 ± 0.8	2.0	0
TBP	0.9 ± 0.2	8.6 ± 0.8	3.4	1.7 ± 0.8

Sr(NO₃)₂ by DCH18C6-A in [C₅mim][Tf₂N] containing various amounts of TBP, summarized in Table 1. As reported previously,⁶ the nearest neighbor coordination environment of strontium in the Sr(DCH18C6)(H₂O)₂²⁺ cation extracted into [C₅mim][Tf₂N] comprises 12 carbon atoms and 8 oxygen atoms, 6 from the crown ether and two from water molecules occupying axial coordination sites. The Sr K-edge EXAFS thus exhibits two major peaks, the first, at 2.7 Å, arising from coordinated oxygen atoms, the second, at 3.5 Å, from crown ether carbon atoms. Addition of TBP has no appreciable effect on the EXAFS observed for the extracted complex. In all cases, the number of coordinated oxygen atoms remains as 8, two of which occupy axial positions. In addition, in no instance is there evidence of the presence of distal (*i.e.*, uncoordinated) oxygen atoms, which are associated with coordinated nitrate ions and which give rise to a strong, multiple-scattering peak at 4.3 Å. Two distal oxygens are, however, observed in the EXAFS results for extraction into TBP itself, as expected for partitioning of the strontium-nitrate crown ether complex depicted in Fig. 3A. Taken together, these results strongly indicate that a change in the mechanism of extraction does not underlie the decrease in strontium partitioning observed at high concentrations of TBP.

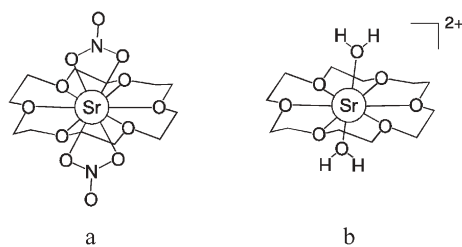
Increased organic phase water content arising from the addition of TBP represents a second possible origin of the increase in strontium extraction observed for many of the TBP-IL mixtures. That is, addition of TBP has previously been demonstrated to increase the water content of various conventional organic solvents,³⁶ and strontium extraction by crown ethers from acidic media has been shown to be favored by high organic phase water content.^{36,37} Both the solubility of water in alkanes and the extraction of strontium from nitric acid into alkanes by crown ethers, for example, increase in direct proportion to the concentration of TBP added.³⁶ Recent work, however, has shown that increasing the water content

of an ionic liquid does not necessarily lead to an increase in metal ion extraction efficiency. In fact, a decrease in D_{Sr} with increasing solvent water content has been observed for extraction by DCH18C6 into [C₂mim][Tf₂N] from acidic nitrate media under certain conditions.⁷ Moreover, Dai *et al.* have reported that the presence of dissolved water is not an important factor in determining the extent of strontium partitioning into RTILs containing crown ethers.³⁸ These studies suggest that increased solubilization of water in the ionic liquid is unlikely to account for the increase in strontium extraction upon TBP addition.

The formation of a synergistic adduct between the strontium-crown ether complex and TBP represents another possible explanation for the observed enhancement of extraction. Takeda³⁹⁻⁴¹ and Hasegawa *et al.*⁴² have shown that under appropriate conditions, any of a number of metal-CE complexes, among them the rubidium and caesium complexes of 12-crown-4 (12C4), 15-crown-5 (15C5), or benzo-15-crown-5 (B15C5),^{39,40} the copper(II) and zinc(II) complexes of 12C4 or 15C5,⁴² and the thallium complex of 15C5,⁴¹ can form 1 : 1 adducts with TBP, and that these adducts can be more extractable than the metal-CE complexes themselves. To investigate the possibility of adduct formation in our system, a continuous variation study, in which the relative proportion of DCH18C6 and TBP in [C₅mim][Tf₂N] was varied while maintaining a constant total ([DCH18C6] + [TBP]) concentration, was carried out. Such studies are well established as a means of determining the stoichiometry of extracted metal complexes and establishing the existence of synergistic interactions between extractants.³⁴ As can be seen from Fig. 4, the values of D_{Sr} observed at a given mole fraction of TBP or DCH18C6 are slightly higher than those calculated on the basis of the sum of the distribution ratios for the individual extractants, assuming first-power dependencies. In addition, a maximum (albeit a not especially well-defined one) is observed in the continuous variation plot at a 1 : 1 TBP : DCH18C6 mole ratio. These results point to the formation of a synergistic adduct between the Sr-DCH18C6 complex and TBP. Further evidence of adduct formation is provided by the results of measurements of the dependence of D_{Sr} on the concentration of TBP at fixed crown ether concentration in [C₅mim][Tf₂N]. If TBP addition is accompanied by 1 : 1 adduct formation (eqn. 1), a log-log plot of D_{Sr} vs. [TBP] would be expected to yield a line of unit slope, and in fact, such a relationship (slope = 0.85 ± 0.06) is observed (Fig. 5).



Thus, as we anticipated, extraction of strontium by DCH18C6 into ILs is susceptible to appreciable synergistic

**Fig. 3** Coordination environments of Sr(NO₃)₂(DCH18C6) in a conventional organic solvent (*e.g.*, 1-octanol) (panel a) and the Sr(DCH18C6)(H₂O)₂²⁺ cation in [C₅mim][Tf₂N] (panel b).

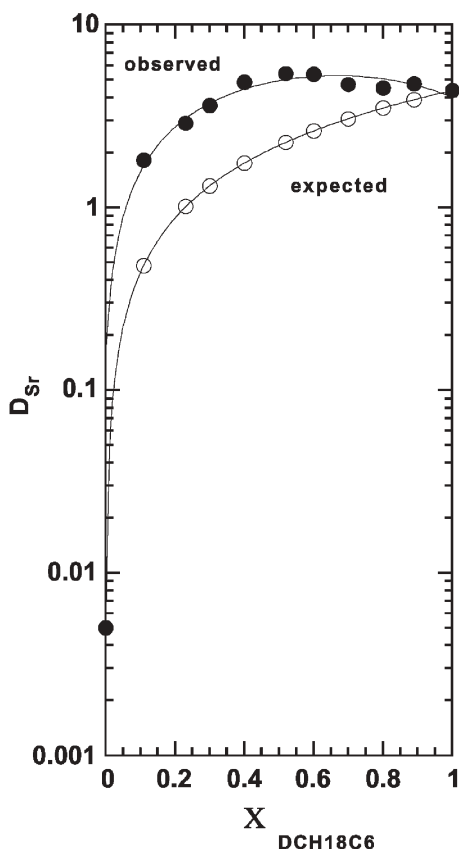
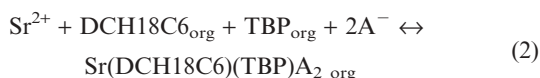


Fig. 4 D_{Sr} vs. mole fraction of DCH18C6 for extraction of strontium by DCH18C6–TBP mixtures in $[\text{C}_5\text{mim}][\text{Tf}_2\text{N}]$. ($[\text{HNO}_3] = 1 \text{ M}$; $[\text{DCH18C6}] + [\text{TBP}] = 0.1 \text{ M}$).

enhancement by addition of a second neutral extractant. This behavior stands in contrast to that of conventional solvents, for which synergistic effects are small or non-existent for systems employing either a pair of neutral extractants (*e.g.*, CE + TBP^{39–42} or CE + tri-*n*-octylphosphine oxide⁴³) or a polar organic solvent and for those not incorporating an organophilic anion (*e.g.*, picrate), A^- , to maintain electroneutrality:^{44,45}



To determine if the synergistic effects in these systems are sufficiently large to outweigh the decline in metal ion extraction efficiency that accompanies increased IL cation hydrophobicity,¹¹ the extraction of strontium by DCH18C6–TBP mixtures into a series of $[\text{C}_n\text{mim}][\text{Tf}_2\text{N}]$ ILs of increasing alkyl chain length, *n*, was measured. As shown previously for Sr^{2+} -DCH18C6 in the absence of TBP, an increase in the length of the alkyl chain in 1-alkyl-3-methylimidazolium bis[(trifluoromethyl)sulfonyl]imides from *n*-pentyl to *n*-hexyl, *n*-octyl, and finally, to *n*-decyl results in a gradual shift in the mechanism of ion transfer from aqueous nitrate media into ionic liquids containing DCH18C6 from cation exchange to nitrate complex partitioning.¹¹ That is, a decreasing percentage of the ion transfer occurs *via* ion exchange as the

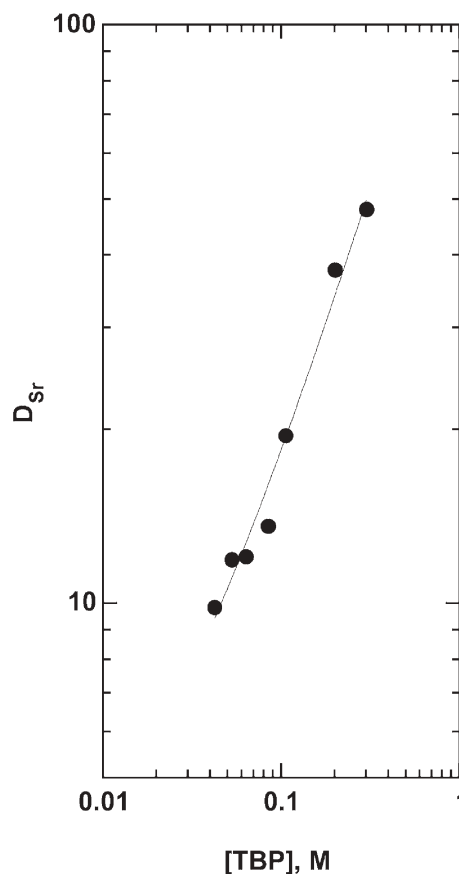


Fig. 5 D_{Sr} extractant dependency for the extraction of strontium by tri-*n*-butylphosphate (TBP) into $[\text{C}_5\text{mim}][\text{Tf}_2\text{N}]$ containing 0.1 M DCH18C6. (Aqueous phase = 1 M HNO_3).

hydrophobicity of the IL cation increases. As shown in Fig. 6, for Sr^{2+} -DCH18C6–TBP systems, the magnitude of the synergistic enhancement observed decreases as the fraction of strontium partitioning occurring *via* ion exchange falls, until for $[\text{C}_{10}\text{mim}][\text{Tf}_2\text{N}]$, addition of TBP yields little or no enhancement (Fig. 7). Thus, the synergistic effect is apparently dependent on the presence of the cationic (and water-bearing) $\text{Sr}(\text{DCH18C6})^{2+}$ complex. Clearly then, synergistic effects arising from combinations of neutral extractants are unlikely to be useful as a means of overcoming the decrease in metal ion extraction efficiency that accompanies increased IL cation hydrophobicity. These effects are, unfortunately, large only for systems in which the extraction efficiency is already high.

Despite this, synergistic interactions between extractants in ILs may still have practical value, particularly if they are accompanied by a significant improvement in the extraction selectivity for the ion of interest over common interferents. With this in mind, the extractant dependency of the distribution of Sr^{2+} , Ca^{2+} and Na^+ between nitric acid and solutions of DCH18C6 in $[\text{C}_5\text{mim}][\text{Tf}_2\text{N}]$ was determined both in the presence and absence of TBP (Fig. 8). In $[\text{C}_5\text{mim}][\text{Tf}_2\text{N}]$, the extraction selectivity ($\text{Sr}^{2+} > \text{Na}^+ > \text{Ca}^{2+}$) is that expected on the basis of the known complexation behavior of DCH18C6.⁴⁶ In a 1 : 1 (v : v) mixture of $[\text{C}_5\text{mim}][\text{Tf}_2\text{N}]$ and TBP, however,

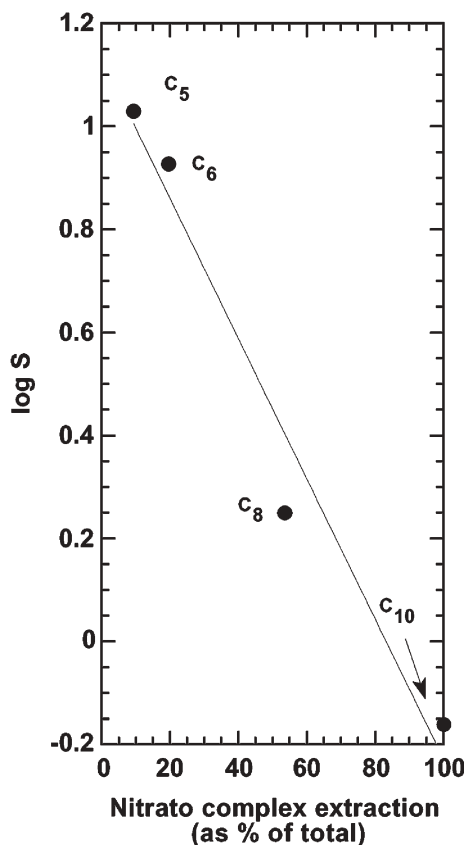


Fig. 6 Variation in the magnitude of the synergistic enhancement of strontium extraction by TBP-DCH18C6 mixtures into $[C_n\text{mim}][\text{TF}_2\text{N}]$ ILs with the fraction of partitioning occurring *via* nitrate complex extraction.¹¹ ($S \equiv$ synergistic factor $= D_{\text{Sr}}(\text{TBP}+\text{CE}) / (D_{\text{Sr}}(\text{TBP}) + D_{\text{Sr}}(\text{CE}))$). Organic phase: 0.1 M DCH18C6 in a 50 : 50 v/v mixture of TBP and the indicated ionic liquid. Aqueous phase: 1 M HNO_3).

appreciable enhancement of the extraction of both Sr^{2+} and Ca^{2+} is observed, while only a modest enhancement is observed for Na^+ , consistent with the expected weaker interaction of the latter with TBP. The result is a significant increase in the extraction selectivity for Sr^{2+} over Na^+ (but not Ca^{2+}) upon addition of TBP. Additional work is required to establish the practical utility of this observation.

Conclusions

The development of environmentally benign metal ion separation systems based upon room-temperature ionic liquids requires an improved understanding of the fundamental aspects of metal ion partitioning into these solvents. Of particular importance is the determination of the extent to which the behavior of IL-based systems can be understood (or predicted) by consideration of the properties of conventional molecular systems. In this context, the results reported here are significant for several reasons. First, they demonstrate that synergistic interactions between extractant molecules can occur in ionic liquids, as is the case in many conventional organic solvents. Moreover, these interactions may yield significant

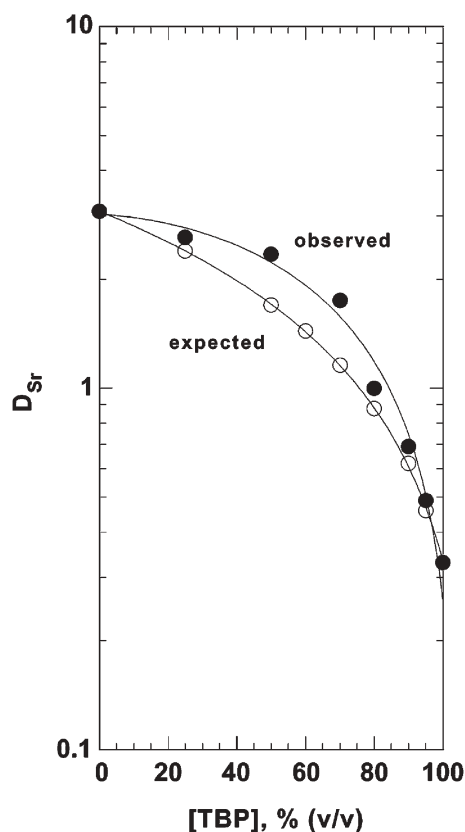


Fig. 7 Effect of co-extractant concentration (expressed as % v/v) on the partitioning of Sr-85 between 1 M HNO_3 and $[\text{C}_{10}\text{mim}][\text{TF}_2\text{N}]$ containing 0.1 M DCH18C6-A.

improvements in both metal ion extraction efficiency and selectivity. Given that appreciable synergistic interactions are not typically observed in polar molecular solvents, for combinations of neutral extractants, or for metal-crown ether complexes not incorporating an organophilic anion, it seems that extraction into many ILs may, in fact, be especially amenable to synergistic enhancement. Finally, as we have noted previously,⁴⁷ despite numerous reports describing synergistic effects between extractants and their use in metal ion separations, predictive guidelines for the design of synergistic systems are lacking. The correlation observed here between the magnitude of the synergistic effect and the fraction of strontium partitioning occurring *via* ion exchange (and therefore, the value of n) for $[\text{C}_n\text{mim}][\text{TF}_2\text{N}]$ ILs is thus noteworthy in that it may represent a first step toward the development of such guidelines for ionic liquid-based extraction systems.

Although our focus in these initial studies has been on combinations of neutral extractants, results obtained in conventional molecular solvents raise the possibility that much greater synergistic effects may be observed in ionic liquids for other extractant combinations (*e.g.*, neutral–acidic). Such combinations may thus offer substantial opportunities for the design of improved IL-based metal ion separation systems. Work addressing these opportunities is now underway in this laboratory.

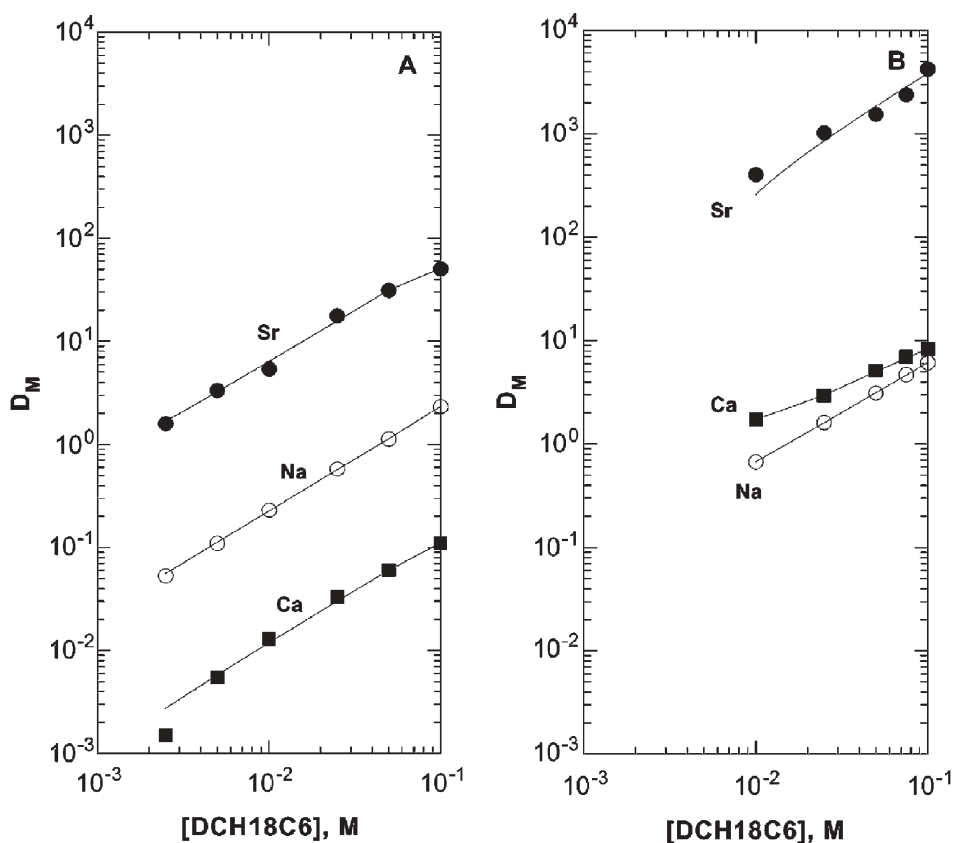


Fig. 8 D_M extractant dependency for the extraction of strontium, calcium, and sodium ions by DCH18C6-A/B in $[C_2mim][Tf_2N]$ in the absence (panel A) or presence (panel B) of TBP (50% v/v). (Aqueous phase = 0.1 M HNO_3).

Acknowledgements

The authors thank Larry R. Sajdak, Jr. for experimental assistance in the initial stages of this work, the Analytical Chemistry Laboratory (Division of Chemical Engineering) for ion chromatographic analyses, and Paul G. Rickert for distillation of TBP and DAAP. This work was performed under the auspices of the Office of Basic Energy Sciences, Division of Chemical Sciences, United States Department of Energy, under contract number W-31-109-ENG-38.

Dominique C. Stepinski, Mark P. Jensen, Julie A. Dzielawa and Mark L. Dietz*

Chemistry Division, Argonne National Laboratory, Argonne, IL 60439.
E-mail: mdietz@anl.gov; Fax: +1 (630) 252-7501;
Tel: +1 (630) 252-3647

References

- 1 Y. Marcus and A. S. Kertes, *Ion Exchange and Solvent Extraction of Metal Complexes*, Wiley-Interscience, London, 1969.
- 2 T. Sekine and Y. Hasegawa, *Solvent Extraction Chemistry*, Marcel Dekker, New York, 1977.
- 3 *Preconcentration Techniques for Trace Elements*, ed. Z. B. Alfassi and C. M. Wai, CRC Press, Boca Raton, FL, 1992.
- 4 A. H. Bond, M. L. Dietz and R. Chiarizia, *Ind. Eng. Chem. Res.*, 2000, **39**, 3442.
- 5 M. L. Dietz and J. A. Dzielawa, *Chem. Commun.*, 2001, 2124.
- 6 M. P. Jensen, J. A. Dzielawa, P. Rickert and M. L. Dietz, *J. Am. Chem. Soc.*, 2002, **124**, 10664.
- 7 M. L. Dietz, J. A. Dzielawa, M. P. Jensen and M. A. Firestone, *Conventional aspects of unconventional solvents: Room-temperature ionic liquids as ion-exchangers and ionic surfactants*, in *Ionic Liquids as Green Solvents: Progress and Prospects*, ed. R. D. Rogers and K. R. Seddon, American Chemical Society, Washington, DC, 2003, pp. 526–543.
- 8 M. L. Dietz, M. P. Jensen, J. V. Beitz and J. A. Dzielawa, *Room-temperature ionic liquids as diluents for the liquid-liquid extraction of metal ions: promise and limitations*, in *Hydrometallurgy 2003-Volume 1: Leaching and Solution Purification*, ed. C. A. Young, A. M. Alfantazi, C. G. Anderson, D. B. Dreisinger, B. Harris, and A. James, TMS (The Minerals, Metals and Materials Society), Vancouver, BC, Canada, 2003, pp. 929–939.
- 9 A. E. Visser, M. P. Jensen, I. Laszak, K. L. Nash, G. R. Choppin and R. D. Rogers, *Inorg. Chem.*, 2003, **42**, 2197.
- 10 M. P. Jensen, J. Neuefeind, J. V. Beitz, S. Skanthakumar and L. Soderholm, *J. Am. Chem. Soc.*, 2003, **125**, 15466.
- 11 M. L. Dietz, J. A. Dzielawa, I. Laszak, B. A. Young and M. P. Jensen, *Green Chem.*, 2003, **5**, 682.
- 12 M. J. Earle and K. R. Seddon, *Pure Appl. Chem.*, 2000, **72**, 1391.
- 13 J. F. Brennecke and E. J. Maginn, *AIChE J.*, 2001, **47**, 2384.
- 14 *Ionic Liquids: Industrial Applications for Green Chemistry*, ed. R. D. Rogers and K. R. Seddon, American Chemical Society, Washington, DC, 2002.
- 15 D. Zhao, M. Wu, Y. Kuo and E. Min, *Catal. Today*, 2002, **74**, 157.
- 16 *Ionic Liquids as Green Solvents*, ed. R. D. Rogers and K. R. Seddon, American Chemical Society, Washington, DC, 2003.
- 17 *Ionic Liquids in Synthesis*, ed. P. Wasserscheid and T. Welton, Wiley-VCH, Weinheim, FRG, 2003.
- 18 S. A. Forsyth, J. M. Pringle and D. R. MacFarlane, *Aust. J. Chem.*, 2004, **57**, 113.
- 19 J. G. Huddleston, A. E. Visser, W. M. Reichert, H. D. Willauer, G. A. Broker and R. D. Rogers, *Green Chem.*, 2001, **3**, 156.
- 20 M. A. Beno, M. Engbretson, G. Jennings, G. S. Knapp, J. Linton, C. Kurtz, U. Rütt and P. A. Montano, *Nucl. Instrum. Methods A*, 2001, **467–468**, 699.

- 21 R. Prins and D. E. Koningsberger, *X-ray Absorption: Principles, Applications, Techniques for EXAFS, SEXAFS, and XANES*, Wiley-Interscience, New York, 1988.
- 22 M. Newville, *J. Synchrotron Rad.*, 2001, **8**, 322.
- 23 A. L. Ankudinov, B. Ravel, J. J. Rehr and S. D. Conradson, *Phys. Rev. B*, 1998, **58**, 7565.
- 24 P. C. Junk and J. W. Steed, *J. Chem. Soc., Dalton Trans.*, 1999, 407.
- 25 M. Caceci, G. R. Choppin and Q. Liu, *Solvent Extr. Ion Exch.*, 1985, **3**, 605.
- 26 S. M. Khalifa, H. F. Aly, J. D. Navratil and F. A. Shehata, *Solvent Extr. Ion Exch.*, 1987, **5**, 1057.
- 27 *Principles of Solvent Extraction*, ed. J. Rydberg, C. Musikas and G. R. Choppin, Marcel Dekker, New York, 1992.
- 28 K. L. Nash, *Studies of the thermodynamics of extraction of f-elements in Solvent Extraction for the 21st Century, Vol. 1*, ed. M. Cox, M. Hidalgo and M. Valiente, Society of the Chemical Industry, London, 2001, pp. 555–559.
- 29 W. W. Schulz and J. D. Navratil, *Science and Technology of Tributyl Phosphate, Vol. 1*, CRC Press, Boca Raton, FL, 1984.
- 30 W. W. Schulz, L. L. Burger and J. D. Navratil, *Science and Technology of Tributyl Phosphate, Vol. 3*, CRC Press, Boca Raton, FL, 1990.
- 31 E. P. Horwitz, M. L. Dietz, R. Chiarizia and H. Diamond, *Anal. Chim. Acta*, 1992, **266**, 25.
- 32 G. W. Mason and H. E. Griffin, *Demonstration of the Potential for Designing Extractants with Preselected Extraction Properties: Possible Application to Nuclear Fuel Reprocessing*, in *Actinide Separations*, ed. J. D. Navratil and W. W. Schulz, American Chemical Society, Washington, DC, 1980, pp. 89–99.
- 33 E. P. Horwitz, D. G. Kalina, H. Diamond, G. F. Vandegrift and W. W. Schulz, *Solvent Extr. Ion Exch.*, 1985, **3**, 75.
- 34 E. P. Horwitz and D. G. Kalina, *Solvent Extr. Ion Exch.*, 1984, **2**, 179.
- 35 S. N. V. K. Aki, J. F. Brennecke and A. Samanta, *Chem. Commun.*, 2001, 413.
- 36 M. L. Dietz, E. P. Horwitz and R. D. Rogers, *Solvent Extr. Ion Exch.*, 1995, **13**, 1.
- 37 E. P. Horwitz, M. L. Dietz and D. E. Fisher, *Solvent Extr. Ion Exch.*, 1990, **8**, 199.
- 38 S. Dai, Y. H. Ju and C. E. Barnes, *J. Chem. Soc., Dalton Trans.*, 1999, 1201.
- 39 Y. Takeda, *Bull. Chem. Soc. Jpn.*, 1981, **54**, 526.
- 40 Y. Takeda, *Bull. Chem. Soc. Jpn.*, 1983, **56**, 2589.
- 41 Y. Takeda, *Bull. Chem. Soc. Jpn.*, 1989, **62**, 2379.
- 42 Y. Hasegawa, H. Miyata and S. Yoshida, *Bull. Chem. Soc. Jpn.*, 1986, **59**, 3003.
- 43 Y. Hasegawa, K. Suzuki and T. Sekine, *Chem. Lett.*, 1981, 1075.
- 44 W. F. Kinard, W. J. McDowell and R. R. Shoun, *Sep. Sci. Technol.*, 1980, **15**, 1013.
- 45 W. F. Kinard and W. J. McDowell, *J. Inorg. Nucl. Chem.*, 1981, **43**, 2947.
- 46 R. M. Izatt, K. Pawlak, J. S. Bradshaw and R. L. Bruening, *Chem. Rev.*, 1991, **91**, 1721.
- 47 M. L. Dietz, A. H. Bond, B. P. Hay, R. Chiarizia, V. J. Huber and A. W. Herlinger, *Chem. Commun.*, 1999, 1177.

Characteristics of methoxycarbonylation of aromatic diamine with dimethyl carbonate to dicarbamate using a zinc acetate catalyst

Toshihide Baba,^{*a} Akane Kobayashi,^b Yukio Kawanami,^a Koji Inazu,^a Akio Ishikawa,^a Tsuneo Echizenn,^a Kazuhito Murai,^a Shinji Aso^c and Masamitsu Inomata^c

Received 1st September 2004, Accepted 22nd December 2004

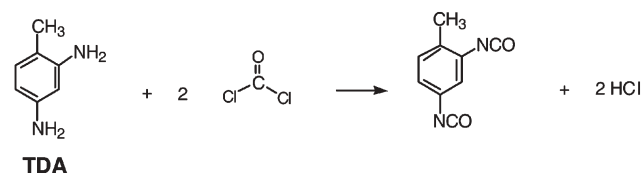
First published as an Advance Article on the web 18th January 2005

DOI: 10.1039/b413334j

The methoxycarbonylation of aromatic diamines such as 2,4-toluene diamine with dimethyl carbonate using $\text{Zn}(\text{OAc})_2 \cdot 2\text{H}_2\text{O}$ as a catalyst is examined to determine the influence of reaction variables on the yields of mono- and di-carbamates. These reactions yield dimethyltoluene-2,4-dicarbamate in 98% yield over 2 h at 453 K. An induction period is observed in the reaction of aromatic amines with dimethyl carbonate, but this induction period is almost completely eliminated by pretreating the catalyst with methanol. The role of methanol is investigated based on infrared absorption measurements, and a mechanism for dimethyl carbonate activation is proposed. Observed differences between the reactivities of aromatic and aliphatic amines for methoxycarbonylation are attributed to differences in the basicities of NH_2 groups in these amines.

Introduction

Alkyl carbamates are widely used as raw materials in agrochemicals, dyestuffs, and pharmaceuticals,^{1,2} and are utilized in organic synthesis as protecting groups for amine functionality.³ Alkyl carbamates are also precursors of isocyanates, with conversion occurring under heat.⁴ Among the isocyanates, 2,4-toluene diisocyanate and 4,4'-diphenylmethane diisocyanate are useful for the production of polyurethane and in many other applications. These aromatic diisocyanates are commercially synthesized by the reaction of phosgene with the corresponding aromatic diamines such as 2,4-toluene diamine (TDA). The reaction, however, has serious drawbacks; phosgene is an extremely toxic reagent, and a stoichiometric amount of HCl, which causes severe corrosion, is produced as a byproduct.



The methoxycarbonylation of an aromatic diamine (such as TDA) with dimethyl carbonate (DMC) and pyrolysis of the resulting carbamate represents an attractive synthetic route for obtaining isocyanates, as there is no need to use phosgene.⁵ Our group has already reported that $\text{Bi}(\text{NO}_3)_3$ and $\text{Sm}(\text{OAc})_3$ catalyze the reaction of 1,6-hexanediamine (HDA) with DMC to dimethylhexane-1,6-dicarbamate,⁶ and that the methoxycarbonylation of TDA with DMC to produce dimethyltoluene-2,4-dicarbamate proceeds using zinc acetate as a catalyst.⁷ In the methoxycarbonylation of these alkyl amines with DMC, the reactivity of the aliphatic amine is usually

higher than that of the aromatic amine. Thus, the methoxycarbonylation of HDA proceeds at around 350 K, while that of TDA proceeds at around 450 K.

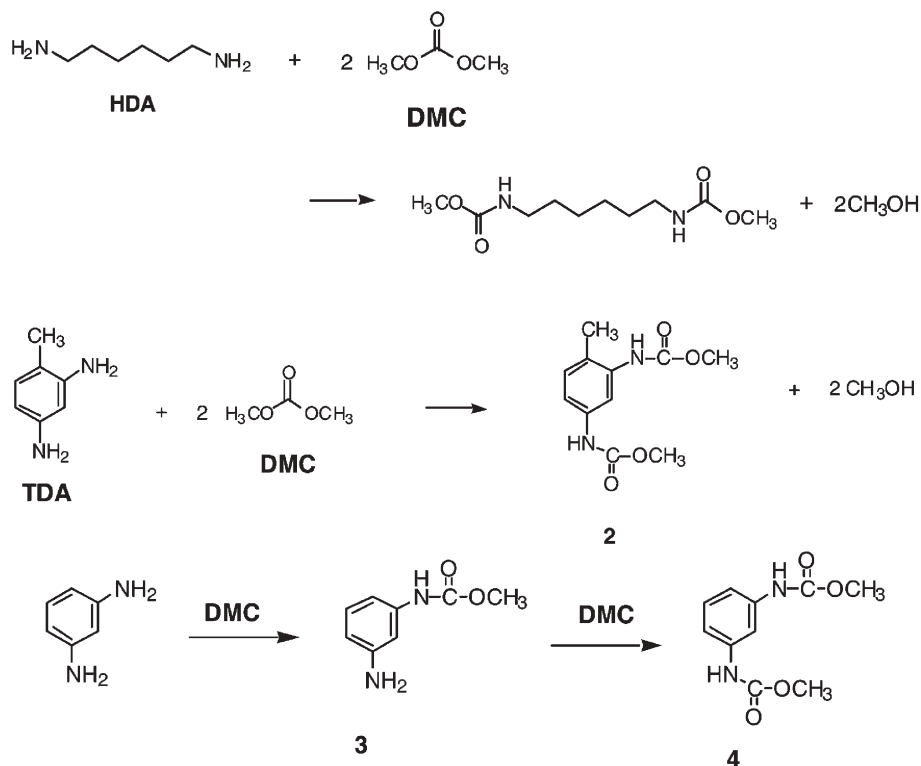
In this work, the methoxycarbonylation of TDA with DMC using $\text{Zn}(\text{OAc})_2 \cdot 2\text{H}_2\text{O}$ as a catalyst was examined in more detail, examining the influence of reaction variables on the yields of the mono- and di-carbamates of TDA. The characteristics of the reaction behavior are also discussed in comparison with the methoxycarbonylation of *m*-phenylenediamine (*m*-PhDA), which is one of the simplest aromatic diamines and which only affords a dicarbamate, dimethyl phenylene-1,3-dicarbamate (**4**). The DMC activation mechanism is also discussed based on the infrared (IR) absorption spectra of $\text{Zn}(\text{OAc})_2 \cdot 2\text{H}_2\text{O}$ in the presence or absence of reactants, and the difference between the reactivities of aromatic and aliphatic diamines is clarified.

Results and discussion

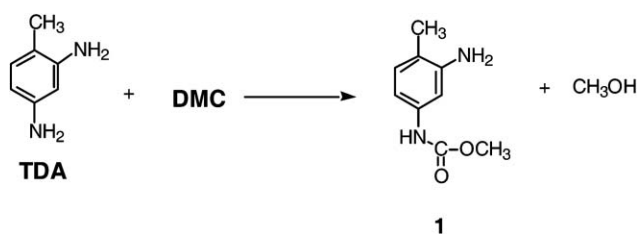
Catalytic activities of zinc and lead carboxylates for methoxycarbonylation

As $\text{Zn}(\text{OAc})_2 \cdot 2\text{H}_2\text{O}$ has been shown to give dimethyltoluene-2,4-dicarbamate **2** in 98% yield in the reaction of TDA with DMC at 453 K,⁷ the catalytic activities of various metal carboxylates for the methoxycarbonylation of TDA and *m*-PhDA with DMC was examined at this temperature (453 K). The catalyst, of the form $\text{Zn}(\text{OAc})_2 \cdot 2\text{H}_2\text{O}$, was dissolved in DMC and *m*-PhDA or TDA to achieve a homogenous reaction system. The metal acetates dissolved in both aromatic and aliphatic amines. The $\text{Zn}(\text{OAc})_2 \cdot 2\text{H}_2\text{O}$ selectively gave **2** or dimethyl phenylene-1,3-dicarbamate (**4**) in high yields together with the corresponding monocarbamates (methyl-3-amino-4-methyl phenyl carbamate (**1**) or methyl-3-aminophenyl carbamate (**3**)). The results are listed in Table 1.

*tbaba@chemenv.titech.ac.jp



In the methoxycarbonylation of TDA, the structure of the monocarbamate of TDA has been identified based on NOE in ^1H NMR spectra and ^{13}C NMR data.⁶ According to the results of NMR measurements, the monocarbamate is methyl-3-amino-4-methyl phenyl carbamate (**1**), the selectivity for which based on TDA was more than 99%. This indicates that the methoxycarbonylation of TDA with DMC predominated, as expressed by the following initial reaction.



The selective formation of monocarbamate **1** is possibly explained by the different basicities of NH_2 groups in the methyl anilines. The relevant $\text{p}K_{\text{a}}$ values are listed in Table 2.

Table 1 The methoxycarbonylation of TDA or *m*-PhDA with DMC, using $\text{Zn}(\text{OAc})_2 \cdot 2\text{H}_2\text{O}$

Reactant	TDA	<i>m</i> -PhDA
Conversion (%)	100	100
DMC	17	14
Yield (%)		
Monocarbamate	1	3
Dicarbamate	98	92
Selectivity (%) ^a	46	52

Zn(OAc)₂·2H₂O 0.4 mmol, aromatic diamines 4.0 mmol, DMC 100 mmol, reaction temperature 453 K, reaction time 2 h.
^a Selectivity based on DMC converted.

The basicity of 4-methyl aniline is highest among the present methyl anilines, suggesting that the higher the basicity of the NH_2 group, the higher the reactivity of the amine. Thus, the basicity of the NH_2 group at the 4 position in TDA is stronger than that at the 2 position.

To verify this hypothesis, the frontier electron densities of the NH_2 groups in TDA were calculated using MOPAC PM3. The calculated frontier electron densities of NH_2 groups at the 2 and 4 positions in TDA are 0.30 and 0.38, respectively. Although these are relative values, this result supports the notion that the basicity of the NH_2 group at the 4 position in TDA is higher than that at the 2 position.

Effect of DMC/TDA molar ratio on the yields of **1** and **2**

The effect of the DMC/TDA molar ratio on the yields of **1** and **2** was examined by changing the amount of DMC while maintaining constant initial amounts of TDA (4.0 mmol) and $\text{Zn}(\text{OAc})_2 \cdot 2\text{H}_2\text{O}$ (0.4 mmol). The results are shown in Fig. 1. The conversion of TDA increased with increasing DMC, reaching 100% at a DMC/TDA molar ratio of higher than 10. The conversion of DMC decreased with increasing DMC, but varied only slightly at DMC/TDA molar ratios higher than 10.

The yields of **1** and **2** were found to be strongly dependent on the amount of DMC (DMC/TDA molar ratio). At a DMC/TDA molar ratio of 2.5, **1** and **2** were formed in almost equivalent yields, accompanied by the *N*-methylation of TDA.

Table 2 $\text{p}K_{\text{a}}$ values of various amines

Amine	Butylamine	HDA	Aniline	Methylaniline		
				<i>o</i>	<i>m</i>	<i>p</i>
$\text{p}K_{\text{a}}$	10.63	9.83; 10.93	4.65	4.57	4.95	5.23

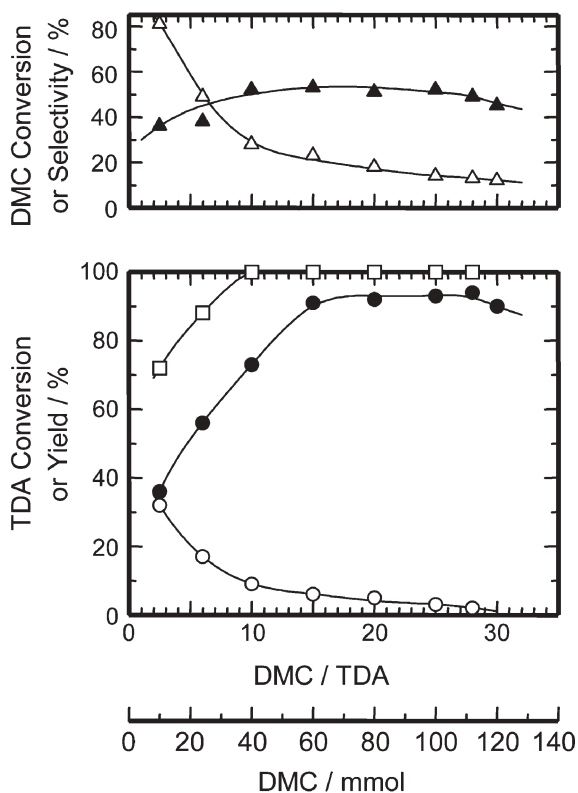


Fig. 1 Effect of DMC/TDA molar ratio on TDA conversion, yields of 1 and 2, and selectivity for 2. TDA: 4.0 mmol. $\text{Zn}(\text{OAc})_2 \cdot 2\text{H}_2\text{O}$: 0.4 mmol. Reaction temperature: 453 K. Reaction time: 2 h. (□) TDA conversion, (Δ) DMC conversion, (○) yield of 1, (●) yield of 2, (▲) selectivity for 2 based on DMC.

The formation of **2** became predominant with increasing DMC/TDA molar ratio, reaching *ca.* 92% at DMC/TDA molar ratios between 15 and 25, and then decreasing to 86% at a DMC/TDA molar ratio of 30.

The selectivity for **2** based on DMC was also found to depend on the amount of DMC. The selectivity increased with the DMC/TDA molar ratio to *ca.* 52% at DMC/TDA molar ratios between 10 and 25. However, at DMC/TDA molar ratios higher than 28, the selectivity for **2** based on DMC decreased, attributable to the decomposition of DMC at such high concentrations. Thus, the optimum DMC/TDA molar ratio was determined to be in the range 20–25.

Effect of the amount of $\text{Zn}(\text{OAc})_2 \cdot 2\text{H}_2\text{O}$

The effect of the amount of $\text{Zn}(\text{OAc})_2 \cdot 2\text{H}_2\text{O}$ catalyst on the yields of **1** and **2** was examined at 453 K using a DMC/TDA molar ratio of 25. The results are shown in Fig. 2. The conversion of TDA without the catalyst was 12%, but neither **1** nor **2** were produced and the reaction was accompanied by *N*-methylation. The conversion of TDA increased sharply with increasing catalyst concentration up to 0.02 mmol of $\text{Zn}(\text{OAc})_2 \cdot 2\text{H}_2\text{O}$, increasing more gradually thereafter to reach 100% conversion at 0.04 mmol ($\text{Zn}(\text{OAc})_2 \cdot 2\text{H}_2\text{O}/\text{TDA} = 0.01$). However, the conversion of DMC was found to be largely independent of the amount of catalyst, remaining relatively constant at *ca.* 14%.

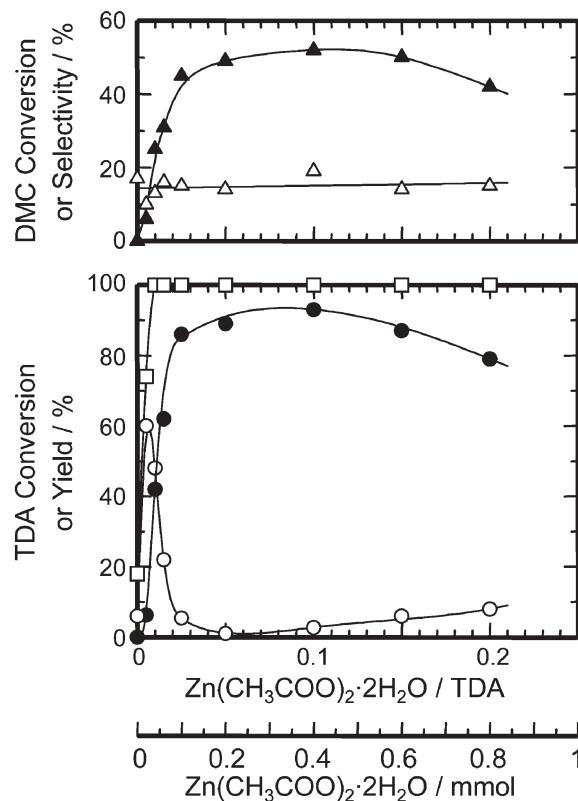


Fig. 2 Effect of $\text{Zn}(\text{OAc})_2 \cdot 2\text{H}_2\text{O}/\text{TDA}$ molar ratio on TDA conversion, yields of 1 and 2, and selectivity for 2. TDA: 4.0 mmol. DMC: 100 mmol. Reaction temperature: 453 K. Reaction time: 2 h. (□) TDA conversion, (Δ) DMC conversion, (○) yield of 1, (●) yield of 2, (▲) selectivity for 2 based on DMC.

The yield of **1** also increased sharply with increasing $\text{Zn}(\text{OAc})_2 \cdot 2\text{H}_2\text{O}$, reaching a maximum of 60% at 0.04 mmol of $\text{Zn}(\text{OAc})_2 \cdot 2\text{H}_2\text{O}$. With further increasing catalyst concentration, the yield decreased to a minimum of 2.5% and then increased slightly again.

The yield of **2** increased with catalyst concentration, reaching 92% yield at 0.4 mmol of the catalyst. The selectivity for **2** based on DMC also increased with catalyst concentration, reaching a maximum of 52% at the maximum yield of **2** (Fig. 2). Therefore, the optimum $\text{Zn}(\text{OAc})_2 \cdot 2\text{H}_2\text{O}/\text{TDA}$ molar ratio was found to be around 0.1.

Effect of reaction temperature

The effect of reaction temperature on reaction behavior was examined by reacting TDA (4 mmol) with DMC (100 mmol) at temperatures from 398 to 473 K for 2 h when $\text{Zn}(\text{OAc})_2 \cdot 2\text{H}_2\text{O}$ (0.4 mmol) was used as a catalyst. The results are shown in Fig. 3. The conversion of TDA increased sharply in a narrow temperature range from 393 to 413 K, and remained near 100% above 414 K. The conversion of DMC gradually increased with reaction temperature.

At 393 K, the dominant carbamate product was **1**, and the yield of **1** reached a maximum of 64% at 403 K. The formation of **2** was observed at reaction temperatures higher than 403 K. The yield of **2** increased with reaction temperature, reaching a maximum at 453 K. At 463 K, the yield of **2** was lower due to

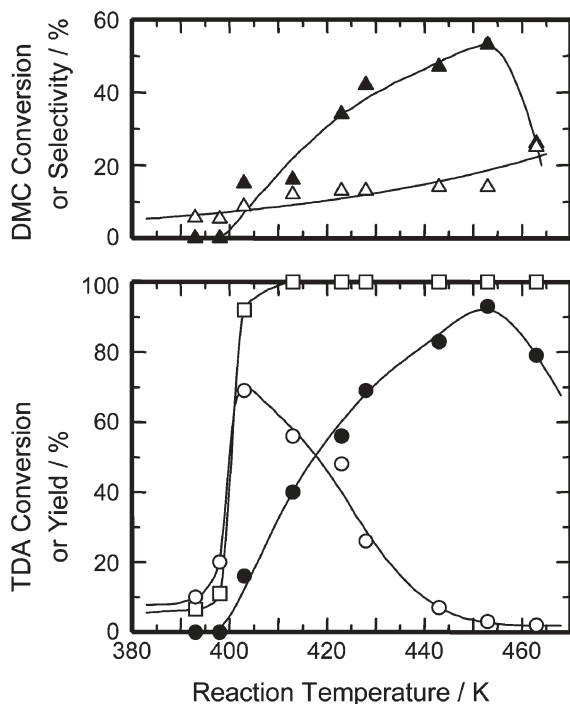


Fig. 3 Effect of reaction temperature on TDA conversion, yields of **1** and **2**, and selectivity for **2**. TDA: 4.0 mmol. DMC: 100 mmol. $\text{Zn}(\text{OAc})_2 \cdot 2\text{H}_2\text{O}$: 0.4 mmol. Reaction time: 2 h. (\square) TDA conversion, (Δ) DMC conversion, (\circ) yield of **1**, (\bullet) yield of **2**, (\blacktriangle) selectivity for **2** based on DMC.

the decomposition of **2** and reduced selectivity for **2** based on DMC.

In the reaction of *m*-PhDA with DMC, the same temperature dependence was observed, as shown in Fig. 4. The conversion of *m*-PhDA increased sharply in a narrow temperature range between 398 and 413 K, above which the conversion of *m*-PhDA remained at close to 100%. At reaction temperatures lower than 403 K, **3** was the only carbamate product, with a maximum yield of 32% at 403 K. The formation of **4** was not observed below 393 K, but the yield of **4** increased sharply above this temperature over a narrower temperature range than the increase in the yield of **2** in the reaction of TDA with DMC. The selectivity for **4** based on DMC increased sharply from 8% to a maximum of 75% with increasing reaction temperature from 403 to 413 K.

The sharp increase in TDA conversion over a narrow temperature range around 400 K (see Fig. 3) was further examined by analyzing the change in the yields of **1** and **2** with reaction time at 453 K using $\text{Zn}(\text{OAc})_2 \cdot 2\text{H}_2\text{O}$ as a catalyst. As shown in Fig. 5, the yield of **1** increased with reaction time to a maximum of 42% after 75 min. In contrast, **2** was not detected in the first 30 min, yet the yield of **2** increased suddenly to 76% by 90 min, reaching a maximum of 92% after 120 min.

A clearer induction phenomenon was observed in the methoxycarbonylation of *m*-PhDA with DMC using $\text{Zn}(\text{OAc})_2 \cdot 2\text{H}_2\text{O}$ as a catalyst. Fig. 6 shows the change in the yields of **3** and **4** with reaction time at 453 K. The formation of **3** was scarcely observed in the first 50 min, but the yield of **3** then increased suddenly in a short period to a maximum of

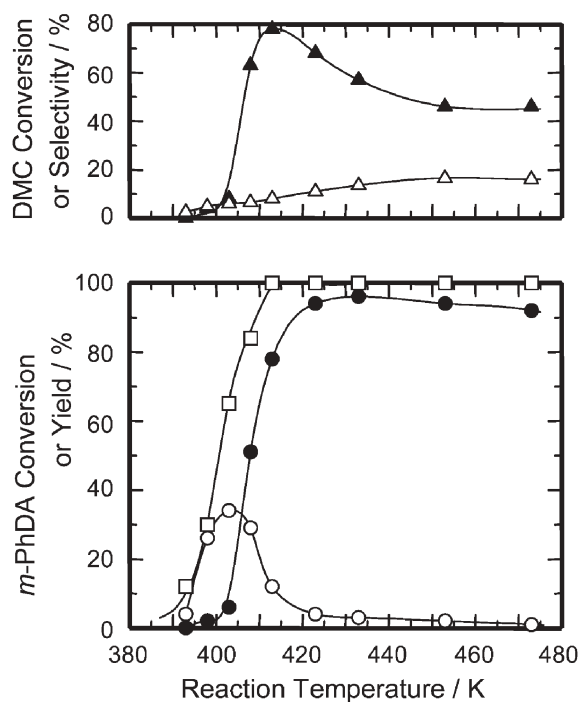


Fig. 4 Effect of reaction temperature on *m*-PhDA conversion, yields of **3** and **4**, and selectivity for **4**. *m*-PhDA: 4.0 mmol. DMC: 100 mmol. $\text{Zn}(\text{OAc})_2 \cdot 2\text{H}_2\text{O}$: 0.4 mmol. Reaction time: 2 h. (\square) *m*-PhDA conversion, (Δ) DMC conversion, (\circ) yield of **3**, (\bullet) yield of **4**, (\blacktriangle) selectivity for **4** based on DMC.

32% after 70 min. Similarly, the formation of **4** was not observed in the first 60 min, but the yield of **4** then increased rapidly over a short period while the yield of **3** decreased sharply beyond 70 min.

Therefore, induction is common in the methoxycarbonylation of aromatic amines, suggesting that the catalyst is

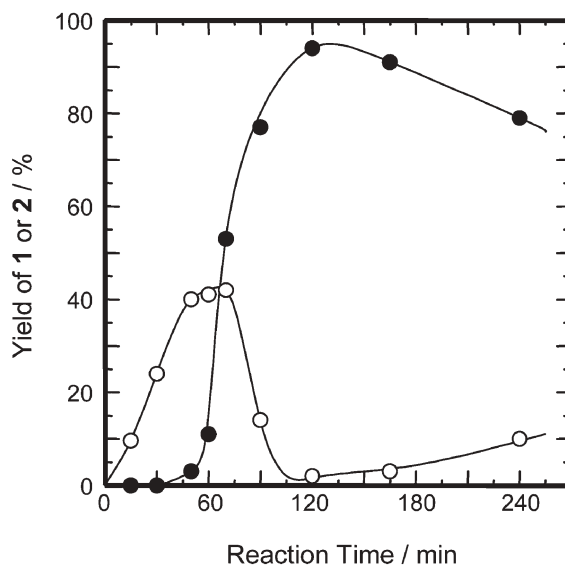


Fig. 5 Effect of reaction time on yields of **1** and **2**. TDA: 4.0 mmol. DMC: 100 mmol. $\text{Zn}(\text{OAc})_2 \cdot 2\text{H}_2\text{O}$: 0.4 mmol. Reaction temperature: 453 K. (\circ) Yield of **1**, (\bullet) yield of **2**.

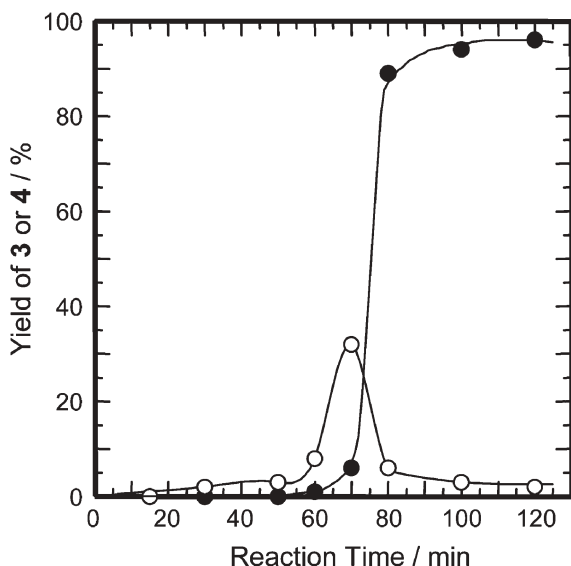


Fig. 6 Effect of reaction time on yields of **3** and **4**. *m*-PhDA: 4.0 mmol. DMC: 100 mmol. Zn(OAc)₂·2H₂O: 0.4 mmol. (○) Yield of **3**, (●) yield of **4**.

transformed into an active form in the induction period. Fu and Ono reported that induction was observed in the methoxycarbonylation of aniline with DMC using PbO catalysts and proposed a mechanism in which PbO is transformed into an active species by reaction with DMC.⁸

Transformation of the catalysts into the active form

Transformation of Zn(OAc)₂·2H₂O catalyst in the reaction of *m*-PhDA or TDA with DMC is supported by the formation of methyl acetate, which is presumably produced by the reaction of acetate anions coordinated to Zn²⁺ with DMC (or methanol formed by the decomposition of DMC). Thus, active species are considered to form by the reaction of Zn(OAc)₂·2H₂O with reactants (such as DMC) or reaction products (such as methanol).

To verify this hypothesis, the catalytic activities of Zn(OAc)₂·2H₂O pretreated under various conditions were examined at 453 K. As the methoxycarbonylation of *m*-PhDA with DMC proceeds within 2 h (see Fig. 6), the transformation of Zn(OAc)₂·2H₂O into the active form was monitored over the same period. The results are listed in Table 3.

Methanol and DMC pretreatment increased the activity of the catalyst for this reaction, whereas pretreatment with *m*-PhDA and methyl acetate appeared to have no effect on the formation of **3** and **4**. As methanol is formed by the decomposition of DMC, it is difficult to distinguish the effect of methanol on the catalytic activity from that of DMC.

Methanol presumably takes part in the transformation of Zn(OAc)₂·2H₂O into the catalytically active species. To examine the effect of methanol, the reaction of aniline, which is the simplest aromatic amine, with DMC was carried out in the absence and presence of methanol. The reaction temperature was set at 393 K, at which no appreciable methoxycarbonylation of TDA or *m*-PhDA with DMC occurs.

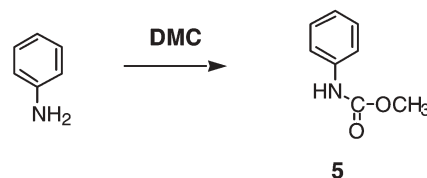


Table 3 Effect of pretreatment of Zn(OAc)₂·2H₂O with various compounds on the yields of **3** and **4**

Pretreatment	Conversion (%)		Yield (%)	
	<i>m</i> -PhDA	DMC	3	4
No treatment ^a	8	21	7	0.4
DMC ^b	79	30	23	55
CH ₃ OH ^c	81	24	21	58
<i>m</i> -PhDA ^d	12	17	4	0.7
Methyl acetate ^e	6	18	6	0.6

Reaction temperature 433 K, reaction time 2 h. ^a *m*-PhDA 4 mmol, DMC 100 mmol, Zn(OAc)₂·2H₂O 0.4 mmol. ^b Zn(OAc)₂·2H₂O (0.4 mmol) was treated with DMC (100 mmol) at 453 K for 1 h, and then the reaction was carried out by adding *m*-PhDA (4 mmol) at 433 K. ^c Zn(OAc)₂·2H₂O (0.4 mmol) was treated with CH₃OH (25 mmol) at 453 K for 1 h, and then the reaction was carried out by adding *m*-PhDA (4 mmol) and DMC (100 mmol) at 433 K. ^d Zn(OAc)₂·2H₂O (0.4 mmol) was treated with *m*-PhDA (4 mmol) at 453 K for 1 h, and then the reaction was carried out by adding DMC (100 mmol) at 433 K. ^e Zn(OAc)₂·2H₂O (0.4 mmol) was treated with methyl acetate (25 mmol) at 453 K for 1 h, and then the reaction was carried out by adding *m*-PhDA (4 mmol) and DMC (100 mmol) at 433 K.

The change in the yield of methyl *N*-phenyl carbamate (**5**) with reaction time is shown in Fig. 7. The methoxycarbonylation of aniline with DMC was accelerated by the addition of methanol, as expected.

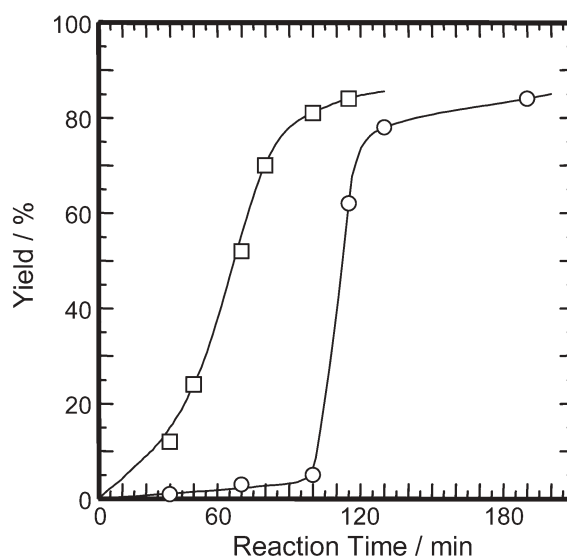


Fig. 7 Effect of methanol on yield of methyl *N*-phenyl carbamate in the methoxycarbonylation of aniline with DMC. Aniline: 11 mmol. DMC: 178 mmol. Zn(OAc)₂·2H₂O: 0.4 mmol. Reaction temperature: 393 K. (○) Without methanol, (□) with 11 mmol of methanol.

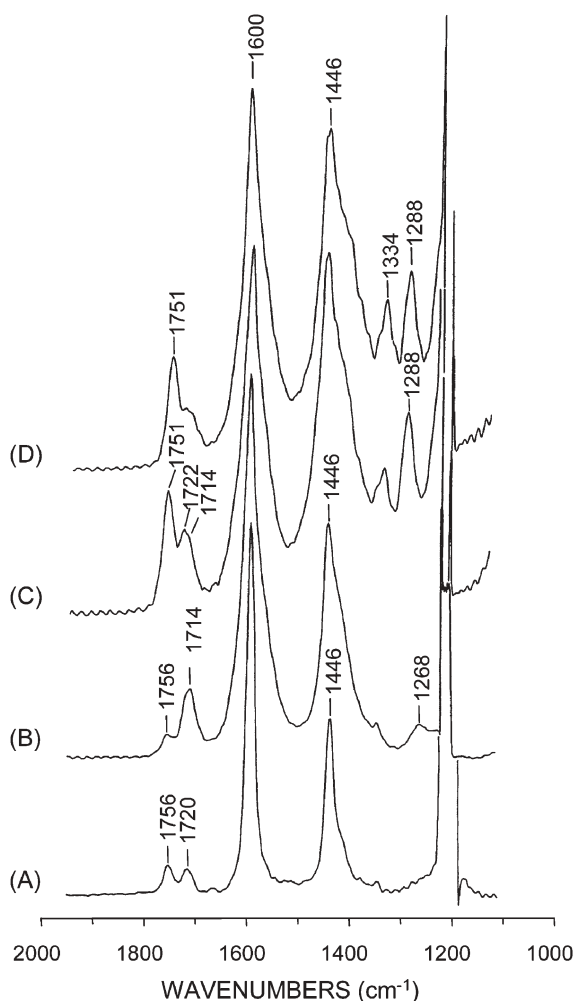
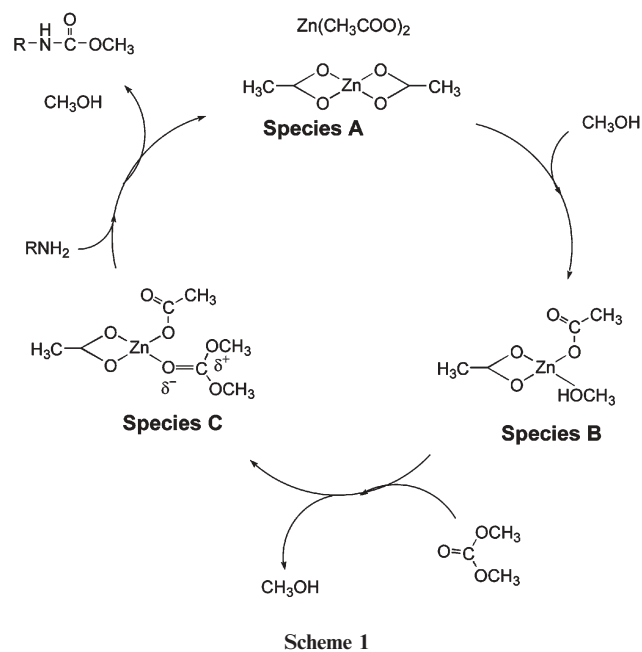


Fig. 8 Effect of methanol on structure of $\text{Zn}(\text{OAc})_2 \cdot 2\text{H}_2\text{O}$ catalyst. IR spectra were recorded at room temperature. (A) Sample A (0.1 mmol $\text{Zn}(\text{OAc})_2 \cdot 2\text{H}_2\text{O}$ dissolved in 20 ml CHCl_3), (B) Sample B (2.5 mmol methanol added to Sample A), (C) Sample C (0.4 mmol of DMC added to Sample B), (D) Sample D (0.16 mmol butyl amine added to Sample C).

Measurements of IR spectra of $\text{Zn}(\text{OAc})_2 \cdot 2\text{H}_2\text{O}$

The role of methanol was further examined using the IR spectra of $\text{Zn}(\text{OAc})_2 \cdot 2\text{H}_2\text{O}$ obtained in the absence and presence of methanol at room temperature. The results are illustrated in Fig. 8. Samples for IR analysis were prepared by dissolving 0.1 mmol of $\text{Zn}(\text{OAc})_2 \cdot 2\text{H}_2\text{O}$ in CHCl_3 (20 ml) (Sample A). Spectral bands at 1600 and 1446 cm^{-1} were obtained, assigned to the carboxyl stretching frequencies of asymmetry ($\nu_a(\text{COO})$) and symmetry ($\nu_s(\text{COO})$) for the bidentate carboxylate group to Zn^{2+} , as shown in Scheme 1, **Species A**.^{9,10} The band at 1600 cm^{-1} also has a component from dissolved water, arising from the $\text{Zn}(\text{OAc})_2 \cdot 2\text{H}_2\text{O}$. The weak bands above 1700 cm^{-1} in Sample A may be due to acetic acid derived from acetate ligands.

To confirm the effect of methanol pretreatment on the catalytic activity of $\text{Zn}(\text{OAc})_2 \cdot 2\text{H}_2\text{O}$, 2.5 mmol of methanol was added to Sample A at room temperature to give Sample B. The IR spectrum of Sample B exhibited two new bands at 1714



and 1268 cm^{-1} . The IR spectrum of $\text{Ge}(\text{OAc})_4$ includes bands at 1719 and 1271 cm^{-1} assigned to the C=O and C–O stretching modes of monodentate carboxylate groups,¹¹ and in $\text{CrO}_2(\text{OAc})_2$, these stretching modes have been observed at 1710 and 1240 cm^{-1} , respectively.¹² Thus, methanol is considered here to transform the bidentate coordination of CH_3COO^- anions to monodentate coordination, as shown in Scheme 1, **Species B**. This change in coordination possibly causes DMC to coordinate to Zn^{2+} , thereby activating the DMC.

To test this hypothesis, 0.4 mmol of DMC was added to Sample B to give Sample C. The IR spectrum displayed new bands at 1751, 1722 and 1290 cm^{-1} and a weakening of the bands at 1714 ($\nu_a(\text{COO})$) and 1268 cm^{-1} ($\nu_s(\text{COO})$), the asymmetric and symmetric stretching modes of CH_3COO^- anions. As the bands at 1751 and 1288 cm^{-1} , assigned to C=O and C–O stretching modes, were observed for DMC in CHCl_3 , the new band at 1722 cm^{-1} is attributed to the C=O stretching mode of DMC coordinated to Zn^{2+} cations, as shown in Scheme 1, **Species C**. The bands at 1751 and 1290 cm^{-1} therefore represent DMC molecules that have not coordinated to Zn^{2+} cations. However, the band near 1200 cm^{-1} due to C–O stretching of DMC molecules coordinated to Zn^{2+} cations unfortunately could not be resolved as it was obscured by the other strong peaks near 1200 cm^{-1} (Spectrum A).

Transformation of the bidentate coordination of CH_3COO^- anions to monodentate coordination facilitates the coordination of DMC molecules to Zn^{2+} cations, thereby activating the carbonyl groups of DMC. This suggests that DMC coordinated to Zn^{2+} cations reacts with amine. To test this hypothesis, butyl amine was added as an amine to Sample C to give Sample D. Butyl amine was selected based on its ability to react with DMC at room temperature to form methyl *N*-butyl carbamate. The $\text{p}K_a$ value of butyl amine is 10.61, which is much higher than that of aromatic amines such as aniline ($\text{p}K_a = 4.65$). The IR spectrum of Sample D shows a weakening of the band at 1722 cm^{-1} , indicating that

Zn²⁺-coordinated DMC reacts with butyl amine to form methyl *N*-butyl carbamate, as shown in Scheme 1.

Reactivities of *m*-PhDA and TDA and their monocarbamates

As shown in Figs. 3 and 4, the reactivity of TDA is higher than that of *m*-PhDA, as the formation of **1** proceeds at a lower reaction temperature than that of **3**. The different reactivities of TDA and *m*-PhDA can possibly be explained by the different basicities of these two compounds. The p*K*_a values of aniline and 4-methyl aniline are 4.65 and 5.23, respectively. Although the p*K*_a values of *m*-PhDA are not known, the estimated values for *o*-phenylene diamine are 4.65 and 1.86, indicating that the basicity of NH₂ groups in TDA at the 4 position is stronger than that in *m*-PhDA. Thus, the formation of **1** proceeds more readily than the formation of **3**. However, the reactivity of **3** is higher than that of **1**. Similarly, while the formation of **4** proceeds more readily than the formation of **2** at 453 K, the yield of **4** reaches 87% in 80 min (Fig. 6), compared to 2 h to reach nearly the same yield of **2**. The frontier electron density of NH₂ groups in **1** is 0.52, while that in **3** is 0.62. Thus, the different reactivities of **1** and **3** can also be explained by the different basicities of NH₂ groups.

Conclusions

The Zn(OAc)₂·2H₂O-catalyzed methoxycarbonylation of TDA with DMC produced dicarbamate **2** in high yield at around 450 K. The methoxycarbonylation of aromatic amines involved almost no induction period after the Zn(OAc)₂·2H₂O catalyst was pretreated with methanol. Methoxycarbonylation was also enhanced in the presence of methanol. Infrared spectra revealed that methanol changes the bidentate coordination of CH₃COO⁻ anions to Zn²⁺ cations of Zn(OAc)₂·2H₂O to monodentate coordination, facilitating the coordination of DMC to Zn²⁺ and activating the DMC molecules for the reaction with amines. The reactivity of amines with DMC was found to depend on the basicity of the amines. Thus, the methoxycarbonylation of aromatic amines, the basicities of which are lower than those of aliphatic amines, proceeded at *ca.* 100 K higher than that of aliphatic amines.

Experimental

Catalysts and reaction procedures

Metal salts such as Zn(OAc)₂·2H₂O were used as received unless otherwise noted. DMC of guaranteed grade was purified by distillation before use, while TDA, *m*-PhDA, and aniline of guaranteed grade were used without further purification. An excess quantity of DMC with respect to aromatic diamines was preferably used in the reactions, as it also acts as a solvent.

The reactions were carried out in a Teflon vessel placed in a 50 cm³ stainless-steel autoclave with a magnetic stirrer. The reaction and manipulation of the reaction mixture were carried out under a nitrogen atmosphere.

Identification and quantitative analysis of reaction products

The reaction products were identified by gas chromatography-mass spectrometry (GC-MS) and ¹H and ¹³C nuclear magnetic resonance (NMR). ¹H and ¹³C NMR spectra were recorded on a JEOL ECP 400 spectrometer, while GC-MS analysis of the reaction products was performed on a Shimadzu GCMS-OP 5000 spectrometer. The NMR data of the monocarbamate **1** obtained in this work were in good agreement with those reported in the literature.⁵ The monocarbamates of TDA have also been identified by analysis of the nuclear Overhauser effect (NOE) in the ¹H NMR spectra.⁶

The conversions of diamines and the yields of reaction products were determined by high-performance liquid chromatography (HPLC), while the conversion of DMC was measured by gas chromatography. Propylbenzene was used as an internal standard to determine both the conversions of diamines and the yields of reaction products. Unless otherwise noted, the yields of reaction products are expressed based on the amount of diamine charged.

IR measurements and calculation of electron density

Infrared absorption spectra of zinc acetate in solution were recorded on a JEOL JIR-WINSPEC50 Fourier Transform infrared (FT-IR) spectrophotometer at room temperature. Frontier electron densities of NH₂ groups in various amines and their corresponding monocarbamates were calculated by MOPAC PM3.¹³

Toshihide Baba,*^a **Akane Kobayashi**,^b **Yukio Kawanami**,^a **Koji Inazu**,^a **Akio Ishikawa**,^a **Tsuneeo Echizen**,^a **Kazuhito Murai**,^a **Shinji Aso**^c and **Masamitsu Inomata**^c

^aDepartment of Environmental Chemistry and Engineering, Tokyo Institute of Technology, G1-14 4259 Nagatsuta, Midori-ku, Yokohama 226-8502, Japan. E-mail: tbaba@chemenv.titech.ac.jp; Fax: +81-45-924-5480

^bDepartment of Chemical Engineering, Tokyo Institute of Technology, Ookayama 2-12-1, Meguro-ku, Tokyo, Japan

^cMistui Chemicals Inc., Sodegaura-shi, Nagaura 580-32, Chiba 299-0265, Japan

References

- P. Piccardi, *Chim. Ind. (Milan)*, 1986, **68**, 108.
- T.-T. Wu, J. Huang, N. D. Arrington and G. M. Dill, *J. Agric. Food Chem.*, 1987, **35**, 817.
- T. Greene and P. G. M. Wuts, *Protective Groups in Organic Synthesis*, John Wiley & Sons, New York, 2nd edn., 1991, p. 315.
- V. L. K. Valli and H. Alper, *J. Org. Chem.*, 1995, **60**, 257.
- M. Aresta, A. Dibebdetto and E. Quaranta, *Green Chem.*, 1999, **1**, 237.
- R. G. Deleon, A. Kobayashi, T. Yamauchi, J. Ooishi, M. Sasaki, F. Hirata and T. Baba, *Appl. Catal., A: Gen.*, 2002, **225**, 43.
- T. Baba, A. Kobayashi, T. Yamauchi, H. Tanaka, S. Aso, M. Inomata and Y. Kawanami, *Catal. Lett.*, 2002, **82**, 193.
- Z.-H. Fu and Y. Ono, *J. Mol. Catal.*, 1994, **91**, 399.
- N. W. Alcock, V. M. Tracy and T. C. Waddington, *J. Chem. Soc., Dalton Trans.*, 1976, 2243.
- K. Nakamoto, *Infrared Spectra of Inorganic and Coordination Compounds*, John Wiley & Sons, New York, 1970, p. 222.
- B. P. Straughan, W. Moore and R. McLaughlin, *Spectrochim. Acta., Part A*, 1986, **42**, 451.
- R. Kapoor, R. Sharma and P. Kapoor, *Z. Naturforsch., B*, 1984, **39**, 1702.
- J. J. P. Stewart, *J. Comput. Chem.*, 1989, **10**, 209.

Materials and Technologies for Sustainable Chemistry

MTSC

1-5 June 2005 Tallinn, Estonia



**Conference on
Knowledge-based
Materials and
Technologies for
Sustainable Chemistry**

**COST Action D29 workshop
of WG-s and MC meeting**

www.sustainchem.ttu.ee

Ehitajate tee 5, 19086 Tallinn, Estonia



1918
TALLINNA TEHNIKAÜLIKOOL
TALLINN UNIVERSITY OF TECHNOLOGY



The University of
Nottingham



SIXTH FRAMEWORK
PROGRAMME



Downloaded on 02 November 2010
Published on 24 February 2005 on http://pubs.rsc.org | doi:10.1039/B50274F

24110429-colour

Fast Publishing? Ahead of the field

To find out more about RSC Journals, visit

www.rsc.org/journals

An electronic archive containing approximately 195,000 articles and 1.2 million pages of ground-breaking chemical science papers published from 1841-1996.



RSC Journals Archive

It offers:

- Rapid location of articles via full-text searching
- Reference linking in articles published after 1990
- A range of purchase options and pricing to suit individual requirements and budgets
- The flexibility of accessing archive information from your desktop
- A secure, cost-effective solution for the storage and retrieval of research journals
- Coverage from prestigious journals such as ChemComm, The Analyst, Dalton Transactions, Organic & Biomolecular Chemistry and the Journal of Materials Chemistry

'It is very exciting to be able to search the full-text of approximately 195,000 papers (from 1841-1996)...The RSC is to be commended for providing both electronic access and full-text searching of this significant historical literature.'

Dana L. Roth, Caltech, USA

www.rsc.org/archive